Using Remote Sensing Data to Model Habitat Selection and Forage Quality for Herbivores in High Northern Latitudes in a Changing Climate

A Dissertation
Presented in Partial Fulfillment of the Requirements for the
Degree of Doctor of Philosophy
with a
Major in Natural Resources
in the
College of Graduate Studies
University of Idaho
by

Jyoti S. Jennewein

Major Professor: Jan Eitel, Ph.D.
Committee Members: Lee Vierling, Ph.D.; Sophie Gilbert, Ph.D.; Arjan Meddens, Ph.D.; Mark Hebblewhite Ph.D.
Department Administrator: Lee Vierling, Ph.D.

December 2020

Authorization to Submit Dissertation

This dissertation of Jyoti S. Jennewein, submitted for the Degree of Doctor of Philosophy with a Major in Natural Resources and titled "Using Remote Sensing Data to Model Habitat Selection and Forage Quality for Herbivores in High Northern Latitudes in a Changing Climate," has been reviewed in final form. Permission, as indicated by the signatures and the dates below, is now granted to submit final copies to the College of Graduate Studies for approval.

Major Professor: _____ Date: _____
Jan Eitel, Ph.D.

Committee Members: _____ Date: _____
Lee Vierling, Ph.D.

_____ Date: _____
Sophie Gilbert, Ph.D.

_____ Date: _____
Arjan Meddens, Ph.D.

_____ Date: _____
Mark Hebblewhite, Ph.D.

Department Administrator: _____ Date: _____
Lee Vierling, Ph.D.

Abstract

Landscapes located in high northern latitudes (≥ 60°N) are changing at a rate two to three times the global mean. Research is needed to assess the current state of northern latitude regions to best identify the impacts of climate change, which can inform the advancement of policies and management strategies. In response to warming induced landscape changes, management agencies are identifying practical "adaptive strategies" that may mitigate the negative effects of climate change. One such strategy in wildlife management is to evaluate and enhance monitoring programs, and to consider incorporating new tools to augment monitoring efforts.

Geospatial tools are one set of technologies that may enhance evaluation and monitoring for wildlife management. These tools enable spatial data to be collected, analyzed, and visualized in ways that assist in planning and management activities. Two common geospatial tools used in wildlife management are (1) mobile Global Positioning Systems (GPS) that can be housed in collars worn by a variety of species, and (2) remote sensing, which collects noncontact information regarding the physical and biological characteristics from a given target using reflected or emitted radiation.

The second chapter of this dissertation incorporates remotely sensed products in conjunction with GPS-telemetry from four Alaska moose populations to assess how habitat selection changes in response to increased temperatures. Both male and female moose in all populations increasingly, and nonlinearly, selected for denser canopy cover as ambient temperature increased during summer, where initial increases in the conditional probability of selection were initially sharper then leveled out as canopy density increased above ~50%. However, the magnitude of selection response varied by population and sex. In two of the three populations containing both sexes, females demonstrated a stronger selection response for denser canopy at higher temperatures than males. We also observed a stronger selection response in the most southerly and northerly populations compared to populations in the west and central Alaska.

The third and fourth chapters of this dissertation explore the development of remote sensing approaches to characterize, monitor, and map forage quality in high latitude regions of Alaska. I used hyperspectral data in conjunction with plant structural metrics derived from digital photographs and unmanned aerial vehicle structure from motion photogrammetry. My

results suggested that spectral vegetation indices calculated from hyperspectral remote sensing are an appropriate method for estimating important forage quality metrics such as dietary fibers (Chapter 3) – hemicellulose, cellulose, neutral detergent fiber, acid detergent fiber, acid detergent fiber, and silica – as well as integrated forage metrics (Chapter 4) – digestible protein and dry matter digestibility. My results also indicated that incorporating shrub structure is an important, and often unconsidered, aspect of remotely sensed forage quality metrics.

Acknowledgements

This dissertation would not have been possible without the support of my graduate committee and other scientific mentors. First, Drs. Jan Eitel and Lee Vierling provided me with the best mentorship I have received to date. From my early first queries about remote sensing and landscape ecology to the more in-depth questions related to field methodology and analytical techniques, they both have shaped me into the scientist I am today. In addition to their scientific support, I feel fortunate to have grown as a person under their mentorship and will carry many life lessons forward with me. Second, thank you to Dr. Arjan Meddens for his immense help with many technical aspects of learning how to calibrate satellite imagery to writing effective code. Third, thank you to Dr. Mark Hebblewhite for his expertise and time teaching me the importance of grounding my papers in wildlife ecology as well as many fast-paced conversations that broadened my perspective on wildlife management, collaboration, and science generally. Fourth, thank you to Dr. Sophie Gilbert for her expertise and guidance on wildlife management and how to engage in successful collaborations. In addition to my committee, I would like to thank Dr. Pete Robichaud for his additional mentorship regarding remote sensing, post-fire science, and how important it is to connect research to land management agencies to have the biggest impact.

I would like to thank additional research collaborators Dr. Peter Mahoney, Dr. Jeremy Pinto, Dr. Ryan Long, Dr. Natalie Boelman, Andrew Maguire, Dr. Mary Engels, Ben Busack, and William Weygint. This work also benefitted tremendously from agency collaborators Tom Paragi, Kyle Joly, Kim King-Jones, Kalin Kellie, Dr. Scott Brainerd, Graham Frye, Glenn Stout, and Erin Julianus. Thank you to all the above-mentioned mentors and collaborators for taking the time to challenge me and help me grow into a more effective and well-rounded scientist.

This research was funded by National Aeronautics and Space Administration's (NASA) Arctic Boreal Vulnerability Experiment (ABoVE) grant numbers: NNX15AT89A and NNX15AW71A as well as NASA's Idaho Space Grant Consortium (ISGC). These sources of financial support enabled me to explore important wildlife management related research questions, and for that I am truly grateful.

Dedication

This body of work is dedicated to my wonderful family. First, the completion of this dissertation was only possible with the love and support of my husband and partner Ben Busack. This work would not have been possible without your encouragement, sense of humor, and contributions to the research itself. Thank you for your endless patience. I am also grateful to my sweet daughter, Elowyn Finley, for bringing light and joy into my life every day. Next, I would like to thank my brother, mother, and father for their unwavering support and confidence in me. Finally, I would like to thank my in-laws for their support, understanding, and help with childcare. Without all of you this achievement would not have been possible.

Table of Contents

List of Tables

List of Figures

Statement of Contribution

The introduction (Chapter 1) and conclusion (Chapter 5) were sole authored. In Chapters 2-4, the listed co-authors primarily acted in advisory roles and in some cases aided in the technical aspects of coding.

Chapter 1: Introduction

High northern latitude regions (≥ 60°N) are undergoing rapid changes in response to increased temperatures from global climate change. These landscape changes include alterations in biogeochemical and hydrological cycles, primary production, and biodiversity through shifts in species distribution and fitness (Post et al., 2009; Walther et al., 2002). Changing wildfire regimes are also profoundly affecting habitats – the geographic area that contains the suite of physical and biological conditions needed to maintain species viability. In North American boreal systems, annual area burned doubled in the last half century (Kasischke & Turetsky, 2006). Such changes in habitat structure may provide new forage resources for herbivores (Beck et al., 2011; Kelly et al., 2013) but may also limit the thermal cover available to heat sensitive species like moose (*Alces alces*).

Additionally, climate driven ecosystem changes strongly affect rural northern communities. Reduced travel and access to important resources (Cold et al., 2020) as well as forecasted decreases in most subsistence species (Brinkman et al., 2016) impact rural northern communities substantially. Habitat changes complicate resource management and affect existing management plans and harvest guidelines, which may further stress the availability of important resources for northern communities. Research is needed to assess the current state of northern latitude regions to best identify the impacts of climate change, which can inform the advancement of policies and management strategies.

The National Aeronautics and Space Administration's (NASA) Arctic-Boreal Vulnerability Experiment (ABoVE) was developed to address questions regarding warming induced ecosystem changes in North American Arctic and boreal regions (ABoVE, 2014). One of ABoVE's six science themes is to evaluate how flora and fauna are responding to environmental change. The work presented in this dissertation falls under the ABoVE designation. Specifically, I developed models for mapping and monitoring forage quality for herbivores and advanced knowledge regarding habitat selection of an important ecosystem engineer (moose) in response to temperatures. This dissertation sought to provide new forage habitat monitoring tools for wildlife managers and identify important structural habitat features for moose, which may inform future managements plans for foraging habitats and moose in a changing climate.

In response to warming induced landscape changes, management agencies are identifying practical "adaptive strategies" that may mitigate the negative effects of climate change (Mawdsley et al., 2009). One such strategy in wildlife management is to evaluate and enhance monitoring programs, and to consider incorporating new tools to augment monitoring efforts (Mawdsley et al., 2009). Geospatial tools are one set of technologies that may enhance evaluation and monitoring for wildlife management. These tools enable spatial data to be collected, analyzed, and visualized in ways that assist in planning and management activities. For instance, Global Positioning Systems (GPS) estimate spatial positions of habitat features using time and distance relationships using satellites. Stationary GPS locations can be used to mark important habitat features such as water bodies and forest boundaries, that can then be imported into Geographic Information Systems (GIS) for analysis. Modern advances in GPS technology also enabled the creation of mobile units that can be housed in collars worn by a variety of species (Kays et al., 2015). These GPS locations track movements that can be associated with habitat selection at a variety of spatial scales that span from selection of specific food items to the geographic range of a species (Johnson, 1980).

Another important geospatial tool in wildlife management is remote sensing, which collects noncontact information regarding the physical and biological characteristics from a given target (e.g., vegetation) using reflected or emitted radiation. These collections most often occur on platforms such as aircrafts and satellites, but also include unmanned aerial vehicles (UAVs) and ground-based assessments from proximal sensors. Optical remote sensing approaches measure reflected light from the ultraviolet (10–380 nm), visible (400–700 nm), near infrared (NIR; 701–1399 nm), and shortwave infrared (SWIR; 1400–2500 nm) regions and can be used to estimate vegetation characteristics such as plant water content, plant structural components, and foliar chemistry (Xue & Su, 2017).

The second chapter of this dissertation incorporates remotely sensed products in conjunction with GPS-telemetry from four Alaska moose populations to assess how habitat selection changes in response to increased temperatures. Moose are well-adapted for cold weather and can experience heat stress year-round (McCann et al., 2013; Renecker & Hudson, 1986; Street et al., 2015; Thompson et al., 2019). Moose often use behavioral strategies to mitigate the effects of warming by moving to areas of denser and taller forest cover (Demarchi & Bunnell, 1995; Melin et al., 2014; van Beest et al., 2012) or areas that provide

convective cooling from water (Street et al., 2015). However, the majority of previous work on moose thermoregulation occurred in the southern portion of moose range in North America or in high latitude regions of Europe (Lenarz et al., 2010; Melin et al., 2014; van Beest et al., 2012). Hence, it was the goal of my second chapter to gain an improved understanding of whether ambient temperature elicits a behavioral in high-northern latitude moose populations in North America is increasingly important as these ecosystems are undergoing massive changes from climate change (Markon et al., 2018).

Remote sensing approaches are also commonly employed by wildlife management agencies to quantify, monitor, and map forage resources for herbivores (Macander et al., 2020; Merems et al., 2020; Walton et al., 2013). In high northern latitudes, the increased abundance and geographic extent of shrubs (Myers-Smith et al., 2011; Sturm et al., 2001) is enabling the expansion of herbivore habitat for moose, snowshoe hares (*Lepus americanus*), and ptarmigan (*Lagopus lagopus, L. muta*) (Tape et al., 2016; Zhou et al., 2020). However, the impact of climate warming on forage quality is less clear, and will likely vary depending on region and species (Elmendorf et al., 2012; Hansen et al., 2006; Lenart et al., 2002; Turunen et al., 2009). For instance, as temperatures warm and more nitrogen is available for plant uptake, chemical deterrents in subarctic plants also decline (De Long et al., 2016), thereby increasing digestibility. In contrast, observed increases in forage biomass from warming has coincided with a decline in caribou (*Rangifer tarundus*) populations indicating that forage quality has decreased even as quantities or forage increased (Fauchald et al., 2017). Forage quality strongly influences herbivore life-history traits like maternal body condition, pregnancy rates, and survival (Parker et al., 2009). Monitoring approaches that characterize wide portions of the landscape used by wildlife are urgently needed because forage quality influences herbivore behavior and populations, which can have cascading effects on ecosystem structure and function (Kielland et al., 2006; Schmitz et al., 2018).The third and fourth chapters of this dissertation explore the development of remote sensing approaches to characterize, monitor, and map forage quality in high latitude regions of Alaska.

In summary, my three research chapters add important information to a growing body of research on habitat changes or animal behavior in high northern latitudes. Such information may help inform future studies related to movement behaviors of heat-sensitive species and

monitoring and mapping forage quality across the landscape, which may contribute to sound policy and management plans.

Literature Cited

Beck, P. S. A., Goetz, S. J., Mack, M. C., Alexander, H. D., Jin, Y., Randerson, J. T., & Loranty, M. M. (2011). The impacts and implications of an intensifying fire regime on Alaskan boreal forest composition and albedo. *Global Change Biology*, *17*(9), 2853–2866.

Brinkman, T. J., Hansen, W. D., Chapin, F. S., Kofinas, G., BurnSilver, S., & Rupp, T. S. (2016). Arctic communities perceive climate impacts on access as a critical challenge to availability of subsistence resources. *Climatic Change*, *139*(3–4), 413–427.

Cold, H. S., Brinkman, T. J., Brown, C. L., Hollingsworth, T. N., Brown, D. R. N., & Heeringa, K. M. (2020). Assessing vulnerability of subsistence travel to effects of environmental change in interior Alaska. *Ecology and Society*, *25*(1).

De Long, J. R., Sundqvist, M. K., Gundale, M. J., Giesler, R., & Wardle, D. A. (2016). Effects of elevation and nitrogen and phosphorus fertilization on plant defence compounds in subarctic tundra heath vegetation. *Functional Ecology*, *30*(2), 314–325.

Demarchi, M. W., & Bunnell, F. L. (1995). Forest cover selection and activity of cow moose in summer. *Acta Theriologica*, *4*(1), 23–36.

Dussault, C., Ouellet, J.-P., Courtois, R., Huot, J., Breton, L., & Larochelle, J. (2004). Behavioural responses of moose to thermal conditions in the boreal forest. *Ecoscience 11*(3), 321–328).

Elmendorf, S. C., Henry, G. H. R., Hollister, R. D., Björk, R. G., Bjorkman, A. D., Callaghan, T. V., Collier, L. S., Cooper, E. J., Cornelissen, J. H. C., Day, T. A., Fosaa, A. M., Gould, W. A., Grétarsdóttir, J., Harte, J., Hermanutz, L., Hik, D. S., Hofgaard, A., Jarrad, F., Jónsdóttir, I. S., … Wookey, P. A. (2012). Global assessment of experimental climate warming on tundra vegetation: Heterogeneity over space and time. *Ecology Letters*, *15*(2), 164–175.

Fauchald, P., Park, T., Tømmervik, H., Myneni, R., & Hausner, V. H. (2017). Arctic greening from warming promotes declines in caribou populations. *Science Advances*, *3*(4). https://doi.org/10.1126/sciadv.1601365

Hansen, A. H., Jonasson, S., Michelsen, A., & Julkunen-Tiitto, R. (2006). Long-term experimental warming, shading and nutrient addition affect the concentration of phenolic compounds in arctic-alpine deciduous and evergreen dwarf shrubs. *Oecologia*, *147*(1), 1–11.

Johnson, D. H. (1980). The comparison of usage and availability measurements for evaluating resource preference. *Ecology*, *61*(1), 65–71.

Kasischke, E. S., Hayes, D. J., Billings, S., Boelman, N., Colt, S., Fisher, J., Goetz, S., Griffith, P., Grosse, G., Hall, F., Harriss, R., Karchut, J., Larson, E., Mack, M., McGuire, A. D., McLennan, D., Metsaranta, J., Miller, C., Rawlins, M., … Wullscheger, S. (2014). A concise experiment plan for the Arctic-Boreal Vulnerability Experiment. http://above.nasa.gov/acep/acep_final_pdf.pdf. Accessed 1/25/2015.

Kasischke, Eric S, & Turetsky, M. R. (2006). Recent changes in the fire regime across the North American boreal region—Spatial and temporal patterns of burning across Canada and Alaska. *Geophysical Research Letters*, *33*(9), L09703.

Kays, R., Crofoot, M. C., Jetz, W., & Wikelski, M. (2015). Terrestrial animal tracking as an eye on life and planet. *Science*, *348*(6240), aaa2478.

Kelly, R., Chipman, M. L., Higuera, P. E., Stefanova, I., Brubaker, L. B., & Sheng, F. (2013). Recent burning of boreal forests exceeds fire regime limits of the past 10,000 years. *Proceedings of the National Academy of Sciences*, *110*(32), 13055–13060.

Kielland, K., Bryant, J. P., & Ruess, R. W. (2006). Mammalian herbivory, ecosystem engineering, and ecological cascades in Alaskan boreal forest. In *Alaska's Changing Boreal Forest.* Edited by FS Chapin III, MW Oswood, K. Van Cleve, LA Viereck, and DL Verbyla. Oxford University Press, New York, 211–226.

Lenart, E. A., Bowyer, R. T., Hoef, J. Ver, & Ruess, R. W. (2002). Climate change and caribou: effects of summer weather on forage. *Canadian Journal of Zoology*, *80*(4), 664–678.

Lenarz, M. S., Fieberg, J., Schrage, M. W., & Edwards, A. J. (2010). Living on the Edge: Viability of Moose in Northeastern Minnesota. *Journal of Wildlife Management*, *74*(5), 1013–1023.

Macander, M. J., Palm, E. C., Frost, G. V, Herriges, J. D., Nelson, P., Roland, C., Russell, K. L. M., Suitor, M. J., Bentzen, T. W., Joly, K., Goetz, S., & Hebblewhite, M. (2020). Lichen cover mapping for caribou ranges in interior Alaska and Yukon. *Environmental Research Letters*, *15*(5), 055001.

Markon, C., Gray, S., Berman, M., Eerkes-Medrano, L., Hennessy, T., Huntigton, H., Littell, J., McCammon, M., Thoman, R., & Trainor, S. (2018). Alaska. In D. R. Reidmiller, C. W. Avery, D. R. Easterling, K. E. Kunkel, K. L. M. Lewis, T. K. Maycock, & B. C. Stewart (Eds.), *Impacts, Risks, and Adaptation in the United States: Fourth National Climate Assessment, Volume II* (pp. 11-85–1241).

Mawdsley, J. R., O'Malley, R., & Ojima, D. S. (2009). A review of climate-change adaptation strategies for wildlife management and biodiversity conservation. *Conservation Biology*, *23*(5), 1080–1089.

McCann, N. P., Moen, R. A., & Harris, T. R. (2013). Warm-season heat stress in moose (*Alces alces*). *Canadian Journal of Zoology*, *91*(12), 893-898.

Melin, M., Matala, J., Mehtätalo, L., Tiilikainen, R., Tikkanen, O. P., Maltamo, M., Pusenius, J., & Packalen, P. (2014). Moose (*Alces alces*) reacts to high summer temperatures by utilizing thermal shelters in boreal forests - an analysis based on airborne laser scanning of the canopy structure at moose locations. *Global Change Biology*, *20*(4), 1115–1125.

Merems, J. L., Shipley, L. A., Levi, T., Ruprecht, J., Clark, D. A., Wisdom, M. J., Jackson, N. J., Stewart, K. M., & Long, R. A. (2020). Nutritional-landscape models link habitat use to condition of mule deer (*Odocoileus hemionus*). *Frontiers in Ecology and Evolution*, *8*(98), 1–13.

Myers-Smith, I. H., Forbes, B. C., Wilmking, M., Hallinger, M., Lantz, T., Blok, D., Tape, K. D., Macias-fauria, M., Sass-klaassen, U., & Esther, L. (2011). Shrub expansion in tundra ecosystems: Dynamics, impacts and research priorities. *Environmental Research Letters*, *6*(4), 045509.

Parker, K. L., Barboza, P. S., & Michael, P. (2009). Nutrition integrates environmental responses of ungulates. *Functional Ecology*, *23*(1), 57–69.

Post, E., Forchhammer, M. C., Bret-harte, M. S., Callaghan, T. V, Christensen, T. R., Elberling, B., Fox, A. D., Gilg, O., Hik, D. S., Høye, T. T., Ims, R. A., Jeppesen, E., Klein, D. R., Madsen, J., Mcguire, A. D., Rysgaard, S., Schindler, D. E., Stirling, I., Tamstorf, M. P., … Aastrup, P. (2009). Ecological dynamics across the arctic associated with recent climate change. *Science*, *325*(5946), 1355-1358.

Renecker, L. A., & Hudson, R. J. (1986). Seasonal energy expenditures and thermoregulatory responses of moose. *Canadian Journal of Zoology*, *64*(2), 322–327.

Schmitz, O. J., Wilmers, C. C., Leroux, S. J., Doughty, C. E., Atwood, T. B., Galetti, M., Davies, A. B., & Goetz, S. J. (2018). Animals and the zoogeochemistry of the carbon cycle. *Science*, *362*(1127), 1–10.

Street, G. M., Rodgers, A. R., & Fryxell, J. M. (2015). Mid-day temperature variation influences seasonal habitat selection by moose. *Journal of Wildlife Management*, *79*(3), 505–512.

Sturm, M., Racine, C., Tape, K., Cronin, T. W., Caldwell, R. L., & Marshall, J. (2001). Increasing shrub abundance in the Arctic. *Nature*, *411*(6837), 546-547.

Tape, K. D., Gustine, D. D., Ruess, R. W., Adams, L. G., & Clark, J. A. (2016). Range expansion of moose in Arctic Alaska linked to warming and increased shrub habitat. *PLoS ONE*, *11*(7), 1–12.

Thompson, D. P., Barboza, P. S., Crouse, J. A., Mcdonough, T. J., Badajos, O. H., & Herberg, A. M. (2019). Body temperature patterns vary with day, season, and body condition of moose (*Alces alces*). *Journal of Mammalogy*, *100*(5), 1466–1478.

Turunen, M., Soppela, P., Kinnunen, H., Sutinen, M. L., & Martz, F. (2009). Does climate change influence the availability and quality of reindeer forage plants? *Polar Biology*, *32*(6), 813–832.

van Beest, F. M., Moorter, B. Van, & Milner, J. M. (2012). Temperature-mediated habitat use and selection by a heat-sensitive northern ungulate. *Animal Behaviour*, *84*(3), 723–735. https://doi.org/10.1016/j.anbehav.2012.06.032

Walther, G., Post, E., Convey, P., Menzel, A., Parmesan, C., Beebee, T. J. C., Fromentin, J., I, O. H., & Bairlein, F. (2002). Ecological responses to recent climate change. *Nature*, *416*(6879), 389–395.

Walton, K. M., Spalinger, D. E., Harris, N. R., Collins, W. B., & Willacker, J. J. (2013). High spatial resolution vegetation mapping for assessment of wildlife habitat. *Wildlife Society Bulletin*, *37*(4), 906–915.

Xue, J., & Su, B. (2017). Significant remote sensing vegetation indices: A review of developments and applications. *Journal of Sensors*.

Zhou, J., Tape, K. D., Prugh, L., Kofinas, G., Carroll, G., & Kielland, K. (2020). Enhanced shrub growth in the Arctic increases habitat connectivity for browsing herbivores. *Global Change Biology*, *26*, 3809–3820.

Chapter 2: Behavioral modifications by a large-northern herbivore to mitigate warming conditions

Authors: Jyoti S. Jennewein, Mark Hebblewhite, Peter Mahoney, Sophie Gilbert, Arjan J.H. Meddens, Natalie Boelman, Kyle Joly, Kim Jones, Kalin A. Kellie, Scott Brainerd, Lee A. Vierling, and Jan U.H. Eitel

Accepted for publication: *Movement Ecology*

Abstract

Temperatures in arctic-boreal regions are increasing rapidly and pose significant challenges to moose (*Alces alces*), a heat-sensitive large-bodied mammal. Moose act as ecosystem engineers, by regulating forest carbon and structure, below ground nitrogen cycling processes, and predator-prey dynamics. Previous studies showed that during hotter periods, moose displayed stronger selection for wetland habitats, taller and denser forest canopies, and minimized exposure to solar radiation. However, previous studies regarding moose behavioral thermoregulation occurred in Europe or southern moose range in North America. Understanding whether ambient temperature elicits a behavioral response in high-northern latitude moose populations in North America may be increasingly important as these arctic-boreal systems have been warming at a rate two to three times the global mean. We assessed how Alaska moose habitat selection changed as a function of ambient temperature using a step-selection function approach to identify habitat features important for behavioral thermoregulation in summer (June-August). We used Global Positioning System telemetry locations from four populations of Alaska moose (n=169) from 2008 to 2016. We assessed model fit using the quasi-likelihood under independence criterion and conduction a leave-one-out cross validation. Both male and female moose in all populations increasingly, and nonlinearly, selected for denser canopy cover as ambient temperature increased during summer, where initial increases in the conditional probability of selection were initially sharper then leveled out as canopy density increased above ~50%. However, the magnitude of selection response varied by population and sex. In two of the three populations containing both sexes, females demonstrated a stronger selection response for denser canopy at higher temperatures than males. We also observed a stronger selection response in the most southerly and northerly populations compared to populations in the west and central Alaska. The impacts of climate change in arctic-boreal regions increase landscape heterogeneity through

processes such as increased wildfire intensity and annual area burned, which may significantly alter the thermal environment available to an animal. Understanding habitat selection related to behavioral thermoregulation is a first step toward identifying areas capable of providing thermal relief for moose and other species impacted by climate change in arctic-boreal regions.

Introduction

Global temperatures are drastically increasing (Intergovernmental Panel on Climate Change [IPCC], 2014), which directly affect animal behavior and fitness (Brivio et al., 2019; van Beest et al., 2012; Walker et al., 2019). When ambient temperatures rise above an animal's thermal neutral zone, they use physiological and behavioral mechanisms to dissipate heat and mitigate thermal stress. For instance, additional energy may be spent to augment the cardiovascular and respiratory systems enabling evaporative cooling but may also lead to dehydration (Clarke & Rothery, 2008; McCann et al., 2013; Renecker & Hudson, 1986). Consequentially, increases in ambient temperature may contribute to a negative energy balance within an animal (Bourgoin et al., 2011; Timmermann & McNicol, 1988; van Beest & Milner, 2013). Energetic requirements of mammals vary by season and traits (e.g., body mass, lactation). Summer is an important season for mammals as they need to recover from winter food deficits, lactate and rear young, and store fat (Cameron et al., 1993; Rönnegård et al., 2002; Timmermann & McNicol, 1988). Climate change puts further stress on these important activities, which may, in turn, limit the ability of mammals to meet energetic requirements for reproduction and survival (Elmore et al., 2017; Lenarz et al., 2009; Vors & Boyce, 2009). Recent work suggests that large-bodied mammals respond more strongly to climate change, when compared to smaller-bodied mammals, through contraction or expansion of elevational ranges and also experience increased extinction risk (McCain & King, 2014).

Moose (*Alces alces*) are an important, large-bodied mammal vulnerable to increasing temperatures because they are well-adapted to cold climates (Renecker & Hudson, 1986; Schwartz & Renecker, 2007). Moose also act as ecosystem engineers, by regulating forest carbon and structure, below ground nitrogen cycling processes, and predator-prey dynamics (Bump et al., 2009; Christie et al., 2014; Kielland & Bryant, 1998; McLaren & Peterson, 1994). According to the seminal physiological study by Renecker and Hudson (1986), moose

reached their upper critical temperature threshold at 14°C in summer where they increased their heart and respiration rates, while open-mouthed panting began at 20°C. However, recent works call these thresholds into question and suggest there is no static temperature threshold where free-ranging moose become heat stressed (Thompson et al., 2019, 2020). Similarly, behavioral changes are often observed at temperatures that exceeds the upper critical summer threshold proposed by Renecker and Hudson (1986) (Broders et al., 2012; Melin et al., 2014).

Behavioral alterations elicited by changes in temperature influence both resource selection patterns and movement rates. For example, previous studies showed that during hotter periods, moose displayed stronger selection for riparian or wetland habitats (Renecker & Schwartz, 2007; Street et al., 2015), taller and denser forest canopies that provide thermal cover (Demarchi & Bunnell, 1995; Melin et al., 2014; van Beest et al., 2012), and minimized exposure to solar radiation (McCann et al., 2013). Additionally, moose may also decrease their activity and movement rates in response to warmer daytime temperatures (Montgomery et al., 2019; Street et al., 2015).

Moose thermoregulatory behaviors are indeed a 'hot topic' in applied ecology because of rising temperatures related to climate change and their important ecosystem role (e.g., Melin et al., 2014; Montgomery et al., 2019; Street et al., 2015). However, most previous studies occurred in Europe or the southern end of moose range in North America (Lenarz et al., 2009; Melin et al., 2014; van Beest et al., 2012). Understanding whether ambient temperature elicits a behavioral response in high-northern latitude (i.e., ≥ 60°N) moose populations in North America may be increasingly important as these arctic-boreal systems have been warming at a rate two to three times the global mean (Arctic Monitoring and Assessment Programme [AMAP], 2017; IPCC, 2014; Screen, 2014; Wolken et al., 2011) and current projections anticipate continued increases in temperature (IPCC, 2014; Markon et al., 2018). Thus, it is important to explore how movement patterns of moose, a heat-sensitive large-bodied mammal, are influenced by changes in temperature at the northern extent of their range.

Accordingly, our study objective was to assess Alaska moose (*Alces alces gigas*) habitat selection as a function of ambient temperature. We tested the hypothesis that moose modified resource selection in response to ambient temperature as predicted by physiological models. To accomplish this, we used Global Positioning System (GPS) -telemetry locations

from four Alaska moose populations (*n*=169 moose; Figure 2.1 & Table 2.1) from 2008 to 2016 that were located in four unique ecoregions (Nowacki et al., 2003). We combined moose GPS locations with remotely sensed products important to thermoregulatory behaviors. We analyzed only summer months (June-August) because of their importance in moose life history and because thermal stress is most likely to occur in summer (Dussault et al., 2004; van Beest et al., 2012). Each population was analyzed independently and separated into male and female subsets because fine-scale movements vary by sex and local habitat characteristics (Joly et al., 2015; Joly et al., 2016; Leblonde et al., 2010). We predicted that Alaska moose exhibit a detectable behavioral response to increasing summer temperatures, and, that as temperature increased moose would select for cooler locations, such as thermal refugia provided through increased canopy cover, areas closer to water, and/or low exposure to solar radiation.

Methods and Materials

Study areas

All four study areas span a mixture of subarctic and arctic boreal forest vegetation including black spruce (*Picea mariana*), alders (*Alnus* spp.), willows (*Salix* spp.), Alaska birch (*Betula neoalaskaa*), white spruce (*Picea glauca)*, quaking aspen (*Populus* tremuloides), and balsam poplar (*Populus balsmifera*). The upper Koyukuk region located in the Brooks Mountain Range (Figure 2.1) is rugged and varies from 500 to 2600 m above sea level (Alaska Department of Fish and Game [ADFG], 2006). Wildfire is common in this region, which experiences strongly continental climate patterns where summers are short, but temperatures can exceed 30°C (Joly et al., 2015). Average daily summer (June-August) temperature ranged from 7.5°C to 15°C from 1986 to 2016 (National Oceanic and Atmospheric Administration [NOAA], 2019). The Tanana Flats region is located south of Fairbanks, where the alluvial plane from the Alaska Mountain Range slopes northward making meandering rivers and oxbow lakes common (ADFG, 2006). Elevation ranges from 0 to 700m, however the highest elevations occurred in the northern portion of the Alaska Mountain Range (ADFG, 2006). The Tanana region experiences dry-continental climate, and average daily summer temperature ranged from 11°C to 19.5°C from 1986 to 2016 (NOAA, 2019). The Innoko region lies in southwest Alaska and includes a portion of the lower Yukon River. Meandering waterways, oxbow lakes and floods are common in the lowlands while upland areas experience more

wildfire disturbance (Paragi et al., 2017). Elevation varies little (30 – 850 m) and average daily summer temperatures ranged from 9.5°C to 17.5°C from 1989 to 2016 (NOAA, 2019). The Susitna moose range lies south of Alaska Mountain Range, and is characterized by numerous wetlands, hilly moraines, black spruce woodlands, and mountains. Elevation varies widely from 400 to 3500 m. This region is primarily located in temperate-continental climate, with some exposure to temperate coastal climates in the southern portion of the range (ADFG, 2006). Average daily summer temperatures ranged from 11.5°C to 19°C from 1988 to 2016 in this region (NOAA, 2019).

Moose Data

All capture protocols and handling protocols adhered to the Alaska Animal Care and Use Committee approval process (#07–11) as well as the Institutional Animal Care and Use Committee Protocol (#09-01). Moose in all regions were darted from helicopter (Robison R-44) and injected using carfentanil citrate (Wildnil® Wildlife Pharmaceuticals, Incorporated, Fort Collins, CO) and xylazine hydrochloride (Anaset ®; Lloyd Laboratories, Shenandoah, IA). Moose were instrumented with GPS radio-collars with three and a half to eight-hour fix rates (Table 2.1). Specifically, moose were fitted with the following collars from Telonics Inc. (Telonics, Mesa, AZ): Koyukuk – GW-4780, Tanana –TGW-4780-3, Susitna – TGW-4780-2, Innoko –CLM-340.

Statistical analyses

Habitat Selection

We used a step-selection function (SSF) to assess moose behavioral responses to changing temperatures. SSF's model habitat selection in a used-available design that accounts for changing availability of resources at any point in time (Fortin et al. 2005; Thurfjell et al. 2014). We aggregated moose datasets to a near eight-hour fix rate to enable regional comparisons of behavior (Table 2.1). We chose this modeling framework because it allows for assessments of fine-scale habitat selection, and the effect of temperature on large herbivore movement behavior are most pronounced at fine to intermediate spatial and temporal scales (van Beest et al., 2011). To sample availability, we generated ten-paired available locations based on empirical distributions of an individual's step length and turning angles between sampling intervals, which were estimated using the 'ABoVE-NASA' R package (Gurarie et al., 2018). We used conditional-logistic regression (CLR, Hosmer &

Lemeshow 2000) in the 'survival' R package (Therneau, 2015) to compare each used location with the concurrent available locations at the same point in time and space (i.e., one stratum contained one used point and ten randomly generated available points). The equation can be written as:

Equation 1. $w^*(\mathrm{x})=\frac{exp(\beta 1\mathrm{x}1+\beta 2\mathrm{x}2+\cdots+\beta \mathrm{nxn}+e)}{1+exp(\beta 1\mathrm{x}1+\beta 2\mathrm{x}2+\cdots+\beta \mathrm{nxn}+e)}$

where $w^*(x)$, the relative probability of selection, is dependent on habitat covariates X_1 through X_n, and their estimated regression coefficients $\beta 1$ to βn, respectively. Steps with higher $w^*(x)$ indicate a greater chance of selection. CLR compares strata (i.e., one used point and ten available points) individually, which enabled us to assess selection of fine-scale habitat features rather than broader-scale landscape characteristics (Boyce, 2006). We did not directly incorporate random effects into our SSF models as the analytical techniques for doing this are sparse and often computationally prohibitive for complex model sets (Muff et al., 2020). In our models, we would have a needed to incorporate a random effect of individual for each covariate in the model – the equivalent of random slopes. We believe this would likely have led to convergence issues as our models are already complex (see section regarding temperature interaction terms). Instead, we fit our CLR models with generalized estimating equations (GEE) using a clustering variable of "animal-year" to split the data into statistically independent clusters. This allowed us to account for lack of independence between steps within an individual for a given summer, and provided unbiased (i.e., robust) variance estimates provided there are at least 20 independent clusters and preferably 30 (Prima et al., 2017). Our data all had at least 20 unique animal year clusters, and all but one had greater than 30 (Table 2.1).

Habitat covariates

We obtained temperature estimates from the North American Regional Reanalysis (NARR) as opposed to weather stations. NARR provides a suite of highly-temporally dynamic (eight times daily; 32 km) set of meteorological variables (Mesinger et al., 2006). We annotated NARR temperature estimates using the environmental-data automated track annotation (Env-DATA) system available from Movebank (Dodge et al., 2013). To ensure accuracy of these temperature estimates, we performed a validation exercise on the two populations of moose which included temperature sensors on their collars (Innoko and Koyukuk). We found a moderate relationship between the two (Appendix 1.1 (A1.1); R^2=

0.47 – 0.58, RMSE= 3.88 – 4.43°C). NARR temperature estimates represent an ambient, neighborhood temperature, allowing us to investigate how moose respond to ambient variation in temperature via fine-scale selection for environmental characteristics that are likely to create cooler microclimates. We excluded ambient temperature as a main effect within CLR models because it did not vary within strata, and only included it as an interaction term with other covariates.

Moose may move to areas that provide thermal cover when temperatures increase such as denser canopied forests (Melin et al., 2014). In our models, a United States Geological Survey (USGS) percent canopy product for 2010 (30 m cell size, Hansen et al., 2013) was used as an index of thermal cover. Moose use canopy cover for purposes other than thermoregulation such as predator avoidance (Timmermann & McNicol, 1988). However, by considering the interaction between temperature and canopy cover, it is likely that we captured behavioral thermoregulation in our models.

We assessed the importance of water habitats in behavioral thermoregulation using a distance-to-water covariate. We estimated this covariate from Pekel and colleague's (2016) percent global surface water map, which quantified global surface water from 1984 to 2015. We used the R 'raster' package (Hijmans, 2019) to estimate the Euclidian distance of the nearest water pixel (30m cell size) from a given moose location. Elevation estimations (in meters) were extracted from the ArcticDEM (version 6, 5m cell size; Porter et al., 2018). The solar radiation index (SRI; Keating et al., 2007) was estimated mathematically as a function of latitude, aspect, and slope using the 'RSAGA' package (Brenning, 2008) – which were derived from the ArcticDEM, with the resultant values representing the hourly extraterrestrial radiation striking an arbitrarily oriented surface (Keating et al., 2007).

We chose to consider only continuous covariates as predictors to represent habitat as dynamic and continuous (*sensu* Coops & Wulder, 2019). Covariates were standardized by dividing them by two times their standard deviation (Gelman, 2008), allowing coefficients to be directly comparable across models. Collinearity was assessed using Pearson correlation coefficients, if correlation coefficients between predictors exceeded 0.70 we excluded collinear metrics from being present in the same model (Dormann et al., 2013).

Two-way temperature interactions

We considered both linear and nonlinear interactions between habitat covariates and ambient temperature as nonlinear processes are widespread in ecology particularly in response to climate change (Burkett et al., 2005; Walther, 2010). In total, three model variants for each population-sex partition were considered: (1) a *base model* that included habitat covariates as described above with no interaction terms or consideration of temperature, (2) *linear interaction models* where habitat covariates sequentially interacted with temperature linearly, and (3) *spline interaction models* where habitat covariates sequentially interacted nonlinearly with temperature using natural cubic splines. Because nonlinear terms are at risk of overfitting models, we constrained any nonlinear relationships explored in the spline interactions to two or three knots in CLR models using the 'splines' package (R Core Team, 2019).

Habitat selection model evaluation and validation

We evaluated model fit for each population-sex partition using the quasi-likelihood under independence criterion (QIC; Pan, 2001) because it is well suited for case-control models (Craiu et al. 2008). Finally, predictive ability of model variants were assessed using leave-one-out cross validation (LOOCV), which is a k-fold cross validation variant (Boyce et al., 2002) where each individual animal is sequentially left out and predicted based on the remaining data. Mean Spearman rank coefficients were used to determine the predictive ability of model variants. For each population-sex partition, the model with the highest correlation coefficients from LOOCV and lowest QIC was considered the best. All spatial processing and statistical analyses were conducted in the statistical software R version 3.6.1 (R Core Team, 2019).

Results

In total seven base, 28 linear interaction, and 28 spline interaction models were estimated. For the sake of parsimony, only the most biologically significant results are presented and summarized by sex and population. Elevation was collinear with distance-to-water in the Innoko population, we retained the latter because of its known importance in moose ecology (Renecker & Schwartz, 2007; Street et al., 2015). In all but one case (Koyukuk males), spline-based models where percent canopy interacted with temperature outperformed linear interaction and base models and are thus the only models discussed (Table 2.2 and 2.3). In contrast to the strong habitat selection responses of moose for canopy cover, we did not find evidence for other behavioral thermoregulation strategies. For example, we found no support

that Alaska moose altered resource selection with increasing summer temperatures in response to topography (i.e., more northerly, cooler slopes), elevation (with the exception of one population), nor hydrology (i.e., by selecting to be closer to water).

Females

The best fit spline models across all four populations occurred when percent canopy interacted with temperature using two to three knots. These spline interaction models had significant improvements in model fit compared to both the base models (ΔQIC= -108 to -284; Table 2.2) and the linear interaction models (not shown). Cross validation scores for spline interaction models experienced small to moderate improvements when compared to the base model (ΔLOOCV= +1% to +10%; Table 2.3).

In summer, female moose in all four regions selected for increased canopy cover nonlinearly as temperature increased (Figure 2.2). However, the magnitude of the selection response to thermal cover was most pronounced in the most southerly region (Susitna; $\beta_{\%canopy1}$ = 33.90, p<0.001; $\beta_{\%canopy2}$ = 20.09, p<0.001; Table 4) as well as the most northerly region (Koyukuk; $\beta_{\%canopy1}$ =24.91, p<0.001; $\beta_{\%canopy2}$ =20. 03, p<0.001). Although the effect of canopy cover was reduced in both the Innoko moose ($\beta_{\%canopy1}$ = 14.82, p<0.001; $\beta_{\%canopy2}$ = 9.01, p<0.001) and the Tanana moose ($\beta_{\%canopy1}$ = 4.71, p<0.001; $\beta_{\%canopy2}$ = 8.97, $\beta_{\%canopy3}$ = 7.70, p<0.001), both populations still revealed highly statistically significant results indicating female moose selected nonlinearly for increased canopy cover as temperature increased.

Female moose in the Koyukuk and Susitna regions also showed an increased affinity for water demonstrated in the significant negative beta coefficients for the "distance-to-water" predictor (Table 2.4), suggesting that moose in these regions preferred to be closer to water. Additionally, we observed additional selection behaviors in the Innoko and Susitna female moose. Female moose in the Innoko population showed an avoidance of areas of high solar radiation (β_{SRI} = -0.18, p<0.001), while females in the Susitna population showed an avoidance of higher elevation locations ($\beta_{elevation}$= -1.21, p<0.001), but these results were independent of temperature.

Males

For males, the best fit spline models in the Susitna and Innoko populations were also from percent canopy interacted with temperature (ΔQIC= -142 and -97 respectively; Table

2.3). For the Koyukuk males, the best fit spline model came from elevation interacted with temperature, but males in this region also saw improved model fit from percent canopy interacted with temperature (ΔQIC= -54). Cross validation scores for spline interaction models (percent canopy interacted with temperature) in all three male populations experienced small to moderate increases when compared to the base model (ΔLOOCV= +3% to +6%).

Male moose in all three populations (no males were collared in the Tanana population, see Table 2.1) selected for increased canopy cover as temperature increased (Figure 2.3). However, like with the females, the response to selection of thermal cover was most pronounced in the most northerly region (Koyukuk; $\beta_{\%canopy1} = 27.84$, $p<0.001$; $\beta_{\%canopy2} = 24.30$, $p<0.001$; Table 2.5) as well as the most southerly region (Susitna; $\beta_{\%canopy1} = 22.51$, $p<0.001$; $\beta_{\%canopy2} =14.71$, $p<0.001$). The effect of canopy cover was reduced in the Innoko males ($\beta_{\%canopy1} = 13.02$, $p<0.001$; $\beta_{\%canopy2} = 8.50$, $p<0.001$), yet the results still revealed highly statistically significant results indicating moose selected for increased canopy cover as temperature increased.

Additionally, male moose in the Susitna population showed increased selection of locations closer to water and, like their female counterparts, avoided areas of higher elevation ($\beta_{elevation}= -1.11$, $p<0.001$). Similarly, Innoko males showed avoidance for areas with increased topographical solar radiation exposure ($\beta_{SRI} = -0.12$, $p<0.001$), but these selection behaviors were independent of temperature.

Discussion

Our results demonstrate that moose at the northern extent of their range altered habitat selection patterns in response to temperature. Across all populations and sexes, moose selected for denser canopy cover as temperature increased, which is consistent with previous studies (Demarchi & Bunnell, 1995; Melin et al., 2014; van Beest et al., 2012), and our prediction that moose would select cooler locations as ambient temperature increased.

Magnitude of selection response to temperature varied by sex and population

Our habitat selection results also demonstrated that the magnitude of moose selection for dense canopy cover at higher temperatures varied between populations and sexes (Figures 2.2 and 2.3; Tables 2.4 and 2.5). In two (Innoko and Susitna) of the three populations containing both male and female moose, females demonstrated a stronger selection response for denser

canopy at higher temperatures than males. This may be linked to calving and nursing demands on female moose (Speakman & Król, 2010) who may more strongly select for denser canopy cover to avoid spending calories to thermoregulate using physiological mechanisms. However, we were unable to distinguish between females with and without calves in this study. This likely influenced our results as females accompanied by their calves tend to increase selection for areas that provide cover for predator avoidance (Dussault et al., 2005; Joly et al., 2016) and drastically change their movements both before and after parturition (Testa et al., 2000).

We also considered whether population differences in selection strength may be related to the availability of thermal cover between regions (i.e., a functional response) where animals alter their habitat selection based on habitat availability (Arthur et al., 1996; Mysterud & Ims, 1998). However, our results cannot entirely be explained by a functional response in habitat selection for thermal cover. For example, the Koyukuk moose showed strong selection for thermal cover as temperature increased but also had the second lowest available canopy cover regionally (37.6%; A1.2). Thus, we do not think a functional response per se explains regional differences in the selection strength, rather we anticipate that it is likely a combination of environmental factors interacting in complex ways to create a suite of unique habitat differences across regions (A1.3). However, to fully understand functional responses in habitat selection one must also consider the different spatial scales of selection (Johnson, 1980; Mysterud & Ims, 1998), as such responses are often evaluated at the landscape or home range scale (Hansen et al., 2009; Hayes & Harestad, 2000; Hebblewhite et al., 2008; Moreau et al., 2012). Thus, the lack of functional response of moose to canopy cover in our study may be related to the fine-scale nature of our analytical framework and not an absence of a functional response of moose to thermal cover.

Implications of habitat selection results within a changing climate

The consistent patterns of resource selection for thermal refugia under increasing temperatures found in this study may have important implications for moose resilience in arctic-boreal landscapes responding to increased temperatures from global climate change. For instance, landscape changes associated with wildfire are generally reducing canopy cover from coniferous species, and annual area burned in North American boreal systems doubled in the last half century (Kasischke & Turetsky, 2006), which is strongly linked to climate and

annual weather patterns (Johnson, 1996; Kasischke et al., 2010). Vegetation in interior Alaska now has less older spruce forests, the most common thermal refugia by moose, and a greater proportion of early successional vegetation than before 1990 (Markon et al., 2018). Burn severity also plays a major role in how boreal forests recover after wildfire (Epting & Verbyla, 2005), where areas of low burn severity in black spruce stands tend to undergo self-replacement succession (Johnstone & Chapin, 2006) and areas of high burn severity favor relay succession of deciduous species over black spruce because of increased exposure of mineral soil and reduced seedbank availability (Johnstone, et al., 2010; Shenoy et al., 2011). For moose, such changes in habitat structure may provide new forage resources (Beck et al., 2011; Kelly et al., 2013), but also may limit the available thermal refugia needed for behavioral thermoregulation immediately after disturbance events prior to vegetation regeneration, or in late spring (March-April) prior to budburst when moose have not yet shed their winter coats.

Limitations and Future Work

Our results showed moose did not select for areas closer to water as temperature increased, which differ from previous observations where moose sought wetland or riparian areas to thermoregulate (Schwartz & Renecker, 2007; Street et al., 2015). We believe our results differed due to the spatial resolution (30m grid cell size) used to represent this behavioral strategy. This restricted detection of smaller aquatic microhabitats important to moose. Unfortunately, no finer-scale map currently exists and limited our ability to study selection for aquatic microhabitats, which may be especially relevant in flatter, more swamp-like areas such as the Tanana and Innoko regions.

Based on our results and limitations encountered we make three broad recommendations for future work regarding animal behavioral thermoregulation. First, future work should investigate the vulnerability and resilience of arctic-boreal animals to structural habitat changes as forage resources increase and thermal cover decreases (e.g., Mason et al., 2017; van Beest et al., 2012). For example, recent work on Alpine ibex (*Capra ibex*) – another heat-sensitive ungulate – indicates that male ibex response to minimize heat stress comes at the expense of optimal foraging (Brivio et al., 2019). Unfortunately, we did not have a detailed forage quality or biomass model calibrated for our study areas and hesitated to use categorical land cover maps because of criticisms regarding their use (Coops & Wulder,

2019). In Alaska, there is not a wide distinction between shrub classes in landcover maps that would enable us to determine if selected shrub habitats correspond to palatable species and foraging behavior. For instance, “shrub" in most vegetative classifications does not distinguish between shade forages (*Salicaceae, Betula neoalaskana)* and shade only (*Alnus*, B. *nana*) species, which is critical for parsing selection behavior. Moose maximize energy intake in the hottest parts of summer, so selection for forage biomass and quality plausibly overrides thermal stress and predation risk for a time. However, we were unable to directly assess this tradeoff due to data limitations.

Second, we suggest testing for differences in female selection and movement relative to presence or absence of offspring. Such a distinction would connect nicely to calls to link behavior and movement to population outcomes (Brodie et al., 2012; Morales et al., 2010) especially when considering the thermal environment as survival and fitness often depend on the availability of suitable habitat to buffer against thermal extremes in a landscape (Elmore et al., 2017).

Finally, a critical next step is to evaluate how habitat selection under thermal stress impacts individual fitness and population dynamics, as temperature plays an important role in limiting fecundity in other mammals (Corlatti et al., 2018; Wells et al., 2016) including moose (Lenarz et al., 2009; Murray et al., 2006). This is especially important as population responses to climate change can vary dramatically. For instance, Joly and colleagues (2011) found the influence of climate on caribou herds in Alaska was not uniform, instead, western populations increased in size while northwestern populations declined as a result of intensity changes in the Pacific Decadal Oscillation. Similarly, using detailed demographic information for caribou (*Rangifer tarandus*), red deer (*Cervus elaphus)*, and elk (*C. canadensis*) across the Northern Hemisphere, Post and colleagues (2009) showed that that different population responses to climate varied in both direction and magnitude.

Conclusion

The impacts of climate change in arctic-boreal regions increase landscape heterogeneity through processes such as increased wildfire intensity and area burned, which can significantly alter the thermal environment available to an animal. Despite recognizing the importance of thermal conditions to animals, there is a distinct lack of research on how animals might respond to climate driven changes in thermal refugia. Our regional assessment

provides insight on how Alaska moose may respond to changes in ambient temperature, where statewide annual temperatures are averaging an increase of 0.4ºC per decade and summer temperatures are projected to increase 2 – 5°C by midcentury (Markon et al., 2018). Understanding habitat selection and movement patterns related to behavioral thermoregulation is a first step toward identifying areas capable of providing thermal relief for moose and other species impacted by climate change.

Literature Cited

Alaska Department of Fish and Game (ADFG) (2006). Our Wealth Maintained: A Strategy for Conserving Alaska's Diverse Wildlife and Fish Resources. Alaska Department of Fish and Game, Juneau, Alaska. https://www.adfg.alaska.gov/static/species/wildlife_action_plan/cwcs_full_document.pdf. Accessed 3/25/2019.

Arctic Monitoring and Assessment Programme (AMAP). (2017). *Snow, Water, Ice, and Permafrost in the Arctic: Summary for Policy-makers*. Oslo, Norway. Retrieved from www.amap.no/swipa. Accessed 2/01/2017.

Arthur, S. M., Manly, B. F. J., & Garner, G. W. (1996). Assessing habitat selection when availability changes. *Ecology*, *77*(1), 215–227.

Beck, P. S. A., Goetz, S. J., Mack, M. C., Alexander, H. D., Jin, Y., Randerson, J. T., & Loranty, M. M. (2011). The impacts and implications of an intensifying fire regime on Alaskan boreal forest composition and albedo. *Global Change Biology*, *17*(9), 2853–2866.

Bourgoin, G., Garel, M., Blanchard, P., Dubray, D., Maillard, D., & Gaillard, J. M. (2011). Daily responses of mouflon (*Ovis gmelini musimon* × *Ovis* sp.) activity to summer climatic conditions. *NRC Research Press*, *89*(9), 765–773.

Boyce, M. S. (2006). Scale for resource selection functions. *Diversity and Distributions*, *12*(3), 269–276.

Boyce, M. S., Vernier, P. R., Nielsen, S. E., & Schmiegelow, F. K. A. (2002). Evaluating resource selection functions. *Ecological Modelling*, *157*(2-3), 281–300.

Brenning, A., 2008. Statistical geocomputing combining R and SAGA: The example of landslide susceptibility analysis with generalized additive models. In J. Boehner, T. Blaschke and L. Montanarella (eds.), SAGA - Seconds Out (= Hamburger Beitraege zur Physischen Geographie und Landschaftsoekologie, vol. 19), p. 23-32.

Brivio, F., Zurmühl, M., Grignolio, S., Hardenberg, J. Von, Apollonio, M., & Ciuti, S. (2019). Forecasting the response to global warming in a heat-sensitive species. *Scientific Reports*, *9*(3048), 1–16.

Brodie, J. F., Post, E. S., Doak, D. F. (2012). *Wildlife Conservation in a Changing Climate.* University of Chicago Press, Chicago, IL.

Broders, H. G., Coombs, A. B., & Mccarron, J. R. (2012). Ecothermic responses of moose (*Alces alces*) to thermoregulatory stress on mainland Nova Scotia. *Alces*, *48*, 53–61.

Bump, J. K., Webster, C. R., Vucetich, J. A., Rolf, O., Shields, J. M., & Powers, M. D. (2009). Ungulate carcasses perforate ecological filters and create biogeochemical hotspots in forest herbaceous layers allowing trees a competitive advantage. *Ecosystems*, *12*(6), 996–1007.

Burkett, V. R., Wilcox, D. A., Stottlemyer, R., Barrow, W., Fagre, D., Baron, J., … Doyle, T. (2005). Nonlinear dynamics in ecosystem response to climatic change: Case studies and policy implications. *Ecological Complexity*, *2*(4), 357–394.

Cameron, R. D., Smith, T., Fancy, S. G., Gerhart, K. L., & White, R. G. (1993). Calving success of female caribou in relation to body weight. *Canadian Journal of Zoology*, *71*(3), 480-486.

Christie, K. S., Ruess, R. W., Lindberg, M. S., & Mulder, C. P. (2014). Herbivores influence the growth, reproduction, and morphology of a widespread Arctic willow. *PLoS ONE*, *9*(7), 1–9.

Clarke, A., & Rothery, P. (2008). Scaling of body temperature in mammals and birds. *Functional Ecology*, *22*(1), 58–67.

Coops, N. C., & Wulder, M. A. (2019). Breaking the Habit(at). *Trends in Ecology & Evolution*, *34*(7), 585–587.

Corlatti, L., Gugiatti, A., Ferrari, N., Formenti, N., Trogu, T., & Pedrotti, L. (2018). The cooler the better? Indirect effect of spring–summer temperature on fecundity in a capital breeder. *Ecosphere*, *9*(6), 1–13.

Craiu, R. V., Duchesne T., & Fortin, D.(2008). Inference methods for the conditional logistic regression model with longitudinal data. *Biometrical Journal, 50*(1), 97–109.

Demarchi, M. W., & Bunnell, F. L. (1995). Forest cover selection and activity of cow moose in summer. *Acta Theriologica*, *4*(1), 23–36.

Dodge, S., Bohrer, G., Weinzierl, R., Davidson, S., Kays, R., Douglas, D., … Wikelski, M. (2013). The environmental-data automated track annotation (Env-DATA) system: Linking animal tracks with environmental data. *Movement Ecology, 1*(1), 3.

Dormann, C. F., Elith, J., Bacher, S., Buchmann, C., Carl, G., Carr, G., … Lautenbach, S. (2013). Collinearity: A review of methods to deal with it and a simulation study evaluating their performance. *Ecography*, *36*(1), 27–46.

Dussault, C., Ouellet, J.-P., Courtois, R., Huot, J., Breton, L., & Larochelle, J. (2004). Behavioural responses of moose to thermal conditions in the boreal forest. *Ecoscience, 11(3), 321-328.*

Dussault, C., Ouellet, J., Courtois, R., Huot, J., Breton, L., & Jolicoeur, H. (2005). Linking moose habitat selection to limiting factors. *Ecography*, *28*(5), 619–628.

Elmore, R. D., Carroll, J. M., Tanner, E. P., Hovick, T. J., Grisham, B. A., Fuhlendorf, S. D., & Windels, S. K. (2017). Implications of the thermal environment for terrestrial wildlife management. *Wildlife Society Bulletin*, *41*(2), 183–193.

Epting, J., & Verbyla, D. (2005). Landscape-level interactions of prefire vegetation , burn severity, and postfire vegetation over a 16-year period in interior Alaska. *Canadian Journal of Forest Research*, *35*(6), 1367–1377.

Fortin, D., Beyer, H. L., Boyce, M. S., Smith, D. W., Duchesne, T., & Mao, J. S. (2005). Wolves influence elk movements: Behavior shapes a trophic cascade in Yellowstone National Park. *Ecology*, *86*(5), 1320–1330.

Gelman, A. (2008). Scaling regression inputs by dividing by two standard deviations. *Statistics in Medicine*, *27*(15), 2865–2873. https://doi.org/10.1002/sim.3107

Gurarie, E., Mahoney, P., LaPoint, S., & Davidson, S. (2018). above: Functions and methods for the Animals on the Move project of the Arctic Boreal Vulnerability Experiment (ABoVE - NASA). R package version 0.11.

Hansen, B. B., Herfindal, I., Aanes, R., Sæther, B.-E., & Henriksen, S. (2009). Functional response in habitat selection and the tradeoffs between foraging niche components in a large herbivore. *Nordic Society Oikos*, *118*(6), 859–872.

Hansen, M.C., Potapov, P.V., Moore, R., Hancher, M., Turubanova, S.A., Tyukavina, A., Thau, D., Stehman, S.V., Goetz, S.J., Loveland, T.R., Kommareddy, A., Egorov, A., Chini, L., Justice, C.O., and Townshend, J.R.G. (2013). High-resolution global maps of forest cover change. *Science*, *342*(6160), 850–853.

Hayes, R. D., & Harestad, A. S. (2000). Wolf functional response and regulation of moose in the Yukon. *Canadian Journal of Zoology*, *78*(1), 60–66.

Hebblewhite, M., & Merrill, E. (2008). Modelling wildlife-human relationships for social species with mixed-effects resource selection models. *Journal of Applied Ecology*, *45*(3), 834–844.

Hijmans R. J. (2019). raster: Geographic Data Analysis and Modeling. R package version 3.0-2. https://CRAN.R-project.org/package=raster

Hosmer, D. W., & Lemeshow, S. (2000). *Applied Logistic Regression* (2nd ed.). John Wiley & Sons, Inc, New York, NY.

Intergovernmental Panel on Climate Change (IPCC), (2014). *Climate Change 2014: Synthesis Report*. Contribution of Working Groups I, II and III to the Fifth Assessment Report of the Intergovernmental Panel on Climate Change [Core Writing Team, R.K. Pachauri and L.A. Meyer (eds.)]. IPCC, Geneva, Switzerland.

Johnson, E. A. (1996). *Fire and vegetation dynamics: Studies from the North American boreal forest*. Cambridge University Press, Great Britian.

Johnson, D. H. (1980). The comparison of usage and availability measurements for evaluating resource preference. *Ecology*, *61*(1), 65–71.

Johnstone, J. F., & Chapin, F. S. III. (2006). Fire interval effects on successional trajectory in boreal forests of northwest Canada. *Ecosystems*, *9*(2), 268–277.

Johnstone, J. F., Hollingsworth, T. N., Chapin, F. S. III., & Mack, M. C. (2010). Changes in fire regime break the legacy lock on successional trajectories in Alaskan boreal forest. *Global Change Biology*, *16*(4), 1281–1295. https://doi.org/10.1111/j.1365-2486.2009.02051.x

Joly, K., Craig, T., Sorum, M. S., McMillan, J. S., & Spindler, M. A. (2015). Variation in fine-scale movements of moose in the upper Koyukuk River drainage, northcentral Alaska. *Alces*, *51*, 97–105.

Joly, K., Klein, D. R., Verbyla, D. L., Rupp, T. S., & Chapin III, F. S. (2011). Linkages between large-scale climate patterns and the dynamics of Arctic caribou populations. *Ecography*, *34*(2), 345–352.

Joly, K., Sorum, M. S., Craig, T., & Julianus, E. L. (2016). The effects of sex, terrain, wildfire, winter severity, and maternal status on habitat selection by moose in north-central Alaska. *Alces*, *52*, 101–115.

Kasischke, E. S., & Turetsky, M. R. (2006). Recent changes in the fire regime across the North American boreal region — Spatial and temporal patterns of burning across Canada and Alaska. *Geophysical research letters, 33(9),* L09703.

Kasischke, E. S., Verbyla, D. L., Rupp, T. S., McGuire, A. D., Murphy, K. A., Jandt, R., … Turetsky, M. R. (2010). Alaska's changing fire regime — implications for the vulnerability of its boreal forests 1. *Candian Journal of Forest Research*, *40*(7), 1313–1324.

Keating, K. A., Gogan, P. J. P., Vore, J. M., & Irby, L. (2007). A simple solar radiation index for wildlife habitat studies. *Journal of Wildlife Management*, *71*(4), 1344–1348.

Kelly, R., Chipman, M. L., Higuera, P. E., Stefanova, I., Brubaker, L. B., & Sheng, F. (2013). Recent burning of boreal forests exceeds fire regime limits of the past 10,000 years. *Proceedings of the National Academy of Sciences*, *110*(32), 13055–13060.

Kielland, K., & Bryant, J. P. (1998). Moose herbivory in Taiga: Effects on biogeochemistry and vegetation dynamics in primary succession. *Oikos 82*(2), 377–383.

Leblond, M., Dussault, C., & Ouellet, J. P. (2010). What drives fine-scale movements of large herbivores? A case study using moose. *Ecography*, *33*(6), 1102–1112.

Lenarz, M. S., Nelson, M. E., Schrage, M. W., & Edwards, A. J. (2009). Temperature mediated moose survival in northeastern Minnesota. *Journal of Wildlife Management*, *73*(4), 503–510.

Markon, C., Gray, S., Berman, M., Eerkes-Medrano, L., Hennessy, T., Huntington, H., … Trainor, S. (2018). Alaska. In D. R. Reidmiller, C. W. Avery, D. R. Easterling, K. E. Kunkel, K. L. M. Lewis, T. K. Maycock, & B. C. Stewart (Eds.), *Impacts, Risks, and Adaptation in the United States: Fourth National Climate Assessment, Volume II* (pp. 11-85–1241). US Global Change Research Program, Washington, DC, USA.

McCain, C. M., & King, S. R. B. (2014). Body size and activity times mediate mammalian responses to climate change. *Global Change Biology*, *20*(6), 1760–1769.

McCann, N. P., Moen, R. A., & Harris, T. R. (2013). Warm-season heat stress in moose (*Alces alces*). *Canadian Journal of Zoology*, *91*(12), 893–898.

McLaren, B. E., & Peterson, R. O. (1994). Wolves, moose, and tree rings on Isle Royale. *Science*, *266*(5190), 1555–1558.

Melin, M., Matala, J., Mehtätalo, L., Tiilikainen, R., Tikkanen, O. P., Maltamo, M., … Packalen, P. (2014). Moose (*Alces alces*) reacts to high summer temperatures by utilizing thermal shelters in boreal forests - an analysis based on airborne laser scanning of the canopy structure at moose locations. *Global Change Biology*, *20*(4), 1115–1125.

Mesinger, F. M., DiMego, G., Kalnay, E., Mitchell, K., Shafran, P. C., Ebiuzaki, W., … Shi, W. (2006). North american regional reanalysis. *American Meterological Society*, *87*(3), 343-360.

Montgomery, R. A., Redilla, K. M., Moll, R. J., Moorter, B. Van, Rolandsen, C. M., Millspaugh, J. J., & Solberg, E. J. (2019). Movement modeling reveals the complex nature of the response of moose to ambient temperatures during summer. *Journal of Mammalogy*, *100*(1), 169-177.

Morales, J. M., Moorcroft, P. R., Matthiopoulos, J., Frair, J. L., Kie, J. G., Powell, R. A., … Haydon, D. T. (2010). Building the bridge between animal movement and population dynamics. *Philosophical Transactions of the Royal Society B: Biological Sciences*, *365*(1550), 2289–2301.

Moreau, G., Fortin, D., Couturier, S., & Duchesne, T. (2012). Multi-level functional responses for wildlife conservation: The case of threatened caribou in managed boreal forests. *Journal of Applied Ecology*, *49*(3), 611–620.

Muff, S., Signer, J., & Fieberg, J. (2020). Accounting for individual-specific variation in habitat-selection studies: Efficient estimation of mixed-effects models using Bayesian or frequentist computation. *Journal of Animal Ecology*, *89*(1), 80–92.

Murray, D. L., Cox, E. W., Ballard, W. B., Whitlaw, H. A., Lenarz, M. S., Custer, T. W., … Fuller, T. K. (2006). Pathogens, nutritional deficiency, and climate influences on a declining moose population. *Wildlife Monographs*, *166*(1), 1-30.

Mysterud, A., & Ims, R. (1998). Functional responses in habitat use: Availability influences relative use in trade-off situations. *Ecology*, *79*(4), 1435–1441.

National Oceanic and Atmospheric Administration (NOAA). (2019). National Centers for Environmental Information, temperature summaries. [FIPS:02]. Retrieved from https://www.ncdc.noaa.gov/cdo-web/search, Accessed 1/6/2020.

Nowacki, G. J., P. Spencer, M. Fleming, and T. Jorgenson (2003), Unified ecoregions of Alaska, *U.S. Geol. Surv. Open File Rep.*, *02-297* (map). https://pubs.er.usgs.gov/publication/ofr2002297

Pan, W. (2001). Akaike's information criterion in generalized estimating equations. *Biometrics*, *57*(1), 120– 125.

Paragi, T. F., Kellie, K. A., Peirce, J. M., & Warren, M. J. (2017). *Movements and Sightability of Moose in Game Management Unit 21E*. Alaska Department of Fish and Game, Juneau.

Pekel, J. F., Cottam, A., Gorelick, N., & Belward, A. S. (2016). High-resolution mapping of global surface water and its long-term changes. *Nature*, *540*(7633), 418–422.

Porter, Claire, Morin, Paul; Howat, Ian; Noh, Myoung-Jon; Bates, Brian; Peterman, Kenneth; Keesey, Scott; Schlenk, Matthew; Gardiner, Judith; Tomko, Karen; Willis, Michael; Kelleher, Cole; Cloutier, Michael; Husby, Eric; Foga, Steven; Nakamura, Hitomi; Platson, Melisa; Wethington, Michael, Jr.; Williamson, Cathleen; Bauer, Gregory; Enos, Jeremy; Arnold, Galen; Kramer, William; Becker, Peter; Doshi, Abhijit; D'Souza, Cristelle; Cummens, Pat; Laurier, Fabien; Bojesen, Mikkel, 2018, "ArcticDEM", https://doi.org/10.7910/DVN/OHHUKH, Harvard Dataverse, V1, 2018, Accessed 10/1/2018.

Post, E., Brodie, J., Hebblewhite, M., Anders, A. D., Maier, J. A. K., & Wilmers, C. C. (2009). Global population dynamics and hot spots of response to climate change. *Bioscience*, *59*(6), 489–497.

Prima, M. C., Duchesne, T., & Fortin, D. (2017). Robust inference from conditional logistic regression applied to movement and habitat selection analysis. *PLoS ONE*, *12*(1), 1–13.

R Core Team (2019). R: A language and environment for statistical computing. R Foundation for Statistical Computing, Vienna, Austria. URL https://www.R-project.org/

Renecker, L. A., & Hudson, R. J. (1986). Seasonal energy expenditures and thermoregulatory responses of moose. *Canadian Journal of Zoology*, *64*(2), 322–327.

Renecker L. A., & Schwartz, C. C. (2007). Food Habits and Feeding Behavior. In: *Ecology and Management of the North American Moose*, 2nd Edition, Franzmann & Schwartz C. C. (Eds). Wildlife Management Institutions, 403-439.

Rönnegård, L., Forslund, P., & Danell, Ö. (2002). Lifetime patterns in adult female mass, reproduction, and offspring mass in semidomestic reindeer (*Rangifer tarandus tarandus*). *Canadian Journal of Zoology*, *80*(12), 2047–2055. https://doi.org/10.1139/Z02-192

Schwartz, C. C., & Renecker L. A. (2007). Nutrition and Energetics. In: *Ecology and Management of the North American Moose*, 2nd Edition, Franzmann & Schwartz C. C. (Eds). Wildlife Management Institutions, 441-478.

Screen, J. A. (2014). Arctic amplification decreases temperature variance in northern mid- to high-latitudes. *Nature Climate Change*, *4*(7), 577–582.

Shenoy, A., Johnstone, J. F., Kasischke, E. S., & Kielland, K. (2011). Persistent effects of fire severity on early successional forests in interior Alaska. *Forest Ecology and Management*, *261*(3), 381–390.

Speakman, J. R., & Król, E. (2010). Maximal heat dissipation capacity and hyperthermia risk: Neglected key factors in the ecology of endotherms. *Journal of Animal Ecology*, *79*(4), 726–746.

Street, G. M., Rodgers, A. R., & Fryxell, J. M. (2015). Mid-day temperature variation influences seasonal habitat selection by moose. *Journal of Wildlife Management*, *79*(3), 505–512.

Testa, J. W., Becker, E. F., & Lee, G. R. (2000). Movements of female moose in relation to birth and death of calves. *Alces*, *36*, 155–162.

Therneau T. (2015). A Package for Survival Analysis in S. version 2.38, https://CRAN.R-project.org/package=survival.

Timmermann, H. R., & McNicol, J. G. (1988). Moose habitat needs. *The Forestry Chronicle*, *64*(3), 238-245.

Thompson, D. P., Barboza, P. S., Crouse, J. A., McDonough, T. J., Badajos, O. H., & Herberg, A. M. (2019). Body temperature patterns vary with day, season, and body condition of moose (*Alces alces*). *Journal of Mammalogy*, *100*(5), 1466-1478.

Thompson, D. P., Crouse, J. A., Jaques, S., & Barboza, P. S. (2020). Redefining physiological responses of moose (*Alces alces*) to warm environmental conditions. Journal of Thermal Biology, 102581.

Thurfjell, H., Ciuti, S., & Boyce, M. S. (2014). Applications of step-selection functions in ecology and conservation. *Movement Ecology*, *2*(4), 1–12.

van Beest, F. M., & Milner, J. M. (2013). Behavioural responses to thermal conditions affect seasonal mass change in a heat-sensitive northern ungulate. *PloS one, 8*(6), e65972.

van Beest, F. M., Moorter, B. Van, & Milner, J. M. (2012). Temperature-mediated habitat use and selection by a heat-sensitive northern ungulate. *Animal Behaviour*, *84*(3), 723–735.

van Beest, F. M., Rivrud, I. M., Loe, L. E., Milner, J. M., & Mysterud, A. (2011). What determines variation in home range size across spatiotemporal scales in a large browsing herbivore? *Journal of Animal Ecology*, *80*(4), 771–785.

Vors, L. S., & Boyce, M. S. (2009). Global declines of caribou and reindeer. *Global Change Biology*, *15*(11), 2626–2633.

Walker, W. H., Meléndez-Fernández, O. H., Nelson, R. J., & Reiter, R. J. (2019). Global climate change and invariable photoperiods: A mismatch that jeopardizes animal fitness. *Ecology and Evolution*, *9*(17), 10044–10054.

Walther, G. R. (2010). Community and ecosystem responses to recent climate change. *Philosophical Transactions of the Royal Society B: Biological Sciences*, *365*(1549), 2019–2024.

Wells, K., O'Hara, R. B., Cooke, B. D., Mutze, G. J., Prowse, T. A. A., & Fordham, D. A. (2016). Environmental effects and individual body condition drive seasonal fecundity of rabbits: identifying acute and lagged processes. *Oecologia, 181*(3), 853–864.

Wolken, J. M., Hollingsworth, T. N., Rupp, T. S., Chapin, F. S., Trainor, S. F., Barrett, T. M., … Yarie, J. (2011). Evidence and implications of recent and projected climate change in Alaska's forest ecosystems. *Ecosphere*, *2*(11), 1-35.

Tables

Table 2.1. Summaries of Alaska moose (*Alces alces gigas*) Global Positioning System (GPS) datasets by study area. Information on the number of fixes and the fix success rate are specific to summer (June 1 – August 31). The number of clusters for each population-sex partition refer to the unique combination of individual-year, which were used in our conditional logistic regression models as a clustering variable for estimating robust variance estimates using generalized estimating equations.

Dataset	Number of moose	Number females (clusters)	Number males (clusters)	Years	Fix rate (hours)	Fix success	Number of fixes
Koyukuk	30	19 (45)	11 (22)	2008-2013	8	91%	F- 11,324 M- 3,949
Susitna	61	38 (71)	23 (36)	2012-2016	8	98%	F- 14,984 M-6,003
Innoko	45	21 (63)	24 (65)	2010-2014	4*	95%	F- 2,319 M- 1,987
Tanana	33	33 (145)	0	2011-2016	3.5*	99%	F- 21,530
Totals:	169	111	58	-	-	96%	F-50,157 M- 11,939

* data with less than 8-hour fix rates were aggregated to near 8-hour fix rates

Table 2.2. Model evaluation (QIC) and cross validation (LOOCV) for female moose organized by population**.** Base models contain no temperature covariates, while spline models incorporate nonlinear interactions between a given covariate and ambient temperature. In this case, "Spline %can2" refers to percent canopy interacted with ambient temperature with two spline segments, while "Spline %can3" refers to percent canopy interacted with ambient temperature with three spline segments. Decreases in QIC indicate a better model fit while increases in LOOCV indicate more predictive ability.

	Koyukuk		**Susitna**		**Innoko**		**Tanana**	
	Base	*Spline %can2*	*Base*	*Spline %can2*	*Base*	*Spline %can2*	*Base*	*Spline %can3*
QIC	47,070	46,918	70,707	70,423	73,361	73,184	102,854	102,746
ΔQIC	-	-152	-	-284	-	-177	-	-108
LOOCV	68%	69%	62%	64%	60%	63%	36%	46%
ΔLOOCV	-	+1%	-	+2%	-	+3%	-	+10%

Note: %can= percent canopy cover

Table 2.3. Model evaluation (QIC) and cross validation (LOOCV) for male moose summary of organized by population. See additional descriptors in Table 3.

	Koyukuk		**Susitna**		**Innoko**	
	Base	*Spline %can2*	*Base*	*Spline %can2*	*Base*	*Spline %can2*
QIC	18,583	18,529	27,919	27,777	62,946	62,849
ΔQIC	-	-54	-	-142	-	-97
LOOCV	42%	45%	57%	62%	50%	56%
ΔLOOCV	-	+3%	-	+5%	-	+6%

Table 2.4. Best habitat selection models by population for female moose (*Alces alces gigas*) in Alaska from the step-selection function analysis. The best models across all four populations occurred when percent canopy interacted with temperature nonlinearly and are presented here. Natural spline (sp) predictors, where percent canopy interacted with temperature, have coefficients estimated for each line segment. Therefore, numbers one through three in the spline predictor terms represent an individual line segment. Only one of four populations (Tanana) has a third set of coefficients. In the Innoko population, elevation was collinear with distance-to-water and was thus excluded. All predictors were standardized by dividing by two times their standard deviation, making coefficients directly comparable. Robust standard errors are reported.

	Population			
	Koyukuk	**Susitna**	**Innoko**	**Tanana**
Predictor	Coefficient (SE)	Coefficient (SE)	Coefficient (SE)	Coefficient (SE)
Elevation	0.09 (0.16)	-1.21 (0.25)***	NA	0.28 (0.39)
sp(Percent Canopy x Temperature) 1	24.91 (3.7)***	33.90 (3.1)***	14.82 (3.32)***	4.71 (1.07)***
sp(Percent Canopy x Temperature)2	20. 03 (3.1)***	20.09 (1.9)***	9.01 (2.14)***	8.97 (2.22)***
sp(Percent Canopy x Temperature)3	NA	NA	NA	7.70 (1.97)***
Percent Canopy	-13.90 (2.2)***	-16.60 (1.6)***	-7.90 (1.92)***	-4.80(1.21)***
Solar Radiation Index	0.02 (0.02)	0.003 (0.02)	-0.18 (0.02)***	-0.0006 (0.02)
Distance-to-Water	-0.66 (0.3)*	-0.48 (0.09)***	-0.22 (0.16)	-0.09 (0.07)

*0.05; **0.01; ***0.001

Table 2.5. Best habitat selection models for male Alaska moose from the step-selection function analysis. Natural spline (sp) predictors, where percent canopy interacted with temperature, have coefficients estimated for each line segment. Numbers one and two in the spline predictors represent an individual line segment. All three populations had temperature-canopy interactions with two-line segments. In the Innoko population, elevation was collinear with distance-to-water and was thus excluded. All predictors were standardized by dividing by two times their standard deviation. Robust standard errors are reported.

	Population		
	Koyukuk	**Susitna**	**Innoko**
Predictor	Coefficient (SE)	Coefficient (SE)	Coefficient (SE)
Elevation	-0.45 (0.37)	-1.11 (0.28)***	NA
sp(Percent Canopy * Temperature)1	27.84 (4.6)***	22.51 (5.5)***	13.02 (3.3)***
sp(Percent Canopy * Temperature)2	24.30 (4.1)***	14.71 (3.8)***	8.50 (2.4)***
Percent Canopy	-16.63 (2.9)***	-11.81 (3.1)***	-17.60 (2.04)***
Solar Radiation Index	0.02 (0.03)	-0.005 (0.003)	-0.12 (0.02)***
Distance-to-Water	0.34 (0.31)	-0.59 (0.11)***	-0.02 (0.33)

*0.05; **0.01; ***0.001

Figures

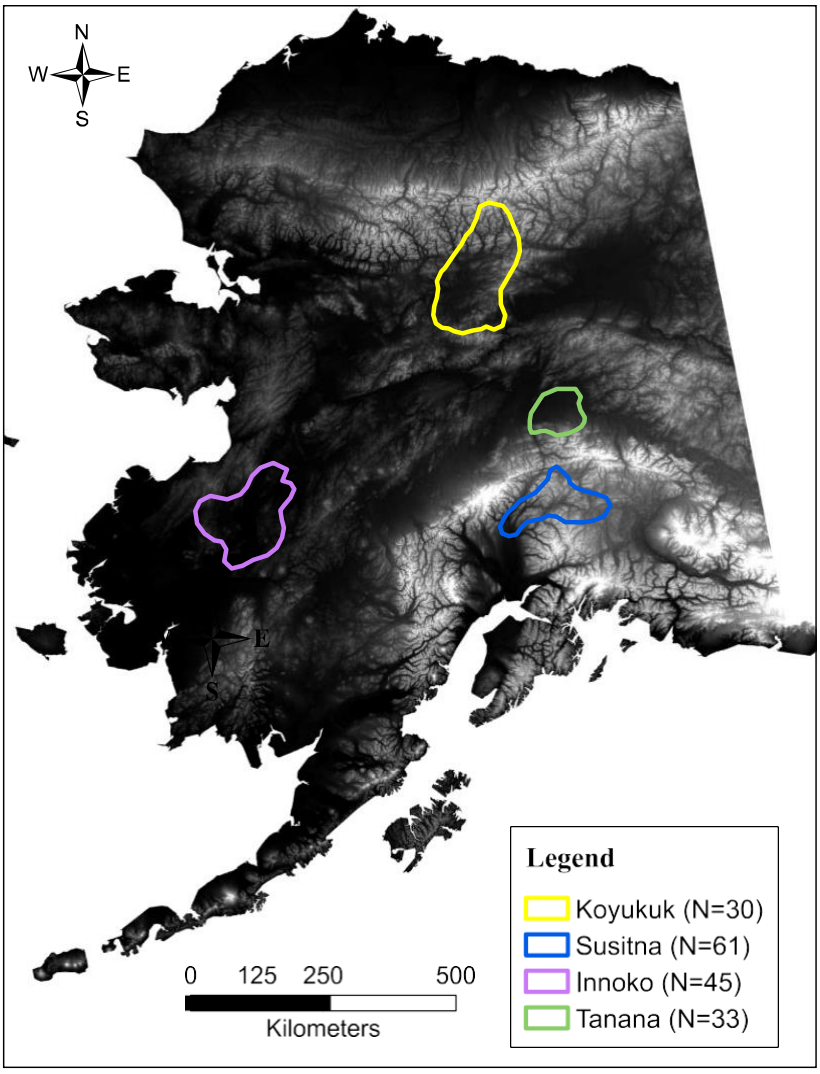

Figure 2.1. Moose (*Alces alces gigas*) study area locations in four distinct ecoregions of Alaska, USA. In total, 169 moose were included in these analyses (111 females; 58 males).

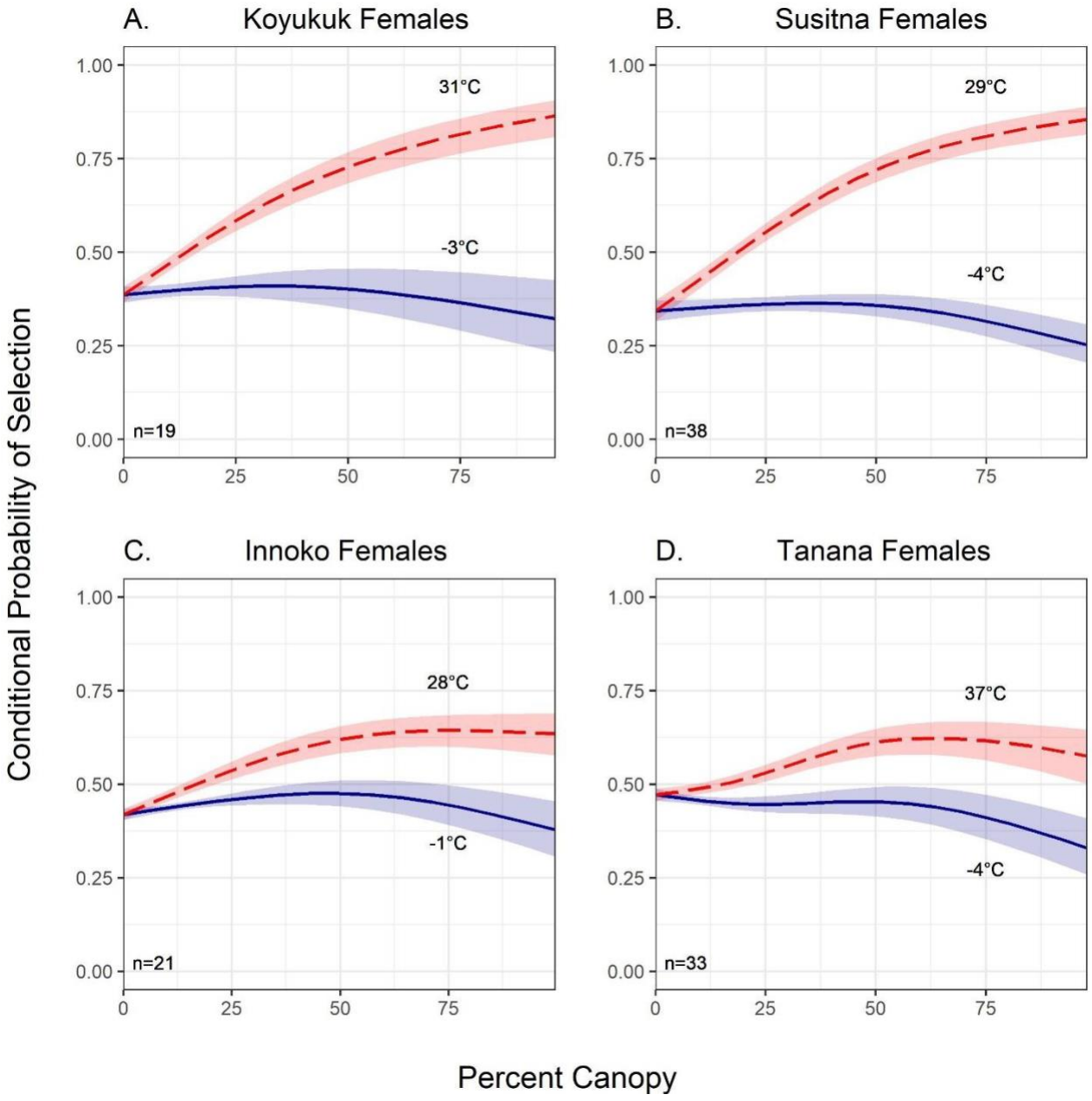

Figure 2.2. Conditional probability of selection of spline-based thermal cover as a function of temperature for Alaskan female moose by region in summer months (June-August). We used natural splines with two to three degrees of freedom to represent the relationship between canopy cover and temperature. The probability of selection of denser canopy increased significantly with temperature during summer for all four regions, where red lines indicated the warmest experienced temperature and the blue lines indicate the coolest experienced temperature by region. Shaded bands represent a 95% confidence interval.

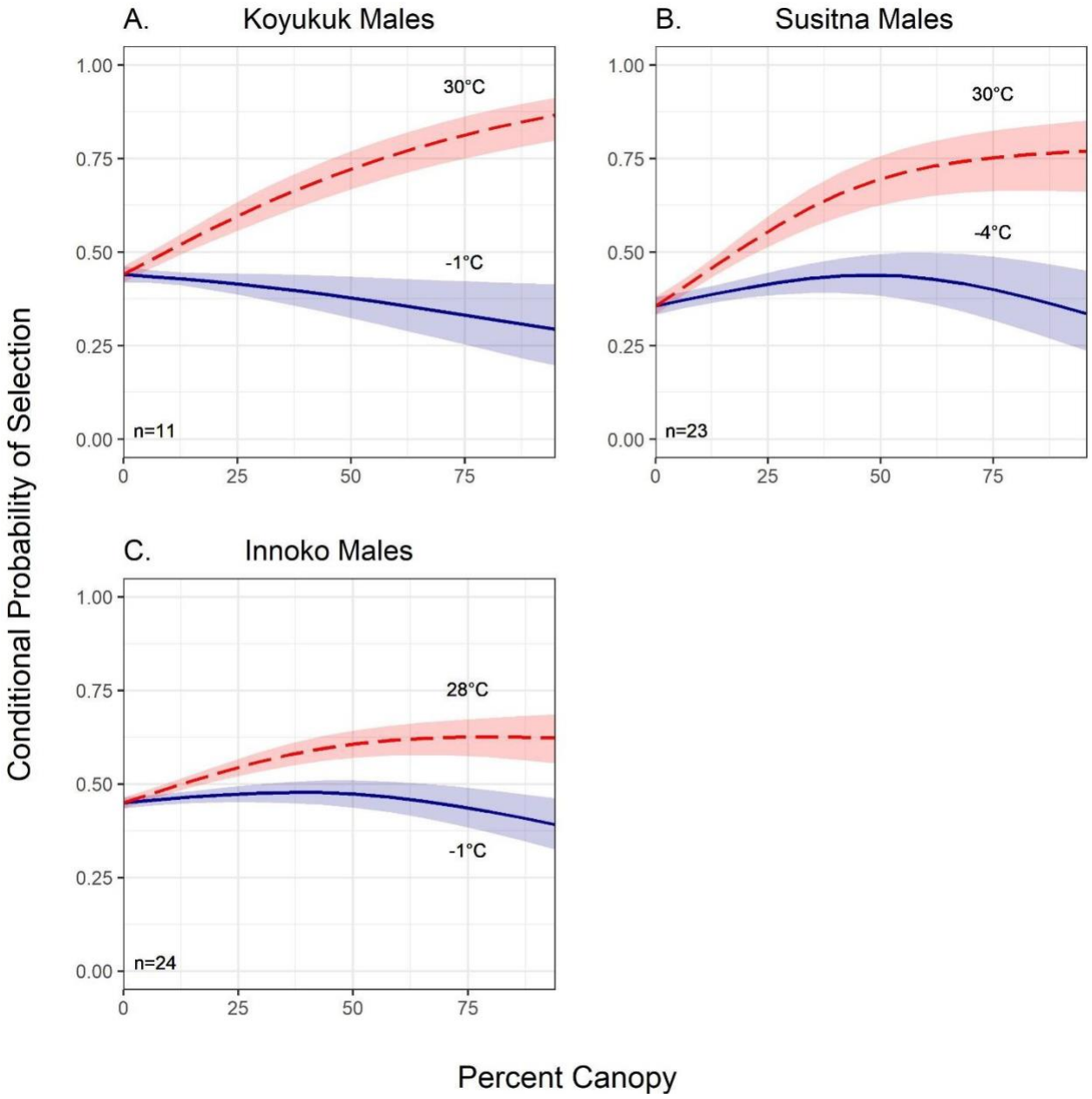

Figure 2.3. Conditional probability of selection of spline-based thermal cover as a function of temperature for Alaskan male moose by region in summer months (June-August). We used natural splines with two to three degrees of freedom to represent the relationship between canopy cover and temperature. The probability of selection of denser canopy increased significantly with temperature during summer for all four regions, where red lines indicated the warmest experienced temperature and the blue lines indicate the coolest experienced temperature by region. Shaded bands represent a 95% confidence interval.

Chapter 3: Toward mapping dietary fibers in northern ecosystems using hyperspectral and multispectral data

Authors: Jyoti S. Jennewein, Jan U.H. Eitel, Jeremiah R. Pinto, Lee A. Vierling,

Published: *Remote Sensing*, August 2020

Abstract

Shrub proliferation across the Arctic from climate warming is expanding herbivore habitat but may also alter forage quality. Dietary fibers—an important component of forage quality—influence shrub palatability, and changes in dietary fiber concentrations may have broad ecological implications. While airborne hyperspectral instruments may effectively estimate dietary fibers, such data captures a limited portion of landscapes. Satellite data such as the multispectral WorldView-3 (WV-3) instrument may enable dietary fiber estimation to be extrapolated across larger areas. We assessed how variation in dietary fibers of *Salix alaxensis* (Andersson), a palatable northern shrub, could be estimated using hyperspectral and multispectral WV-3 spectral vegetation indices (SVIs) in a greenhouse setting, and whether including structural information (i.e., leaf area) would improve predictions. We collected canopy-level hyperspectral reflectance readings, which we convolved to the band equivalent reflectance of WV-3. We calculated every possible SVI combination using hyperspectral and convolved WV-3 bands. We identified the best performing SVIs for both sensors using the coefficient of determination (adjusted R^2) and the root mean square error (RMSE) using simple linear regression. Next, we assessed the importance of plant structure by adding shade leaf area, sun leaf area, and total leaf area to models individually. We evaluated model fits using Akaike's information criterion for small sample sizes and conducted leave-one-out cross validation. We compared cross validation slopes and predictive power (Spearman rank coefficients ρ) between models. Hyperspectral SVIs (R^2 = 0.48–0.68; RMSE = 0.04–0.91%) outperformed WV-3 SVIs (R^2 = 0.13–0.35; RMSE = 0.05–1.18%) for estimating dietary fibers, suggesting hyperspectral remote sensing is best suited for estimating dietary fibers in a palatable northern shrub. Three dietary fibers showed improved predictive power when leaf area metrics were included (cross validation ρ = +2–8%), suggesting plant structure and the light environment may augment our ability to estimate some dietary fibers in northern landscapes. Monitoring dietary fibers in northern

ecosystems may benefit from upcoming hyperspectral satellites such as the environmental mapping and analysis program (EnMAP).

Introduction

Accelerated warming in high latitude regions (i.e., ≥ 60°N) has led to warmer, wetter, and more variable environments (Serreze et al., 2000; Wolken et al., 2011). One consequence of accelerated warming in these regions is the increased abundance and geographic extent of shrubs (Myers-Smith et al., 2011; Sturm et al., 2001). Some herbivores are expanding their ranges to exploit these increased food resources (Tape et al., 2016; Zhou et al., 2020) and also regulate vegetation proliferation through browsing (Bryant, 1987; Christie et al., 2015) and soil fertilization (Butler & Kielland, 2008; Kielland & Bryant, 1998). The effect of herbivores on shrubs is influenced by herbivore density, foraging intensity, and the palatability of shrubs (Christie et al., 2015; Speed et al., 2010). Shrub palatability may be influenced by increased temperatures from environmental change, which has broad ecosystem implications such as alterations to nutrient cycling (Doiron et al., 2014; Zamin et al., 2017).

Characterizing palatability—or forage quality—for herbivores is complex. Nitrogen content, foliar defense compounds, and dietary fibers must all be considered when quantifying forage quality (Felton et al., 2018). Dietary fibers encompass the structural components of plant cell walls, primarily hemicellulose (HMC), cellulose (CLL), and lignin, but can also be quantified in the laboratory for technical fiber fractions: neutral detergent fiber (NDF), acid detergent fiber (ADF), acid detergent lignin (ADL), and acid insoluble ash (AIA, or silica) (Van Soest et al., 1991). Higher fiber levels often increase handling time (i.e., cropping, chewing, and digesting) (Shipley & Spalinger, 1992), and therefore reduce plant palatability. However, CLL and HMC can provide substantial energy for ruminants (up to 80%) (Barboza et al., 2008).

Quantifying and mapping forage resources for herbivores are critical to effective management. Remote sensing provides a means of characterizing and monitoring forage quality across the landscape. Optical remote sensing approaches use reflected light from the ultraviolet (10–380 nm), visible (400–700 nm), near infrared (NIR; 701–1399 nm), and shortwave infrared (SWIR; 1400–2500 nm) regions to estimate plant dynamics. Reflected light from vegetation is influenced by functional group, plant water content, plant structural

components, and foliar chemistry (Xue & Su, 2017). Spectral vegetation indices (SVIs) calculated from spectral data are generated using simple algebraic formulas that enhance a target's spectral signal, and are commonly used to characterize vegetation vigor, growth, and foliar chemistry (Xue & Su, 2017). For example, the normalized difference vegetation index (NDVI) (Rouse Jr et al., 1974) is often used to predict habitat quality and takes the mathematical form of (NIR-Red)/(NIR + Red). However, NDVI often has mixed results when used to track forage resources (Doiron et al., 2013; Johnson et al., 2018). This limitation may be linked to the spectral resolution of broad band imagery that is not able to detect small absorption features associated with foliar biochemical traits.

Hyperspectral instruments sample the electromagnetic spectrum at narrow, contiguous wavelength ranges, which results in hundreds of sampled wavelengths. Generally, wavelengths greater than 700 nm show measurable absorption and scattering features that track dietary fibers such as CLL and lignin (Kokaly et al., 2009), particularly in the SWIR region (Curran, 1989; Elvidge, 1990). HMC and CLL have been accurately estimated using hyperspectral instruments in a variety of ecosystems from grasslands (Knox et al., 2012; Wang et al., 2019) to complex forests (Asner et al., 2014). Similarly, NDF and ADF have also been accurately estimated via hyperspectral remote sensing in semiarid rangelands (Mirik et al., 2005; Starks et al., 2004).

Although SVIs calculated from remotely sensed spectral data have demonstrated their utility in detecting various vegetation characteristics, they also show considerable sensitivity to plant structure such as leaf area index (LAI) (Chen & Cihlar, 1996; Turner et al., 1999). Canopy structural variation strongly influences spectral reflectance characteristics by creating a more complex three-dimensional environment for photons to interact (Asner, 1998; Knyazikhin et al., 2013; Vierling et al., 1997). Thus, plants with higher LAI have a more complex canopy and therefore amplify biochemical signals through scattering in NIR and to a lesser extent the SWIR regions (Asner, 1998).

Complex canopy architecture also influences the light environment within the canopy, impacting photosynthesis, growth, and nutrient quality for herbivores. For instance, diamond leaf willow (*Salix planifolia pulchra*) in Alaska demonstrated varying levels of NDF and ADF between sun and shaded leaves and a decrease in digestibility for willows growing in the sun (Molvar et al., 1993). Similarly, palatable shrubs growing in shaded

conditions had significantly reduced levels of HMC but increased levels of CLL than sunlit shrubs of the same species (Blair et al., 1983). Thus, incorporating plant structural metrics and the distinction between sun and shaded leaves into models designed to predict dietary fibers may improve model performance.

Although hyperspectral instruments can resolve fine-scale foliar chemistry, few hyperspectral satellites exist, and airborne data captures only a small portion of the landscape used by wildlife. However, the high-spatial resolution (< 5 m pixels) of multispectral imagery from WorldView satellites may enable fine-scale forage quality estimation, though the broadband imagery (bandwidth 40–70 nm) lacks the spectral resolution of hyperspectral data. WorldView-2 (WV-2) and WorldView-3 (WV-3) sensors have shown promise in estimating foliar nitrogen content in rangelands (Ramoelo et al., 2015; Zengeya et al., 2012), crop residues in agricultural settings (Hively et al., 2018), and digestible protein in eucalyptus forests (Wu et al., 2019). WorldView satellites also demonstrate utility in mapping percent vegetation cover (Liu et al., 2017) and plant functional type (Langford et al., 2016) in Arctic regions. WV-3 includes eight SWIR bands, yet to our knowledge no study has yet assessed the utility of the WV-3 satellite to map dietary fibers in high latitude settings.

Evaluating sensor performance in measuring dietary fibers in high latitude regions is increasingly important because of the effect of warming on palatable shrubs. Therefore, our overarching objective was to assess whether variation in six dietary fibers could be estimated by using multispectral bands from the WV-3 satellite, relative to hyperspectral data. To control for variations in environmental conditions, we conducted a greenhouse experiment with a highly palatable shrub common in Boreal and Arctic ecosystems, feltleaf willow (*Salix alaxensis* (Andersson)). We collected hyperspectral measures at two time intervals and identified hyperspectral SVIs suitable to remotely sense two functional fibers (HMC and CLL) and four technical fibers (NDF, ADF, ADL, and AIA) collectively called ‘dietary fibers’ hereafter. Second, we assessed the value of incorporating shrub structure and the light environment into our models using leaf area (cm^2) from sun and shaded leaves from each sample. Finally, we evaluated the suitability of the WV-3 satellite to monitor dietary fibers across the landscape using the band equivalent reflectance (BER) for each band by convolving our hyperspectral measures.

We hypothesized that the best SVIs would contain wavelengths > 700 nm (Kokaly et al., 2009) and that the SWIR region (Curran, 1989; Elvidge, 1990) would be best suited for tracking dietary fibers. We also predicted the BER of WV-3 would be able to estimate dietary fibers moderately well because of its eight SWIR bands. Further, we hypothesized that accounting for leaf area would enhance our models because higher levels of LAI have been shown to amplify biochemical signals in the NIR and SWIR regions (Asner, 1998). Finally, we hypothesized that partitioning leaf area into sun and shaded fractions would contribute meaningful differences in model performance because dietary fiber concentrations vary between sunlit and shaded canopies (Blair et al., 1983; Molvar et al., 1993).

Methods and Materials

Greenhouse Procedures

On 13 June 2018, we collected 52 willow (*Salix alaxensis* (Andersson)) cuttings near Coldfoot, AK (67.2524°N, −150.1772°W). We stored cuttings in a chilled cooler for transit, and cuttings were wrapped in moist paper towels and provided water through a plastic reservoir attached to each cut stem. Twenty-four hours later, we processed field cuttings by clipping small wooded stems and current year green stems. We dipped these new clippings in a solution of indol-3-butyric acid (0.2%) rooting hormone and planted them in trays containing a water-saturated, peat moss, and vermiculite (1:1 by volume) media. Trays were placed inside a misting chamber outfitted with a root zone heat mat set to 17 °C.

Available nutrients for high latitude plants are expected to increase as temperatures rise, which in turn increases shrub biomass (Myers-Smith et al., 2011) and therefore dietary fibers. Thus, we simulated a broad range of possible nitrogen (N) concentration scenarios that may occur as the rate of nutrient cycling increases (Appendix 3.1 (A3.1)). Four weeks after the second clipping, when cuttings had generated new roots, we randomly stratified willow cuttings (n = 105) into six groups along a gradient of N-fertilizer treatments: native; +5; +10; +20; +50; and +100 kg N ha^{-1}. After treatment groups were assigned, we transferred rooted-cuttings into larger, 2.3 L Treepot containers (Stuewe & Sons, Inc. Tangent, OR, USA) containing artificial media (peat moss, vermiculite, and perlite; 2:1:1 by volume) and the total amount of N required for the study. N, phosphorus (P), potassium, (K), and micronutrients were delivered via controlled-release fertilizer (Osmocote Plus, 5–6 month, NPK: 15-9-12). Water was provided via subirrigation and timing was determined

gravimetrically (Dumroese et al., 2015). Feltleaf willows grow primarily in riparian areas so gravimetric irrigation targets were set to 70–80% of saturation.

Our samples experienced a large amount of attrition (43%) related to disease (willow rust, *Melampsora* spp.) and pests (aphid outbreak) within the first month of the experiment. Thus, we opted to put the remaining samples into dormancy for the winter and to restart the experiment in March 2019. On 11 January 2019, willows were wrapped in moist paper towels, stored in paper bags inside of a freezer set to −2.2 °C. After 8 weeks in dormancy, willows were thawed at 15.6–18.3 °C for three days. Once willows were thawed, we replanted them using the same procedures outlined previously. Sixty plants were viable from the first round of the experiment. From March through June 2019, greenhouse temperatures averaged 23.6/17.4 °C (day/night), relative humidity averaged 41.7/62.0% (day/night), and photosynthetically active radiation (PAR) peaked at 1190 μmol during the experimental period (March–June 2019).

For each round of sampling, we randomly selected 12 willows for harvest. Although we had planned to conduct a third and fourth round of sampling, our plants again experienced a pest outbreak. Therefore, we only sampled two rounds and obtained 24 samples total—one and two months after planting, 6 May and 2 June, respectively.

Hyperspectral, Leaf Area, and Destructive Vegetation Collection

We collected hyperspectral reflectance readings and associated destructive-vegetation samples from each replicate. We collected canopy spectra using a FieldSpec Pro Full Range Spectroradiometer (Malvern Panalytical Ltd., Malvern, UK). This instrument has a spectral range of 350–2500 nm, with a full-width half-max of 3 nm in the visible and near infrared regions (350–1050 nm), and 10–12 nm in both short-wave infrared regions (900–1850 nm and 1700–2500 nm). Prior to sampling of each plant, dark current and white reference measures were taken using Spectralon panel (Labsphere, Inc., North Sutton, NH, USA).

The fiber optic probe of the instrument (with a 25° field of view) was mounted 50 cm above the highest point of each plant (Figure 3.1C). Each sampled plant was illuminated with a full spectrum lamp (1000 W) mounted at a 60° zenith angle 1.4 m above the ground. To minimize confounding background effects on spectral measurements, a spectrally flat black-foam material was cut and placed around the lowest point of the stem of each willow (Figure 3.1B). Four spectral measurements were taken per willow, and the willow was rotated 90°

each round of sampling. We calculated the mean of these four spectral measurements for analysis.

Immediately after collecting canopy spectra, leaves were harvested, separated into 'shade' and 'sun' categories based on a visual assessment of their position in the canopy and scanned using a portable scanner. We included a reference target of a known area in each scan that enabled us to calculate one-sided leaf area (cm^2) in Image J (Schneider et al., 2012) following methods outlined in (Glozer, 2008). After scanning, leaves were oven dried for 48 h at 30–40 °C. Dried samples were ground and analyzed by the Washington State University Habitat Lab for NDF, ADF, ADL, and AIA using the sequential fiber analysis (Van Soest et al., 1991). We estimated HMC content by subtracting ADF from NDF, and CLL content by subtracting ADL from ADF.

Statistical Analyses

We used R statistical software version 3.6.2 (R Core Team, 2019) for all statistical assessments. We tested for differences in dietary fibers between sample periods using Welch's two sample *t*-test (Welch, 1947) and differences between dietary fibers and N fertilization treatments using a one way analysis of variance (ANOVA) and Tukey's range test (Tukey, 1949) as a post hoc follow up to determine pairwise differences between fertilizer treatments.

We assessed every possible spectral band combination using simple ratio SVIs (Band A/Band B) and also normalized differenced SVIs ((Band A − Band B)/(Band A + Band B)) to track dietary fibers using simple linear models. The best performing SVIs for each dietary fiber were identified using adjusted R^2 values and the root mean square error (RMSE). After identifying the best performing SVIs, we assessed the importance of plant structure by adding shade leaf area, sun leaf area, and total leaf area to linear models individually. We evaluated model fit between model variants using Akaike's information criterion for small sample sizes (AICc) (Burnham & Anderson, 2002; Cavanaugh, 1997) from the 'MuMIn' package (Barton & Barton, 2015). We also conducted leave-one-out cross validation (LOOCV) by excluding one willow from the data set sequentially and testing the predictive power of the remaining willows against the excluded one. We compare the resultant slopes and predictive power using Spearman rank coefficients (ρ) between models.

Band Equivalent Reflectance

The BER provides an assessment of potential sensor performance (Smith et al., 2005). To assess the ability of identified SVIs to scale to the landscape level, SVIs identified from canopy-level hyperspectral data were convolved to WV-3 satellite bands using their BER (Trigg & Flasse, 2000). The spectral response functions of WV-3 were obtained directly from Maxar Technologies (Westminster, CO, USA). The BER data for WV-3 were then used to recompute SVIs. As with the hyperspectral SVIs, we assessed whether adding shade leaf area, sun leaf area, and total leaf area improved our models following the same analytical steps detailed in section 2.3. Since we hypothesized that incorporating leaf area into models would improve model performance, we also investigated the relationships between total leaf area and NDVI, which has been shown to have a strong nonlinear relationship with LAI in high latitude regions (Heiskanen, 2006). Finally, we substituted NDVI for total leaf area in our WV-3 BER models to evaluate the possibility of representing plant structure using only SVIs.

Results

Dietary fibers showed a wide variety of concentrations between samples (A2.2). We observed no difference in fiber concentrations between sampling period ($t = -0.07$ to 1.28, $p > 0.05$) except for HMC ($t = -2.77$, $p = 0.01$) where the first sampling period had significantly more HMC than the second sampling period. Similarly, we found no significant difference between sun and shaded leaf area in either May ($t = -1.13$, $p = 0.27$) or June ($t = 0.29$, $p = 0.78$), nor when sample dates were pooled ($t = -0.88$, $p = 0.38$). We found no statistically significant difference ($p > 0.05$) between N treatments and HMC, ADL, or AIA concentrations. CLL ($F = 5.68$, $p < 0.01$), NDF ($F = 5.51$, $p < 0.01$), and ADF ($F = 4.19$, $p < 0.01$) concentrations differed across N treatments (A2.3).

Hyperspectral Vegetation Indices

As hypothesized, the best SVIs for tracking dietary fibers contained bands > 700 nm, with most wavelengths located in the SWIR region ($R^2 = 0.48–0.68$; RMSE = 0.04–0.91%; Figure 3.2), but with viable SVIs occurring in the NIR region as well (Figure 3.3). HMC was the only fiber that was best predicted using a non-SWIR SVI (794 nm/816 nm). Cross validation scores were good ($\rho = 0.73–0.83$; Table 1), especially for a small sample size. However, all models underpredicted fiber concentration (slopes < 1). Additionally, we saw an improved model fit and predictive ability when adding shaded leaf area metrics to predict

NDF (ΔAICc = −7.65; ΔLOOCV = +8%). Predictive ability also increased slightly when leaf area metrics were added to CLL (ΔLOOCV = +2–3%) and ADF models (ΔLOOCV = +1%), but without improvements in model fit. HMC models also improved (ΔAICc = −3.17; ΔLOOCV = +5%) when sun leaf area was added. No improvements in model fit or predictive power occurred for ADL, or AIA.

Band Equivalent Reflectance of WV-3

We convolved our hyperspectral data to the BER of WV-3 to assess whether dietary fibers could be measured via satellite (Table 3.2; Figure 4). As with the hyperspectral models, the majority of the best performing WV-3 SVIs contained SWIR bands (Figure 3.4). WV-3 models also underpredicted fiber concentration (slopes < 1) and performed poorer (R^2 = 0.13–0.35; RMSE = 0.05–1.18%) than hyperspectral models (R^2 = 0.48–0.68; RMSE = 0.04–0.91%). However, BER SVIs from WV-3 showed some promise in predicting HMC, NDF, and ADF, particularly when leaf area metrics were accounted for in the models (Table 3.2). As with the hyperspectral models, the best improvements in models came when shaded leaf area was added to NDF (R^2 = 0.45; RMSE = 1.03%; LOOCV ρ = 0.78) and ADF (R^2 = 0.40; RMSE = 0.69%; LOOCV ρ =0.76). In contrast, HMC saw the best model improvements when total leaf area was added (R^2 = 0.45; RMSE = 0.55%; LOOCV ρ = 0.72). WV-3 models for CLL showed slight increase in cross validation scores when leaf area metrics were incorporated (ΔLOOCV = +4–5%), but without increased model fit or explained variance. ADL and AIA showed no model fit improvements with the addition of leaf area metrics, which was consistent with our hyperspectral results.

We also assessed how well total leaf area could be represented using NDVI in the WV-3 models. Results showed that total leaf area and NDVI had a nonlinear relationship with moderate strength (R^2 = 0.51; RMSE = 458.79 cm^2; A2.4). When NDVI replaced total leaf area in WV-3 models, we found slight improvements predictive ability (ΔLOOCV = +1–2%; A2.4) for HMC, CLL, ADF, ADL, and AIA, while NDF showed reduced predictive power (ΔLOOCV = −5%) compared to SVI only models.

Discussion

Our results indicate dietary fibers from an important forage species of arctic-boreal willow can be effectively measured with hyperspectral instruments. This finding supports previous work where dietary fibers have been successfully mapped in rangelands (Mirik et al., 2005;

Starks et al., 2004), grasslands (Knox et al., 2012; Wang et al., 2019), and mixed forest landscapes (Asner et al., 2014) using hyperspectral remote sensing. As hypothesized, all of the best performing SVIs contained wavelengths greater than 700 nm (Kokaly et al., 2009), with the majority of SVIs containing bands in the SWIR region (Curran, 1989; Elvidge, 1990).

Incorporating plant structure into hyperspectral models also improved our ability to track and predict HMC, NDF, and ADL (Table 3.1). This is likely related to the wavelengths used in the SVIs for these fibers. The NIR region is most sensitive to changes in plant structure with the initial portion of the SWIR region (1500–2000 nm) also showing sensitivity to changes in LAI (Asner, 1998). In our study, all three of the fibers that showed improvements when leaf area was incorporated had at least one band in their SVIs in these regions. In contrast, the remaining three fibers—CLL, ADF, and AIA—all had SVIs in the latter part of the SWIR region (2000–2500 nm; Figure 2), which is less sensitive to plant structure (Asner, 1998). Additionally, since the SWIR region is influenced by foliar water content, as water comprises 40–80% of weight in green specimens (Elvidge, 1990), future work may benefit from comparing spectral collections from wet and dry samples as this may improve model performance.

We observed model improvements from plant structure in HMC, NDF, and ADL depended on the partitioning leaf area into shaded and sunlit fractions. HMC models improved most when sunlit leaf area was added to models (Table 3.1). One study found that HMC was highly influenced by shade in two palatable shrubs—yaupon (*Ilex vomitoria*) and Japanese honeysuckle (*Lonicera japonica*)—where HMC levels were up to 92% more in sunlit plants than shaded comparisons (Blair et al., 1983). However, due to constraints in the available dry matter for laboratory analyses in our study, we were unable to assess how fiber concentrations varied between sun and shaded leaves. In contrast, the best NDF and ADL models occurred when shaded leaf area was incorporated (Table 3.1). Again, this may be related to the relative amount of these fibers in sun vs. shaded leaves. ADL concentrations in yaupon and honeysuckle leaves were significantly higher in shaded plants (Blair et al., 1983); however, one study found no statistical difference in lignin (ADL) between shaded and sunlit samples of diamond leaf willow (Molvar et al., 1993). This same study found that NDF was significantly higher in sunny willow shoots compared to shaded shoots (Molvar et al., 1993),

which would not explain why our NDF models improved most when shaded leaf area was included. However, other work has shown that NDF content in shaded and sunlit plants varies according to species, where some show higher NDF in shaded plants (Lin et al., 2001). Thus, we anticipate that our results were specific to feltleaf willow and might not be generalized to other shrubs in high latitudes. Our results also suggest in addition to the importance of plant structural characteristics, the light environment plays a critical role in the development of these fibers in feltleaf willow. One remotely sensed product that may parse shaded and sunlit fractions of vegetation canopies is the Earth polychromatic imaging camera's (EPIC) sunlit LAI product (10 km spatial resolution), although it is likely a finer spatial scale would be required to apply this product to high latitude settings as variations in LAI vary substantially across the landscape (Juutinen et al., 2017).

Sun-dependent variations in foliar biochemical composition influence herbivore foraging behavior. Snowshoe hares (*Lepus americanus*) preferred shaded browse shoots from feltleaf willow over sunlit comparisons (Bryant, 1987). Similarly, Sitka black-tailed deer (*Odocoileus hemionus sitkensis*) showed a preference for shade-grown Alaska blueberry (*Vaccinium alaskensis*) over those grown in sunlit clearcuts (Hanley, 1987). Indeed, it appears that digestibility and quality of forage in palatable high-latitude shrubs is greater in shaded plants (Lenart et al., 2002; Molvar et al., 1993). This is likely linked to decreased light available for photosynthesis, which in turn may limit the formation of structural fibers (Molvar et al., 1993; Moore & Jung, 2001) and increased foliar nitrogen and decreased defense compound concentrations (Osier & Lindroth, 1999).

Shrub proliferation in Arctic regions is increasing the range of herbivores such as snowshoe hare, moose (*Alces alces*), and ptarmigan (*Lagopus lagopus*, *L. muta*) (Tape et al., 2016; Zhou et al., 2020). Increases in ambient temperature may lower the digestibility of forage species by increasing lignification (Weladji et al., 2002) and decreasing nitrogen in the late summer (Doiron et al., 2014), but these changes are likely species and region specific (Elmendorf et al., 2012; Lenart et al., 2002). Shading from clouds or canopy may improve forage quality (Lenart et al., 2002; Molvar et al., 1993; Weladji et al., 2002). However, studies have shown that warming may significantly alter forage quality for high latitude herbivores, which may have broader consequences for ecosystem functions such as nutrient cycling (Doiron et al., 2014; Zamin et al., 2017). Thus, as warming continues, the palatability

of shrubs in high latitudes will likely be a function of landscape structure, browsing intensity, and environmental conditions.

Strategies for monitoring variation in forage quality over broad heterogeneous landscapes are needed to account for changes over space and time. To this end, we evaluated the suitability the WV-3 satellite to measure dietary fibers and we predicted its eight SWIR bands would be useful in estimating dietary fibers. Of the eight SWIR bands, six of them comprised the best performing BER SVIs for CLL, NDF, ADF, ADL, and AIA (Figure 3.4). As with the hyperspectral models, the WV-3 models for HMC and NDF saw improvements when plant structural information was included, particularly when shaded leaf area was included (Table 3.2). However, we observed the best HMC model with total leaf area. We also observed that ADL predictions no longer benefitted from including leaf area but ADF models improved when shaded or total leaf area was included.

Few works have evaluated the utility of WorldView satellites for detecting foliar biochemical properties in high latitude regions. Our results suggest that WV-3 can estimate HMC, NDF, and ADF in a palatable high-latitude shrub with moderate accuracy when additional plant structural information is included in models, but that hyperspectral remote sensing approaches are best suited for mapping dietary fibers in feltleaf willow. Therefore, future work may benefit from assessing and using the upcoming German environmental mapping and analysis program (EnMAP) satellite. EnMAP will collect moderate spatial resolution (30 m) hyperspectral imagery (420–2450 nm) and make data freely available (Guanter et al., 2015).

We also evaluated the possibility of using NDVI as a proxy for total leaf area in the WV-3 models (Appendix D). Although we found a moderate-strength nonlinear relationship between total leaf area and NDVI, only HMC showed improved model statistics when NDVI was included. This suggests that additional, non-spectral measures of shrub structure, and possibly leaf water content, may be necessary to pair with SVIs to obtain the best estimates of dietary fibers. Aerial lidar (light detection and ranging) may be used to represent LAI (Jensen et al., 2008; Pope & Treitz, 2013) and may increase our ability to map dietary fibers in high latitude regions when coupled with hyperspectral data.

Due to the controlled setting of our study, we did not evaluate the influence of soil background effects or confounding factors (e.g., shadows) on our ability to estimate dietary

fibers. Similarly, the composite nature of all remotely sensed pixels includes spectral information from multiple constituents, which impedes our ability to remotely sense vegetation properties (Somers et al., 2011). Therefore, techniques such as spectral mixture analysis (Adams & Smith, 1986) or combined spectral indices (Eitel et al., 2009) may be needed to parse the spectral information of the variable of interest from background noise. For example, previous work has demonstrated the influence of soil properties on sensing foliar biochemical properties and plant structural characteristics such as LAI (Darvishzadeh et al., 2008). Finally, our study was limited by disease and pests in the greenhouse. Despite these afflictions that resulted in a small sample size, our results demonstrate the utility of hyperspectral and multispectral sensors to track dietary fibers in a high latitude palatable forage shrub.

Conclusion

This study contributed to an emerging need to estimate and monitor forage quality across wide expanses in high latitude systems. Results demonstrated that hyperspectral data is best suited to estimating dietary fibers in a palatable northern shrub and highlighted the importance of the SWIR region for this purpose. Additionally, information regarding plant structure and the light environment may augment our ability to estimate dietary fibers in these landscapes. Future work should evaluate the efficacy of including plant structure and light environment in addition to passive spectral information to estimate forage quality metrics in a field-based setting.

Literature Cited

Adams, J. B., & Smith, M. O. (1986). Spectral mixture modeling: A new analysis of rock and soil types at the Viking Lander 1 site. *Journal of Geophysical Research*, *91*(B8), 8098– 8112. https://doi.org/10.1029/jb091ib10p10513

Asner, G. P. (1998). Biophysical and biochemical sources of variability in canopy reflectance. *Remote Sensing of Environment*, *64*(3), 234–253. https://doi.org/10.1016/S0034-4257(98)00014-5

Asner, G. P., Martin, R. E., Carranza-jim, L., Sinca, F., Tupayachi, R., Anderson, C. B., & Martinez, P. (2014). Functional and biological diversity of foliar spectra in tree canopies throughout the Andes to Amazon region. *New Phytologist*, *204*, 127–139.

Barboza, P. S., Parker, K. L., & Hume, I. D. (2008). *Integrative wildlife nutrition*. Springer Science & Business Media.

Barton, K., & Barton, M. K. (2015). Package 'MuMIn.' *Version*, *1*, 18.

Blair, R. M., Alcaniz, R., & Harrell, A. (1983). Shade Intensity Influences the Nutrient Quality and Digestibility of Southern Deer Browse Leaves. *Journal of Range Management*, *36*(2), 257–264. https://doi.org/10.2307/3898177

Bryant, J. P. (1987). Feltleaf willow-snowshoe hare interactions: Plant carbon/nutrient balance and floodplain succession. *Ecology*, *68*(5), 1319–1327.

Burnham, K. P., & Anderson, D. R. (2002). A practical information-theoretic approach. *Model Selection and Multimodel Inference, 2nd Ed. Springer, New York*, *2*.

Butler, L. G., & Kielland, K. (2008). Acceleration of vegetation turnover and element cycling by mammalian herbivory in riparian ecosystems. *Journal of Ecology*, *96*, 136–144. https://doi.org/10.1111/j.1365-2745.2007.0

Cavanaugh, J. E. (1997). Unifying the derivations for the Akaike and corrected Akaike information criteria. *Statistics & Probability Letters*, *33*(2), 201–208.

Chen, J. M., & Cihlar, J. (1996). Retrieving leaf area index of boreal conifer forests using landsat TM images. *Remote Sensing of Environment*, *55*(2), 153–162. https://doi.org/10.1016/0034-4257(95)00195-6

Christie, K. S., Bryant, J. P., Gough, L., Ravolainen, V. T., Ruess, R. W., & Tape, K. D. (2015). The role of vertebrate herbivores in regulating shrub expansion in the Arctic: A synthesis. *BioScience*, *65*(12), 1123–1133. https://doi.org/10.1093/biosci/biv137

Curran, P. J. (1989). Remote sensing of foliar chemistry. *Remote Sensing of Environment*, *30*(3), 271–278. https://doi.org/10.1016/0034-4257(89)90069-2

Darvishzadeh, R., Skidmore, A., Atzberger, C., & van Wieren, S. (2008). Estimation of vegetation LAI from hyperspectral reflectance data: Effects of soil type and plant architecture. *International Journal of Applied Earth Observation and Geoinformation*, *10*(3), 358–373. https://doi.org/10.1016/j.jag.2008.02.005

Doiron, M., Gauthier, G., & Lévesque, E. (2014). Effects of experimental warming on nitrogen concentration and biomass of forage plants for an arctic herbivore. *Journal of Ecology*, *102*(2), 508–517. https://doi.org/10.1111/1365-2745.12213

Doiron, M., Legagneux, P., Gauthier, G., & Lévesque, E. (2013). Broad-scale satellite Normalized Difference Vegetation Index data predict plant biomass and peak date of nitrogen concentration in Arctic tundra vegetation. *Applied Vegetation Science*, *16*(2), 343–351. https://doi.org/10.1111/j.1654-109X.2012.01219.x

Dumroese, R. K., Pinto, J. R., & Montville, M. E. (2015). Using container weights to determine irrigation needs: a simple method. *Native Plants Journal*, *16*(1), 67–71. https://doi.org/10.3368/npj.16.1.67

Eitel, J. U. H., Long, D. S., Gessler, P. E., Hunt, E. R., & Brown, D. J. (2009). Sensitivity of Ground-Based Remote Sensing Estimates of Wheat Chlorophyll Content to Variation in Soil Refl ectance. *Soil Science Society of America*, *73*(5), 1715–1723. https://doi.org/10.2136/sssaj2008.0288

Elmendorf, S. C., Henry, G. H. R., Hollister, R. D., Björk, R. G., Bjorkman, A. D., Callaghan, T. V., Collier, L. S., Cooper, E. J., Cornelissen, J. H. C., Day, T. A., Fosaa, A. M., Gould, W. A., Grétarsdóttir, J., Harte, J., Hermanutz, L., Hik, D. S., Hofgaard, A., Jarrad, F., Jónsdóttir, I. S., … Wookey, P. A. (2012). Global assessment of experimental climate warming on tundra vegetation: Heterogeneity over space and time. *Ecology Letters*, *15*(2), 164–175. https://doi.org/10.1111/j.1461-0248.2011.01716.x

Elvidge, C. D. (1990). Visible and near-infrared reflectance characteristics of dry plant materials. *International Journal of Remote Sensing*, *11*(10), 1775–1795.

Felton, A. M., Wam, H. K., Stolter, C., Mathisen, K. M., & Wallgren, M. (2018). The complexity of interacting nutritional drivers behind food selection, a review of northern cervids. *Ecosphere*, *9*(5), 1–25. https://doi.org/10.1002/ecs2.2230

Glozer, K. (2008). Protocol for leaf image analysis--surface area. Availble at: Http://Ucanr. Edu/Sites/Fruittree/Files/49325.Pdf.

Guanter, L., Kaufmann, H., Segl, K., Foerster, S., Rogass, C., Chabrillat, S., Kuester, T., Hollstein, A., Rossner, G., Chlebek, C., Straif, C., Fischer, S., Schrader, S., Storch, T., Heiden, U., Mueller, A., Bachmann, M., Mühle, H., Müller, R., … Sang, B. (2015). The EnMAP spaceborne imaging spectroscopy mission for earth observation. *Remote Sensing*, *7*(7), 8830–8857. https://doi.org/10.3390/rs70708830

Hanley, T. A. (1987). Physical and chemical response of understory vegetation to deer use in southeastern Alaska. *Canadian Journal of Forest Research*, *17*(3), 195–199.

Heiskanen, J. (2006). Estimating aboveground tree biomass and leaf area index in a mountain birch forest using ASTER satellite data. *International Journal of Remote Sensing*, *27*(6), 1135–1158. https://doi.org/10.1080/01431160500353858

Hively, W. D., Lamb, B. T., Daughtry, C. S. T., Shermeyer, J., Mccarty, G. W., & Quemada, M. (2018). Mapping Crop Residue and Tillage Intensity Using WorldView-3 Satellite Shortwave Infrared Residue Indices. *Remote Sensing*, *10*(1657), 1–22. https://doi.org/10.3390/rs10101657

Jensen, J. L. R., Humes, K. S., Vierling, L. A., & Hudak, A. T. (2008). Discrete return lidar-based prediction of leaf area index in two conifer forests. *Remote Sensing of Environment*, *112*(10), 3947–3957. https://doi.org/10.1016/j.rse.2008.07.001

Johnson, H. E., Gustine, D. D., Golden, T. S., Adams, L. G., Parrett, L. S., Lenart, E. A., & Barboza, P. S. (2018). NDVI exhibits mixed success in predicting spatiotemporal variation in caribou summer forage quality and quantity. *Ecosphere*, *9*(10). https://doi.org/10.1002/ecs2.2461

Juutinen, S., Virtanen, T., Kondratyev, V., Laurila, T., Linkosalmi, M., Mikola, J., Nyman, J., Räsänen, A., Tuovinen, J. P., & Aurela, M. (2017). Spatial variation and seasonal dynamics of leaf-Area index in the arctic tundra-implications for linking ground observations and satellite images. *Environmental Research Letters*, *12*(9). https://doi.org/10.1088/1748-9326/aa7f85

Kielland, K., & Bryant, J. P. (1998). Moose herbivory in Taiga: Effects on biogeochemistry and vegetation dynamics in primary succession. *OIKOS*, *82*(2), 377–383.

Knox, N. M., Skidmore, A. K., Prins, H. H. T., Heitkönig, I. M. A., Slotow, R., Waal, C. Van Der, & Boer, W. F. De. (2012). Remote sensing of forage nutrients: Combining ecological and spectral absorption feature data. *ISPRS Journal of Photogrammetry and Remote Sensing*, *72*, 27–35. https://doi.org/10.1016/j.isprsjprs.2012.05.013

Knyazikhin, Y., Schull, M. A., Stenberg, P., Mõttus, M., Rautiainen, M., Yang, Y., Marshak, A., Carmona, P. L., Kaufmann, R. K., Lewis, P., Disney, M. I., Vanderbilt, V., Davis, A. B., Baret, F., Jacquemoud, S., Lyapustin, A., & Myneni, R. B. (2013). Hyperspectral remote sensing of foliar nitrogen content. *Proceedings of the National Academy of Sciences of the United States of America*, *110*(3). https://doi.org/10.1073/pnas.1210196109

Kokaly, R. F., Asner, G. P., Ollinger, S. V, Martin, M. E., & Wessman, C. A. (2009). Characterizing canopy biochemistry from imaging spectroscopy and its application to ecosystem studies. *Remote Sensing of Environment*, *113*, 78–91. https://doi.org/10.1016/j.rse.2008.10.018

Langford, Z., Kumar, J., Hoffman, F. M., Norby, R. J., Wullschleger, S. D., Sloan, V. L., & Iversen, C. M. (2016). Mapping Arctic Plant Functional Type Distributions in the Barrow Environmental Observatory Using WorldView-2 and LiDAR Datasets. *Remote Sensing*, *8*(733), 1–24. https://doi.org/10.3390/rs8090733

Lenart, E. A., Bowyer, R. T., Hoef, J. Ver, & Ruess, R. W. (2002). Climate change and caribou: effects of summer weather on forage. *Canadian Journal of Zoology*, *80*(4), 664–678. https://doi.org/10.1139/z02-034

Lin, C. H., McGraw, M. L., George, M. F., & Garrett, H. E. (2001). Nutritive quality and morphological development under partial shade of some forage species with agroforestry potential. *Agroforestry Systems*, *53*(3), 269–281. https://doi.org/10.1023/A:1013323409839

Liu, N., Budkewitsch, P., & Treitz, P. (2017). Examining spectral reflectance features related to Arctic percent vegetation cover: Implications for hyperspectral remote sensing of Arctic tundra. *Remote Sensing of Environment*, *192*, 58–72. https://doi.org/10.1016/j.rse.2017.02.002

Mirik, M., Norland, J. E., Crabtree, R. L., & Biondini, M. E. (2005). Hyperspectral One-Meter-Resolution Remote Sensing in Yellowstone National Park, Wyoming: I . Forage Nutritional Values. *Society for Range Management*, *58*(5), 452–458.

Molvar, E. M., Bowyer, R. T., & Van Ballenberghe, V. (1993). Moose herbivory, browse quality, and nutrient cycling in an Alaskan treeline community. *Oecologia*, *94*(4), 472–479. https://doi.org/10.1007/BF00566961

Moore, K. J., & Jung, H. J. G. (2001). Lignin and fiber digestion. *Rangeland Ecology & Management/Journal of Range Management Archives*, *54*(4), 420–430.

Myers-Smith, I. H., Forbes, B. C., Wilmking, M., Hallinger, M., Lantz, T., Blok, D., Tape, K. D., Macias-fauria, M., Sass-klaassen, U., & Esther, L. (2011). Shrub expansion in tundra ecosystems: Dynamics, impacts and research priorities. *Environmental Research Letters*, *6*. https://doi.org/10.1088/1748-9326/6/4/045509

Osier, T. L., & Lindroth, R. L. (1999). Effects of light and nutrient availability on Aspen: Growth, phytochemistry, and insect performance. *Journal of Chemical Ecology*, *25*(7), 1687–1714. https://doi.org/10.1023/A:1010352307301

Pope, G., & Treitz, P. (2013). Leaf Area Index (LAI) estimation in boreal mixedwood forest of Ontario, Canada using Light detection and ranging (LiDAR) and worldview-2 imagery. *Remote Sensing*, *5*(10), 5040–5063. https://doi.org/10.3390/rs5105040

R Core Team. (2019). *R: A language and environment for statistical computing*. Vienna, Austria.

Ramoelo, A., Cho, M. A., Mathieu, R., Madonsela, S., Kerchove, R. Van De, Kaszta, Z., & Wolff, E. (2015). Monitoring grass nutrients and biomass as indicators of rangeland quality and quantity using random forest modelling and WorldView-2 data. *International Journal of Applied Earth Observation and Geoinformation*, *43*, 43–54.

Rouse Jr, J. W., Haas, R. H., Schell, J. A., & Deering, D. W. (1974). Paper A 20. *Third Earth Resources Technology Satellite-1 Symposium: The Proceedings of a Symposium Held by Goddard Space Flight Center at Washington, DC on December 10-14, 1973: Prepared at Goddard Space Flight Center*, *351*, 309.

Schneider, C. A., Rasband, W. S., & Eliceiri, K. W. (2012). NIH Image to ImageJ: 25 years of image analysis. *Nature Methods*, *9*(7), 671–675.

Serreze, M. C., Walsh, J. E., Chapin, F. S. I., Osterkamp, T., Dyurgerov, M., Romanovsky, V., Oechel, W. C., Morison, J., Zhang, T., & Barry, R. G. (2000). Observational evidence of recent change in the northern high- latitude environment. *Climatic Change*, *46*, 159–207. https://doi.org/10.1023/A:1005504031923

Shipley, L. A., & Spalinger, D. E. (1992). Mechanics of browsing in dense food patches: Effects of plant and animal morphology on intake rate. *Canadian Journal of Zoology*, *70*(9), 1743–1752. https://doi.org/10.1139/z92-242

Smith, A. M. S., Wooster, M. J., Drake, N. A., Dipotso, F. M., Falkowski, M. J., & Hudak, A. T. (2005). Testing the potential of multi-spectral remote sensing for retrospectively estimating fire severity in African Savannahs. *Remote Sensing of Environment*, *97*(1), 92–115. https://doi.org/10.1016/j.rse.2005.04.014

Somers, B., Asner, G. P., Tits, L., & Coppin, P. (2011). Endmember variability in Spectral Mixture Analysis: A review. *Remote Sensing of Environment*, *115*(7), 1603–1616. https://doi.org/10.1016/j.rse.2011.03.003

Speed, J. D. M., Austrheim, G., Hester, A. J., Mysterud, A., Speed, J. D. M., Austrheim, G., Hester, A. J., & Mysterud, A. (2010). Experimental evidence for herbivore limitation of the treeline. *Ecology*, *91*(11), 3414–3420.

Starks, P. J., Coleman, S. W., & Phillips, W. A. (2004). Determination of Forage Chemical Composition Using Remote Sensing. *Journal of Range Management*, *57*(6), 635–640.

Sturm, M., Racine, C., Tape, K., Cronin, T. W., Caldwell, R. L., & Marshall, J. (2001). Increasing shrub abundance in the Arctic. *Nature*, *411*(May), 546–547.

Tape, K. D., Gustine, D. D., Ruess, R. W., Adams, L. G., & Clark, J. A. (2016). Range expansion of moose in Arctic Alaska linked to warming and increased shrub habitat. *PLoS ONE*, *11*(7), 1–12. https://doi.org/10.1371/journal.pone.0160049

Trigg, S., & Flasse, S. (2000). Characterizing the spectral-temporal response of burned savannah using in situ spectroradiometry and infrared thermometry. *International Journal of Remote Sensing*, *21*(16), 3161–3168.

Tukey, J. W. (1949). Comparing individual means in the analysis of variance. *Biometrics*, 99–114.

Turner, D. P., Cohen, W. B., Kennedy, R. E., Fassnacht, K. S., & Briggs, J. M. (1999). Relationships between leaf area index and Landsat TM spectral vegetation indices across three temperate zone sites. *Remote Sensing of Environment*, *70*(1), 52–68. https://doi.org/10.1016/S0034-4257(99)00057-7

Van Soest, P. J., Robertson, J. B., & Lewis, B. A. (1991). Methods for dietary fiber, neutral detergent fiber, and non- starch polysaccharides in relation to animal nutrition. *Journal of Dairy Science*, *74*, 3583–3597. https://doi.org/10.3168/jds.S0022-0302(91)78551-2

Vierling, L. A., Deering, D. W., & Eck, T. F. (1997). Differences in arctic tundra vegetation type and phenology as seen using bidirectional radiometry in the early growing season. *Remote Sensing of Environment*, *60*(1), 71–82. https://doi.org/10.1016/S0034-4257(96)00139-3

Wang, Z., Townsend, P. A., Schweiger, A. K., Couture, J. J., Singh, A., Hobbie, S. E., & Cavender-bares, J. (2019). Remote Sensing of Environment Mapping foliar functional traits and their uncertainties across three years in a grassland experiment. *Remote Sensing of Environment*, *221*(November 2018), 405–416. https://doi.org/10.1016/j.rse.2018.11.016

Weladji, R. B., Klein, D. R., Holand, Ø., & Mysterud, a. (2002). Comparative reponse of Rangifer tarandus and other nothern ungulates to climatic variability. *Rangifer*, *22*(1), 33–50.

Welch, B. L. (1947). The generalization ofstudent's' problem when several different population variances are involved. *Biometrika*, *34*(1/2), 28–35.

Wolken, J. M., Hollingsworth, T. N., Rupp, T. S., Chapin, F. S., Trainor, S. F., Barrett, T. M., Sullivan, P. F., McGuire, A. D., Euskirchen, E. S., Hennon, P. E., Beever, E. A., Conn, J. S., Crone, L. K., D'Amore, D. V., Fresco, N., Hanley, T. A., Kielland, K., Kruse, J. J., Patterson, T., … Yarie, J. (2011). Evidence and implications of recent and projected climate change in Alaska's forest ecosystems. *Ecosphere*, *2*(11), art124. https://doi.org/10.1890/ES11-00288.1

Wu, H., Levin, N., Seabrook, L., Moore, B., & Mcalpine, C. (2019). Mapping Foliar Nutrition Using WorldView-3 and WorldView-2 to Assess Koala Habitat Suitability. *Remote Sensing*, *11*(215), 1–17. https://doi.org/10.3390/rs11020215

Xue, J., & Su, B. (2017). Significant remote sensing vegetation indices: A review of developments and applications. *Journal of Sensors*. https://doi.org/10.1155/2017/1353691

Zamin, T. J., Côté, S. D., Tremblay, J. P., & Grogan, P. (2017). Experimental warming alters migratory caribou forage quality: *Ecological Applications*, *27*(7), 2061–2073. https://doi.org/10.1002/eap.1590

Zengeya, F. M., Mutanga, O., & Murwira, A. (2012). Linking remotely sensed forage quality estimates from WorldView-2 multispectral data with cattle distribution in a savanna landscape. *International Journal of Applied Earth Observation and Geoinformation*, *21*(1), 513–524. https://doi.org/10.1016/j.jag.2012.07.008

Zhou, J., Tape, K. D., Prugh, L., Kofinas, G., Carroll, G., & Kielland, K. (2020). Enhanced shrub growth in the Arctic increases habitat connectivity for browsing herbivores. *Global Change Biology*, *00*, 1–12. https://doi.org/10.1111/gcb.15104

Tables

Table 3.1. Best performing hyperspectral vegetation index (SVI) results for dietary fibers. These include hemicellulose, cellulose, neutral detergent fiber, acid detergent fiber, acid detergent lignin, and acid insoluble ash and associated variance explained (R^2), root mean square error (RMSE), Akaike's information criterion for small sample sizes (ΔAICc), and leave-one-out cross validation (LOOCV) slope and Spearman rank coefficients (ρ). The first row of each section indicates model statistics for just the SVI model, while subsequent rows show how model statistics change when adding leaf area (LA) from the top of the canopy (sun), bottom of the canopy (shade), or combined sun and shade leaves (total). Comparisons of ΔAICc and ΔLOOCV are in reference to the SVI model only for each fiber.

Models	R^2	RMSE	AICc	ΔAICc	LOOCV Slope	LOOCV ρ	ΔLOOCV
Hemicellulose (HMC)							
SVI	0.68	0.42	34.62	-	0.66	0.73	-
SVI+ LA Sun	0.74	0.37	31.45	−3.17	0.75	0.69	−4%
SVI+ LA Shade	0.69	0.41	35.48	+0.86	0.68	0.77	+4%
SVI+ LA Total	0.72	0.39	32.63	−1.99	0.71	0.73	0
Cellulose (CLL)							
SVI	0.61	0.42	34.48	-	0.59	0.78	-
SVI+ LA Sun	0.59	0.43	37.14	+2.69	0.56	0.80	+2%
SVI+ LA Shade	0.60	0.42	36.90	+2.42	0.55	0.81	+3%
SVI+ LA Total	0.60	0.42	36.97	+2.49	0.56	0.81	+3%
Neutral detergent fiber (NDF)							
SVI	0.51	0.99	75.30	-	0.57	0.79	-
SVI+ LA Sun	0.55	0.93	74.82	−0.40	0.59	0.81	+2%
SVI+ LA Shade	0.67	0.80	67.65	−7.65	0.62	0.87	+8%
SVI+ LA Total	0.62	0.86	71.02	−4.28	0.60	0.85	+6%
Acid detergent fiber (ADF)							
SVI	0.56	0.61	51.31	-	0.53	0.75	-
SVI+ LA Sun	0.53	0.61	54.15	+2.84	0.48	0.76	+1%
SVI+ LA Shade	0.53	0.61	54.20	+2.89	0.50	0.75	0
SVI+ LA Total	0.53	0.61	54.17	+2.86	0.49	0.76	+1%
Acid detergent lignin (ADL)							
SVI	0.48	0.25	9.46	-	0.49	0.83	-
SVI+ LA Sun	0.49	0.25	10.86	+1.46	0.51	0.82	−1%
SVI+ LA Shade	0.51	0.24	9.87	+0.41	0.52	0.82	−1%
SVI+ LA Total	0.51	0.24	10.07	+0.61	0.52	0.82	−1%
Acid detergent ash (AIA)							
SVI	0.58	0.04	−83.54	-	0.57	0.81	-
SVI+ LA Sun	0.56	0.04	−82.77	+0.84	0.55	0.81	0
SVI+ LA Shade	0.58	0.04	−81.94	+1.60	0.58	0.81	0
SVI+ LA Total	0.56	0.04	−80.73	+2.81	0.55	0.81	0

Table 3.2. Best performing band equivalent reflectance (BER) of WorldView3 (WV3) spectral vegetation index (SVI) results for dietary fibers. These include hemicellulose, cellulose, neutral detergent fiber, acid detergent fiber, acid detergent lignin, and acid insoluble ash and associated variance explained (R^2), root mean square error (RMSE), Akaike's information criterion for small sample sizes (ΔAICc), and leave-one-out cross validation (LOOCV) slope and Spearman rank correlations (ρ). The first row of each section indicates model statistics for just the SVI model, while subsequent rows show how model statistics change when adding leaf area (LA) from the top of the canopy (sun), bottom of the canopy (shade), or combined sun and shade leaves (total). Comparisons of ΔAICc and ΔLOOCV are in reference to the SVI model only for each fiber.

Models	R^2	RMSE	AICc	ΔAICc	LOOCV Slope	LOOCV ρ	ΔLOOCV
Hemicellulose (HMC)							
SVI	0.32	0.62	52.65	-	0.27	0.52	-
SVI+ LA Sun	0.41	0.56	50.74	−1.91	0.39	0.72	+20%
SVI+ LA Shade	0.40	0.57	51.38	−1.27	0.38	0.72	+20%
SVI+ LA Total	0.45	0.55	49.29	−3.36	0.43	0.72	+20%
Cellulose (CLL)							
SVI	0.25	0.59	50.10	-	0.22	0.45	-
SVI+ LA Sun	0.23	0.59	52.44	+2.34	0.20	0.50	+5%
SVI+ LA Shade	0.22	0.59	52.66	+2.56	0.18	0.49	+4%
SVI+ LA Total	0.23	0.58	52.44	+2.34	0.19	0.49	+4%
Neutral detergent fiber (NDF)							
SVI	0.31	1.18	83.33	-	0.26	0.67	-
SVI+ LA Sun	0.33	1.14	84.34	+1.01	0.31	0.71	+4%
SVI+ LA Shade	0.45	1.03	79.82	−3.51	0.43	0.78	+11%
SVI+ LA Total	0.39	1.08	82.09	−1.24	0.37	0.78	+11%
Acid detergent fiber (ADF)							
SVI	0.30	0.76	62.10	-	0.28	0.57	-
SVI+ LA Sun	0.34	0.72	62.40	+0.30	0.35	0.66	+9%
SVI+ LA Shade	0.40	0.69	60.43	−2.33	0.38	0.76	+19%
SVI+ LA Total	0.38	0.70	60.92	−2.82	0.38	0.73	+16%
Acid detergent lignin (ADL)							
SVI	0.34	0.28	15.05	-	0.33	0.70	-
SVI+ LA Sun	0.32	0.28	17.51	+2.46	0.32	0.71	+1%
SVI+ LA Shade	0.34	0.28	17.00	+1.95	0.33	0.71	+1%
SVI+ LA Total	0.33	0.28	17.19	+2.14	0.33	0.69	−1%
Acid detergent ash (AIA)							
SVI	0.13	0.05	−66.35	-	0.11	0.31	-
SVI+ LA Sun	0.09	0.05	−63.45	+2.90	0.08	0.31	0
SVI+ LA Shade	0.10	0.05	−63.78	+2.57	0.09	0.31	0
SVI+ LA Total	0.09	0.05	−63.54	+2.81	0.08	0.28	−3%

Figures

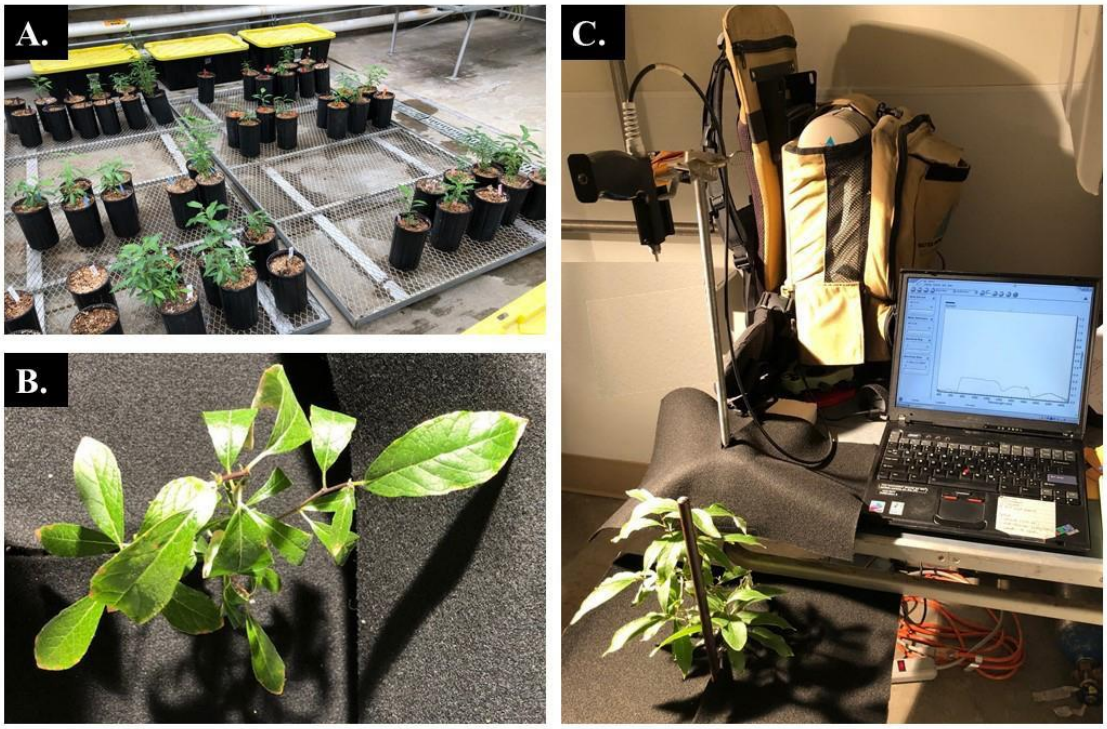

Figure 3.1. Experimental and data collection set up for greenhouse study. Willows were grown in a greenhouse setting (A) and canopy spectra were collected using an FieldSpec Pro Full Range Spectroradiometer (C). A spectrally flat black-foam material below the canopy to avoid introducing soil and background noise (B).

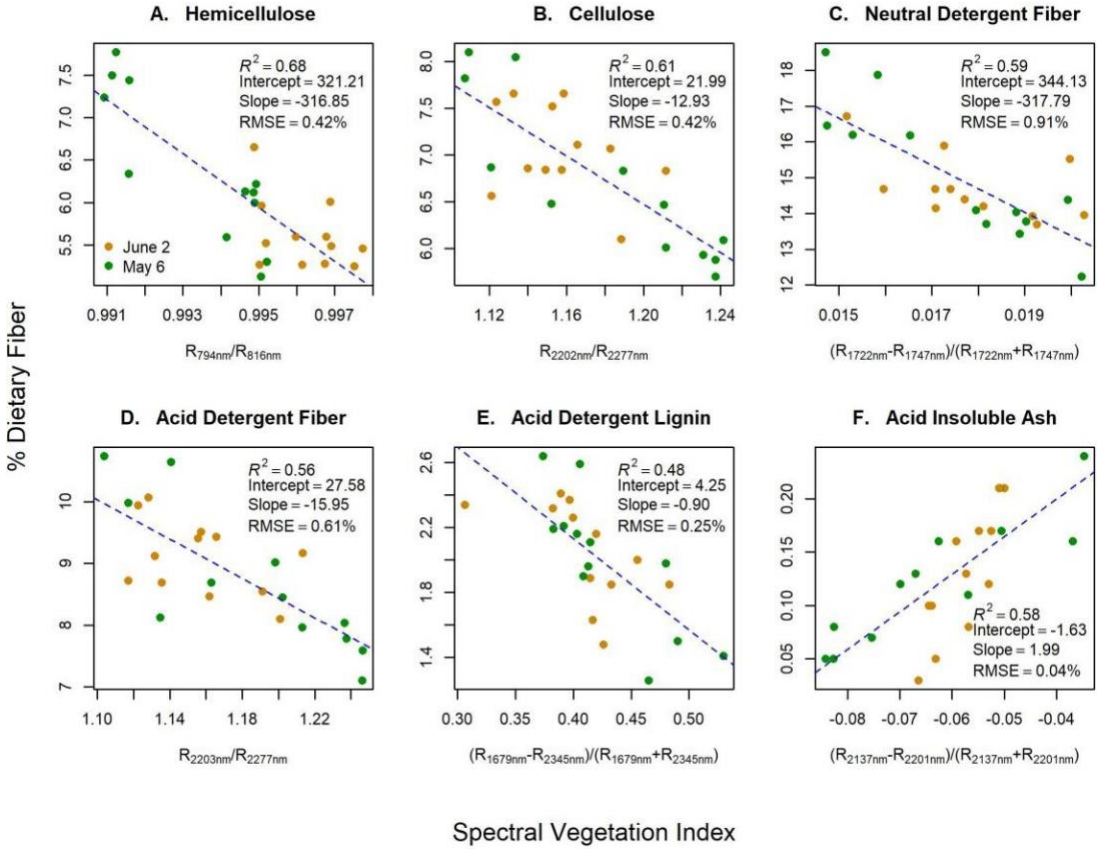

Figure 3.2. Spectral vegetation indices (SVIs) from hyperspectral data for green dietary fibers concentrations (Y-axis) of (A) hemicellulose, (B) cellulose, (C) neutral detergent fiber, (D) acid detergent fiber, (E) acid detergent lignin, and (F) acid insoluble ash. X-axis labels represent the measured reflectance (R) at given wavelengths in nanometers of SVIs.

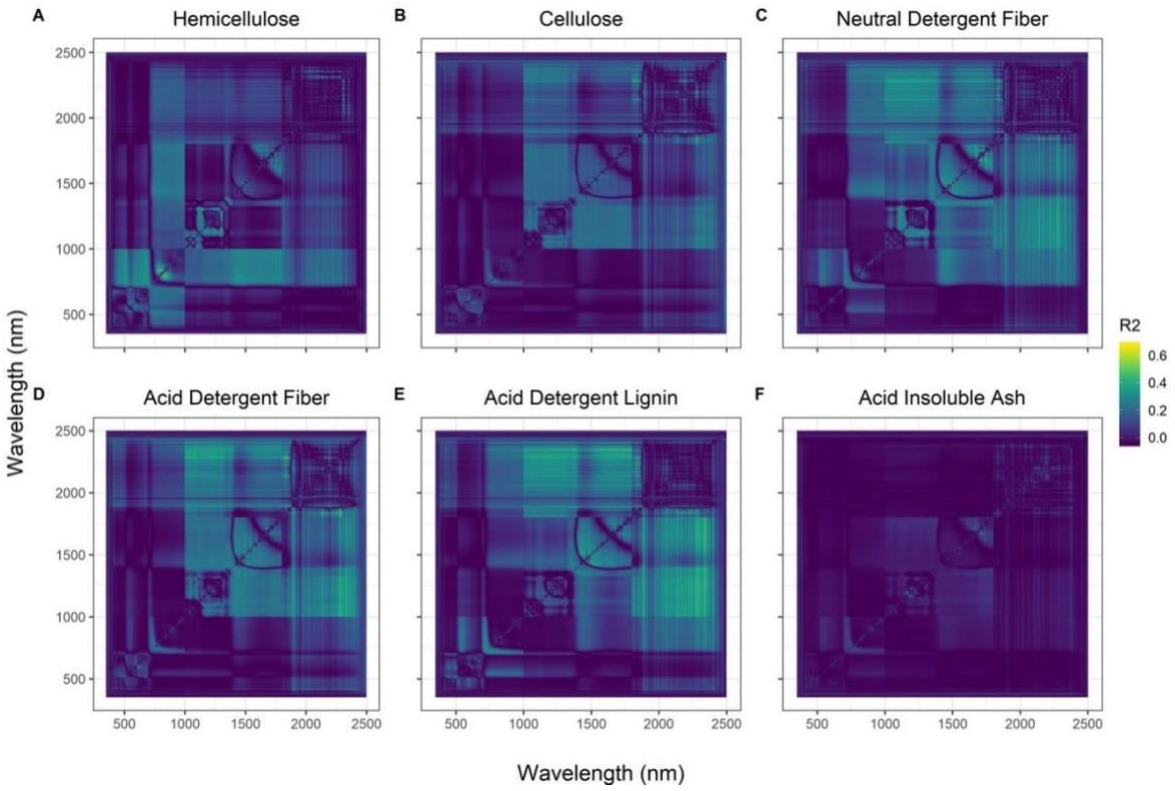

Figure 3.3. Coefficients of determination (R^2) between green dietary fibers (A) hemicellulose (HMC), (B) cellulose (CLL), (C) neutral detergent fiber (NDF), (D) acid detergent fiber (ADF), (E) acid detergent lignin (ADL), and (F) acid insoluble ash (AIA) and simple ratio spectral vegetation indices (SVIs) generated from hyperspectral data. The x- and y-axes are the wavelength (nm) from the spectrometer. The best performing SVIs were R_{794nm}/R_{816nm} for HMC, R_{2202nm}/R_{2277nm} for CLL, $(R_{1722\mathrm{nm}} - R_{1747nm})/(R_{1722nm} + R_{1747nm})$ for NDF, R_{2203nm}/R_{2277nm} for ADF, $(R_{1679nm} - R_{2345nm})/(R_{1679nm} + R_{2345nm})$ for ADL, and $(R_{2137nm} - R_{2201nm})/(R_{2137nm} + R_{2201nm})$ for AIA—where R represents the measured reflectance at given wavelengths in nanometers.

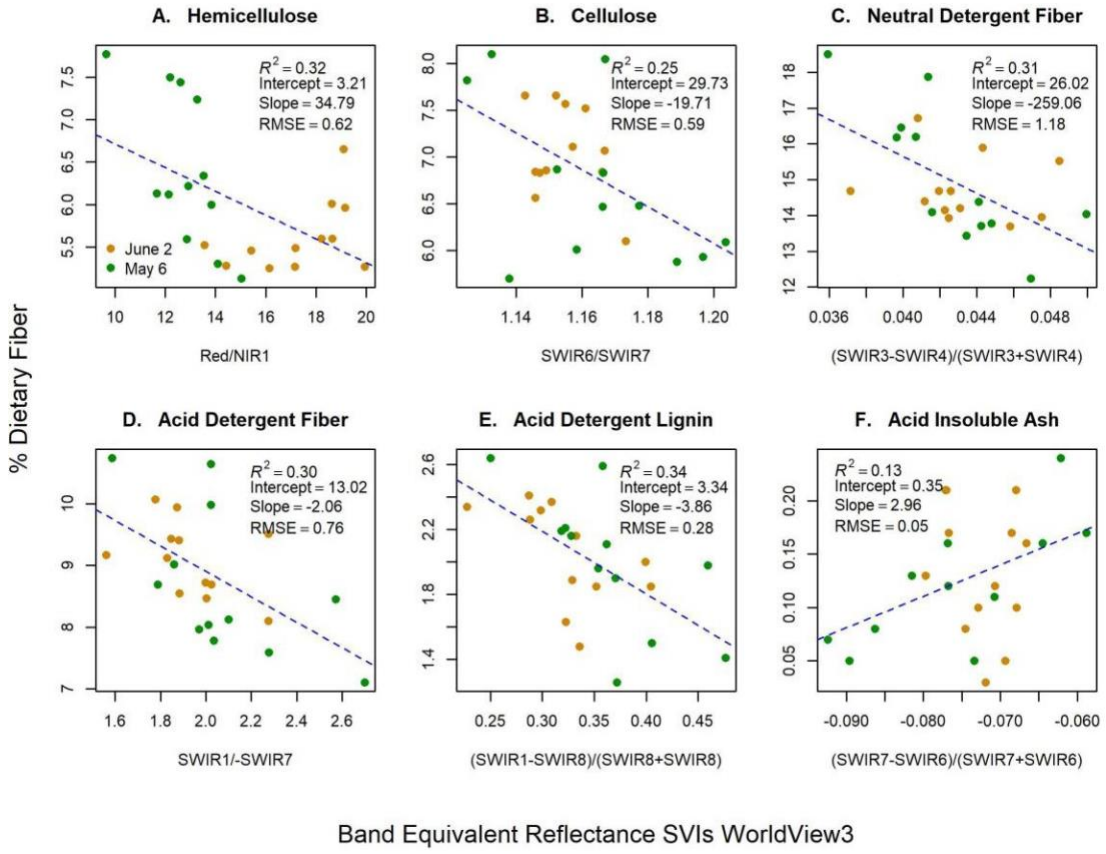

Figure 3.4. Band equivalent reflectance of WorldView-3 (WV-3) spectral vegetation indices (SVIs) for green dietary fibers concentrations (Y-axis) of (A) hemicellulose, (B) cellulose, (C) neutral detergent fiber, (D) acid detergent fiber, (E) acid detergent lignin, and (F) acid insoluble ash. X-axis labels represent the WV-3 bands used to create the best performing SVIs, and contain red, near infrared-1 (NIR1), and shortwave infrared (SWIR) bands.

Chapter 4: Estimating integrated measure of forage quality for northern herbivores by fusing optical and structural remote sensing data

Authors: Jyoti S. Jennewein, Jan U.H. Eitel, Kyle Joly, Ryan Long, Andrew J. Maguire, Lee A. Vierling, William Weygint

In preparation for: *Environmental Research Letters*

Abstract

Northern herbivore ranges are expanding in response to increased forage biomass produced by a warming climate. Forage quality also influences herbivore distributions, but less is known about the effects of climate change on plant biochemical properties. Remote sensing could enable landscape-scale estimations of forage quality, which is of great interest to wildlife managers. Despite the importance of integrated forage quality metrics like digestible protein (DP) and digestible dry matter (DMD), however, few studies have applied remote sensing approaches to estimate and monitor these characteristics. Our objectives were twofold: (1) assess how well DP and DMD can be predicted using hyperspectral remote sensing, and (2) to determine whether incorporating shrub structural metrics affected by browsing would improve our ability to predict DP and DMD. We collected canopy-level spectra, destructive-vegetation samples, and flew unmanned aerial vehicles (UAVs) in areas dominated by willow shrubs in northcentral Alaska in July 2019. Canopy structural metrics were derived from 3-D structural information obtained from UAV imagery using structure from motion photogrammetry. We used generalized least squares regression to account for the spatial autocorrelation of sampled shrubs. The best performing model for DP had two predictors: a spectral vegetation index (SVI) that included a red-edge and shortwave infrared band, and shrub height variability (HVAR; Nagelkerke R^2= 0.81, RMSE= 4.96%, cross validation ρ = 0.85). DMD had three predictors: an SVI that included that used a blue and a red band HVAR, and leaf area index (Nagelkerke R^2= 0.70, RMSE= 1.46%, cross validation ρ = 0.79). Results from our study demonstrate that integrated forage quality metrics like DP and DMD can be successfully quantified using hyperspectral remote sensing data, and that models based on those data can be improved by incorporating additional shrub structural metrics. Modern airborne sensor platforms such as Goddard's LiDAR, Hyperspectral & Thermal Imager (G-LiHT) provide opportunities to fuse data streams from both structural

and optical data, which may enhance our ability to estimate and scale important foliar properties such as DP and DMD.

Introduction

The range of some northern herbivore are expanding in response to increased forage biomass produced by a warming climate (Tape et al., 2016; Zhou et al., 2017, 2020). Herbivore range expansions may also impact nutrient cycling (Doiron et al., 2014; Schmitz et al., 2018; Zamin et al., 2017). For example, high levels of herbivory may accelerate the successional transition of palatable forage species such as willow (*Salix* spp.) to unpalatable species such as alder (*Alnus* spp.) or conifers (Christie et al., 2015; Kielland & Bryant, 1998; Pastor et al., 1988). Such transitions in species composition can alter ecosystem carbon and nitrogen dynamics (Schmitz et al., 2018). For instance nutrient turnover rates may decrease cellulose and defensive chemicals are higher in less palatable species (Pastor et al., 1993). In addition to forage biomass, herbivore distributions have also been linked to variation in forage quality (Ball et al., 2000; Wu et al., 2019).

Forage quality is influenced by the concentration of chemical constituents and have important bottom-up effects on herbivore life-history traits such as maternal body condition, pregnancy rates, and survival (Parker et al., 2009). Characterizing forage quality for herbivores is complex. Fiber, crude protein, and defensive chemical concentrations all play a role in defining forage quality (DeGabriel et al., 2014; Hebblewhite et al., 2008; McArt et al., 2009; Mirik et al., 2005). Despite the importance of these individual chemical constituents, previous studies have called for increased attention to integrated measures of forage quality such as digestible protein (DP) and digestible dry matter (DMD; Foley & Moore, 2005; McArt et al., 2009) because simpler metrics of forage quality such as crude protein do not capture the full range of characteristics that can influence palatability and fitness.

Integrated forage quality metrics such as DP are strongly influenced by the presence of tannins (Hanley et al., 1992; Robbins et al., 1987a; Robbins et al., 1987b), an important plant secondary compound which significantly reduces protein digestion for herbivores by binding to plant proteins and therefore limiting protein digestion (Spalinger et al., 2010). DP is particularly important in northern landscapes because plant available nitrogen is often limited (Sponseller et al., 2016), which in turn limits nitrogen available to herbivores (McArt et al., 2009; White 1993). Because DP estimations reflect a chemical relationship between

the protein precipitating capacity of tannins and the total concentration of protein it can be used as an estimate of forage quality for numerous herbivore species. However, DP does not account for the overall digestibility of forage which varies according to herbivore species.

Body size exerts a strong influence on the digestive capabilities of herbivores (Van Soest, 1996). Smaller body size facilitates selective feeding choices, whereas larger body size increases the overall fraction of digestible forage retained by herbivores (Van Soest, 1996). For instance, moose (*Alces alces*) are large-bodied ruminants whose large size enables even the poorest quality of forage to be digested. DMD is an important integrated forage quality metric that estimates the portion of plant matter that is digestible by an herbivore. DMD estimates vary depending on the herbivore in question. For instance, in vitro DMD can be estimated with fistulated animals. DMD can also be estimated mathematically for ruminants using developed equations that account for the concentration of DP and fiber concentrations (Robbins et al., 1987a; Hanley et al., 1992). Nutritional estimates of forage quality have classically relied on laboratory analyses to quantify forage quality or direct assessments of fistulated animals. However, in the past two decades remote sensing has emerged as a viable, in situ method for assessing forage quality and enables the characterization of broad geographic extents (Knox et al., 2011; Mirik et al., 2005; Skidmore et al., 2010; Youngentob et al., 2012).

Remote sensing enables landscape-scale monitoring of forage quality, which is of great interest to wildlife managers (Vance et al., 2016; Walton et al., 2013). Optical remote sensing approaches use reflected light from the visible (400-700 nm) to the shortwave infrared (SWIR; 1400-2500 nm) and have been used to detect variation in foliar chemistry. To date, much of the optical remote sensing research has focused on detecting individual components of forage quality such as crude protein, fiber, or defense chemicals like condensed tannins (Ferwerda et al., 2006; Jennewein et al., 2020; Mirik et al., 2005; Skidmore et al., 2010; Thulin et al., 2012). Youngentob et al.'s (2012) pioneering work demonstrated that DP and DMD could be successfully estimated across the landscape in *Eucalyptus* trees using hyperspectral remote sensing, which samples reflected light in very narrow (3-10 nm), contiguous spectral bands (Goetz, 2009). Similarly, Wu et al. (2019) provided the first example of successful DP estimation using the multispectral WorldView-3 satellite, which contains much broader spectral bands (30-180 nm) compared to hyperspectral

data. Despite the importance of integrated forage quality metrics like DP and DMD, few studies apply remote sensing approaches to map these characteristics across the landscape and no studies have assessed them in Arctic-boreal regions that are undergoing rapid changes due to warming (Serreze et al., 2000; Verbyla, 2008; Wolken et al., 2011).

Therefore, our first hypothesis (H1) was that integrated forage quality metrics – DP and DMD – in palatable willow shrubs can be predicted using hyperspectral remote sensing. We used hyperspectral remote sensing (as opposed to multispectral) because high spectral resolution data can be directly linked to absorption and scattering features of foliar properties known to influence palatability (Curran, 1989; Elvidge, 1990; Kokaly et al., 2009). We focused on willow species because they are the preferred forage resource for many vertebrate herbivores in Alaska.

Additionally, browsing intensity can drastically alter plant canopy architecture (Christie et al., 2014) and consequentially alter the concentrations of foliar chemical properties that influence palatability (Bryant, 1981; Bryant & Chapin, 1986). For instance, moderate browsing stimulates compensatory growth, which in turn creates bushier shrubs that are frequently re-browsed (Stouter, 2008). In contrast, heavy browsing stunts growth, decreases shrub height, and increases canopy openness (Christie et al., 2014, Kielland & Bryant, 1998). Although plant canopy architecture can be strongly influenced by browsing intensity, ground-based assessments traditionally use only three categories to classify browsing history – unbrowsed, browsed, and broomed (Figure 4.1). Yet variation in broomed architecture can be pronounced (Figure 4.1 A and D) and may indicate distinct functional differences such as added nitrogen from herbivore excreta (Butler & Kielland, 2008; Kielland & Bryant, 1998).

Recently, remote sensing technologies such as lidar (light detection and ranging) have shown utility in assessing vegetation structure for wildlife applications (e.g., Lone et al., 2014; Melin et al., 2016; Vierling et al., 2008). For example, studies in Europe's boreal forests have demonstrated that metrics derived from aerial lidar can successfully detect insect defoliation (Solberg et al., 2006; Vastaranta et al., 2013) and heavy moose browsing (Melin et al., 2016) on young Scots pine (*Pinus sylvestris*) stands. There is also great potential for fusing lidar with optical remote sensing to improve the characterization of ecosystems (Asner et al., 2012; Luo et al., 2017; Torabzadeh et al., 2014). However, the collection of aerial lidar

data may be cost-prohibitive, and 'structure from motion' (SfM) data acquired from unmanned aerial vehicles (UAV) are considered a viable alternative to aerial lidar (Wallace et al., 2016).

Thus, our second hypothesis (H2) was that statistical models for estimating DP and DMD using hyperspectral data would be improved when shrub structural metrics obtained from UAV SfM point clouds were incorporated because herbivores can drastically alter canopy structure (Figure 4.1; Christie et al., 2014). Additionally, because sunlit and shaded leaves in Alaska often differ in their concentrations of important foliar chemicals such as fiber (Molvar et al., 1993) and tannins (Bryant & Chapin, 1986; Klein, 1990; Thompson & Barboza, 2014) that influence the palatability of forage species, we also hypothesized that including the cumulative irradiance (W m^{-2}) incident on a shrub in a growing season would improve models (H3). We predicted that as cumulative irradiance increased, DP and DMD would decrease because nitrogen concentrations increase and fiber decreases in shaded plants (Lenart et al., 2002; Molvar et al., 1993). Similarly, topographic attributes such as aspect and slope influence the amount of solar radiation received by plants. Additionally, elevational gradients influence plant phenology, where higher-elevation plants often have a delayed onset of budburst, which in turn influences migrant herbivore behaviors as they move to "surf the green wave" (Bischof et al., 2012; Mysterud et al., 2017). Thus, our fourth hypothesis was that including topographic attributes from the ArcticDEM would improve our ability to remotely monitor forage quality (H4), because previous work demonstrates that combining hyperspectral data with topographic features such as aspect, slope, and elevation can improve model predictions of forage quality (Knox et al., 2012; Pullanagari et al., 2018).

Methods and Materials

Study area

The upper Koyukuk River drainage in northcentral Alaska (Figure 4.2) contains a wide range of terrain and vegetation including boreal forest dominated by black spruce (*Picea mariana*), alpine tundra and shrubs such as alders, willows, and dwarf birch (*Betula glandulosa*), as well as muskegs and other riparian vegetation such as white spruce (*Picea glauca*) and poplar (*Populus spp.*). Located in the southern end of the Brooks Range, topography is rugged and varies from 80 to 2250 m. The region experiences continental climate patterns. In winter, the average temperature ranges from -22 to -40° C, with snow depths exceeding 60 cm most

winters. In summer, the average temperature ranges from 3 to 16° C, but can also reach >30° C.

Field-based forage-quality assessment study

We collected vegetation spectra and destructive-vegetation samples from willow shrubs along a latitudinal transect in the Koyukuk River drainage (n=45 in July 2019; Figure 4.2). We stratified sites across soil types, elevation, and burn history, because a random sample was unlikely to include the range of nutrient concentrations needed to drive wildlife selection (DeGabriel et al., 2014). We collected spectral information using a FieldSpec Pro Full Range Spectroradiometer (Analytical Spectral Devices, Incorporated), which ranged from 350-2500 nm. This instrument has a full-width half-max spectral resolution of 3 nm in the visible and near infrared (NIR) range (i.e., 350-1050 nm), and 10-12nm in both the NIR and short-wave infrared (SWIR) regions of the electromagnetic spectrum (i.e., 1050-2500nm). We collected canopy spectral signatures under low cloud (<20%) conditions and between 11:00 and 15:00 to minimize confounding effects of illumination geometry. Canopy-level spectra were collected on sun-exposed leaves in each of the four cardinal directions and averaged into a single representative spectral signature to eliminate canopy-level variation in nutrient distribution. Prior to sampling in each direction, dark current and white reference measures were obtained using a Spectralon panel (Labsphere, Inc., North Sutton, New Hampshire, United States). We then calculated spectral vegetation indices (SVIs) indices using all possible band combinations in the simple ratio-type vegetation index (Band A/Band B) and normalized difference-type vegetation index (Band A - Band B)/(Band A + Band B) formats and related them to calculated DP and DMD (H1).

We collected destructive vegetation samples, which we dried at 30-40° C for 12 hours. The Washington State University Habitat Laboratory analyzed each sample for percent: (1) crude protein, (2) neutral detergent fiber, (3) acid detergent fiber, (4) acid detergent lignin, (5) acid insoluble ash, and (6) tannins using the CBB-BSA (2000) methodology. Integrated measures of forage quality were calculated using the Robbins (1987a, 1987b) equations for DP and DMD. Estimates of DMD and DP were quantified on a percent dry matter basis.

Landscape and Shrub Structural Variables

We collected UAV data prior to destructive vegetation samples were taken using a DJI Phantom 4 Pro (Los Angeles, California, USA). Flight elevation ranged from 20 to 25 m above ground level with a frontal and side overlap of 80% resulting in a spatial resolution of 1 cm. To minimize atmospheric interference, flights occurred on sunny days between 11:00 and 15:00. Three-dimensional (3-D) structural information was obtained from UAV imagery using SfM photogrammetry implemented in the Pix4Dmapper software package (Pix4D, 2016). Using CloudCompare (CloudCompare, 2020) open-source software we manually cropped the point cloud to the footprint of sampled shrub crowns and interpolated fine-scale (1 cm) digital surface models (DSMs) that were then processed to obtain information on canopy structural characteristics: coefficient of variation of height (HCV), variance of heights (HVAR), and standard deviation of heights (HSD), using the 'rLiDAR' package (Silva et al., 2017). We focused on these three UAV-based plant structural metrics with the aim of capturing the effect of browsing on willow canopies (H2), because plant canopy architecture may be drastically altered by herbivores thereby altering branching structure and increasing canopy openness (Christie et al., 2014; Kielland & Bryant, 1998), which in turn can influence palatability (Bryant, 1981; Bryant & Chapin, 1986).

As with the UAV-based measures of plant structure, we included leaf area index (LAI) as a potential proxy for browsing history that may capture variation in branching structure and thus foliar nutritional properties that resulted from herbivores (H2). We estimated LAI using hemispherical photos that captured canopy structure of a single shrub in the four cardinal directions. LAI is defined as the amount of leaf area (of a single side of a leaf) per unit ground area. A camera equipped with a 'fisheye' lens was mounted on a stable tripod and levelled prior to collection. When possible, photos were collected under cloudy conditions in the morning or evening to minimize light scattering through the canopy. On sunny days, an umbrella was used to mitigate direction exposure of solar radiation during image collection. Hemispherical photos were processed using Hemiphot (ter Steege, 2018), which uses canopy gap fractions to estimate LAI indirectly.

We also interpolated DSMs (10 cm resolution) for the plots from our UAV SfM point clouds, which were used to model the light environment of the outer portion of sampled willow canopies (H3) using the 'insol' package (Corripio, 2015). This package estimates the instantaneous irradiance (W m^{-2}) for a given location using a DSM and atmospheric (i.e.,

relative humidity, ozone, visibility, air temperature) and surface reflectance (i.e., albedo) properties, which we acquired through the Env-DATA annotation service (Dodge et al., 2013). Based on solar geometry, local topography, surface reflectance, and atmospheric properties we estimated diffuse and direct canopy irradiance for every minute of the summer, which we summed into 'total irradiance' for each shrub location. We modelled the total irradiance experienced by a shrub one week, two weeks, and one month prior to harvest.

Finally, topographic attributes including elevation, aspect, and slope were sourced from the ArcticDEM (Porter et al., 2018) and included as additional landscape metrics to predict DP and DMD (H4). We also used the ArcticDEM to calculate a topographic wetness index (TWI). TWI uses slope and the upstream contributing area to determine topographic effects on hydrological processes. We included topographic wetness in addition to other topographic metrics because TWI has been shown to influence nitrate concentrations (Ogawa et al., 2006), which directly impacts the nitrogen available for plant uptake and hence plant protein levels.

Data Analyses

All data analyses were conducted in R statistical software (R Core Team, 2020). The best performing SVIs were identified using adjusted R^2 values and the root mean square error (RMSE). We used generalized least squares (GLS) regression in the 'nlme' package (Pinheiro et al., 2017) to determine the optimal spatial correlation structure using Akaike Information Criterion (AIC; Akaike, 1974; Table 4.1). After selecting a correlation structure for DP and DMD, we assessed the benefit of adding shrub structure, topographic attributes, and irradiance to models by sequentially adding one additional metric at a time. We evaluated competing models using: (1) AIC, (2) RMSE, and (3) two pseudo R^2 values, the McFadden and Nagelkerke. McFadden R^2 is often used to compare nested models (McFadden & Zarembka, 1974), but values are less comparable to adjusted R^2 from linear regression (i.e., values from 0.2-0.4 indicate excellent fit; Hensher & Stopher, 1979). Nagelkerke R^2 values can range from 0-1, making that metric similar to R^2 from linear regression as an indicator of the overall model predictive strength (Field et al., 2012). We also calculated AIC weights, which sum to one with values ranging from 0 to 1 and may be interpreted as the probability that a given model is the best model (Symonds & Moussalli, 2011) in the set of candidate models for both DP and DMD. Additionally, we conducted

leave-one-out cross validation (LOOCV) by sequentially leaving out one willow at a time and using the remaining observations to predict the excluded one. We compared LOOCV slopes (observed values plotted against predicted values) to assess bias and Spearman rank coefficients (ρ) to quantify predictive ability of these models. The residuals of the GLS models met regression assumptions (i.e., homogeneity of variance, normality of residuals). Finally, we explored combing models that included all predictors that improved model fit (decreases in AIC >2) into a single model for both DP and DMD. Predictors were only combined in the same model if collinearity between them was <0.70 (Dormann et al., 2013).

Results

DP ranged from 1.57% to 13.37% of dry matter, while DMD ranged from 22.73% to 61.76% of dry matter. Models consistently underpredicted DP and DMD (LOOCV slopes <1; Table 4.2). However, we found that hyperspectral SVIs successfully predicted DP (Adjusted R^2 = 0.77, RMSE = 1.42%) and DMD (Adjusted R^2 = 0.61, RMSE = 5.11%), which supported our first hypothesis. The best performing SVI for DP included a red-edge and a SWIR band in the normalized difference format ($(R_{703nm} - R_{1719nm})/(R_{703nm} + R_{1719nm})$). The best performing SVI for DMD included a blue and a red band in the simple ratio format (R_{483nm}/R_{657nm}). Many viable simple ratio SVIs were found for both DP and DMD (Figure 4.3). Of the irradiance options modelled – total irradiance experienced by a shrub one week, two weeks, and one month prior to harvest – the one-week cumulative irradiance before sample harvest produced the best model fit (not shown). Thus, we only included results from this model.

The exponential correlation structure had the lowest AIC for DP (AIC=157.70; Table 4.1) but LOOCV models did not converge using this structure. Thus, we used the spherical correlation structure (AIC=158.79). The best performing SVI showed very strong predictive power (LOOCV ρ =0.88, slope=0.76) and a very low error estimate (RMSE=1.42%; Table 4.2) without the inclusion of any structural metrics (H1). Model fits did improve when two structural metrics were added (H2): HVAR (AIC=154.08, AIC weight=0.56) and HSD (AIC=155.29, AIC weight=0.31) were incorporated, but both models saw a slight decrease in predictive power when compared to the base model using only the SVI (ΔLOOCV ρ = -3%). However, because of the strong correlation (r >0.7) between HSD and HVAR predictors, we

could not create a combined model for DP. Thus, the model with the lowest AIC and highest AIC weight was considered the best model, which included an SVI and HVAR (Figure 4.4).

The exponential correlation structure fit the data for DMD the best (AIC=275.81; Table 4.1), but LOOCV models did not converge using this structure. Thus, we used the rational quadratic correlation structure (AIC=275.94). Using only the SVI, the model showed good predictive power (LOOCV ρ =0.75, slope=0.58) with a low error estimate (RMSE=5.11%; Table 4.2) without the inclusion of any structural metrics (H1). Model fit improved when some structural metrics were added (H2): LAI (AIC=273.98), HVAR (AIC=263.85), and HSD (AIC=267.01) were added to the SVI (Table 4.2). The best performing combined model for DMD included SVI, HVAR, and LAI (Table 4.2; Figure 4; Nagelkerke Pseudo R^2=0.70, AIC=261.09, AIC weight = 0.63, LOOCV ρ = 0.79). Increased error estimates in DMD compared to DP may be related to the relative range of values associated with these estimates, 1.57% to 13.37% for DP and 22.73% to 61.76% for DMD. We observed little evidence that including the light environment (H3) nor topographic attributes (H4) produced model improvements.

Discussion

We assessed how well integrated measures of forage quality – DP and DMD – could be predicted using a fusion of hyperspectral SVIs, shrub structural metrics, topographic attributes, and the light environment. Results from our study demonstrated that DP and DMD could be successfully estimated using hyperspectral remote sensing (H1). Remotely sensed estimates of DP showed a strong correlation with observed estimates and low error (LOOCV ρ = 0.88, RMSE=1.42%); DMD estimates also were highly correlated with measured values, but with higher error (LOOCV ρ = 0.75, RMSE=5.11%). These findings were consistent with previous work in Australian *Eucalyptus* forests where DP (R^2=0.64) and DMD (R^2=0.78) were estimated with high accuracy using hyperspectral remote sensing approaches (Youngentob et al., 2012), though our results suggested DP in northern ecosystems is better predicted than DMD.

Although wavelengths used in the SVIs in this study did not correspond exactly to existing absorption features previously identified for tannins, protein, or fibers (Curran, 1989; Elvidge, 1990; Ferwerda et al., 2006), they were within 25 nm. The SVI for DP contained one wavelength (703 nm) in the red-edge portion of the spectrum, which is known to be

sensitive to chlorophyll and has been used as a proxy for nitrogen content (Eitel et al., 2007; Ramoelo et al., 2012; Wang et al., 2012). DP's second wavelength (1719 nm) was directly adjacent to a known absorption feature of hemicellulose at 1720 nm (Elvide 1990), though numerous tannin absorption features can be found in the shortwave infrared (SWIR; range) region (Ferwerda et al., 2006). In contrast to DP, the wavelengths in DMD's SVI were both in the visible portion of the spectrum (483 nm and 657 nm) and near known spectral features of chlorophyll pigments (Ben-Dor et al., 1997; Curran, 1989), which are often related to plant nitrogen concentrations. This was somewhat surprising because DMD estimates incorporated fiber concentrations that usually have absorption in the SWIR region (Curran, 1989; Elvidge, 1990). For instance, the SWIR region was shown to be sensitive to both DP and DMD in Australian Eucalyptus trees (Youngentob et al., 2012). In our case, we found several viable vegetation indices for DP and DMD (Figure 4.3), many of which also included SWIR wavelengths.

We also observed some improvement in model fit by incorporating shrub structural metrics such as HVAR and LAI (H2). Model fit and AIC weights indicated that the best model for DP included HVAR in addition to the SVI (ΔAIC = -3.62; AIC weight=0.56; Table 4.2), although this addition slightly reduced predictive power (ΔLOOCV= -3%). The best model for DMD included HVAR and LAI, which moderately enhanced predictive power (ΔLOOCV= +4%, AIC weight=0.63; Table 4.2). Herbivores strongly influence plant canopy architecture of palatable species such as willow. Previous work showed browsing influenced shrub height, canopy openness, and branching structure (Christie 2014, 2015; Kielland and Bryant 1998), which in turn can affect the palatability of forage species. To our knowledge, this study was the first to incorporate remotely sensed shrub structural metrics as a proxy for browsing history in models to predict forage quality. Our results indicated that incorporating shrub structure is an important, and often unconsidered, aspect of remotely sensed forage quality metrics.

Based on these findings we suggest that future work should consider shrub structure when using remote sensing to study forage quality metrics. Additionally, because SVIs calculated from passive spectral remote sensing are influenced by plant structural characteristics (Chen & Cihlar, 1996; Eitel et al., 2008; Turner et al., 1999), variation in canopy structure increases the complexity of the three-dimensional space where photons

interact (Asner, 1998; Knyazikhin et al., 2013). This, coupled with the impacts of browsing, suggests a growing need to incorporate structure into remotely sensed models of forage quality to better estimate and map these metrics across the landscape. Modern airborne sensor platforms such as Goddard's LiDAR, Hyperspectral & Thermal Imager (G-LiHT; 1m pixels, with 6 lidar pulses per m^2) provide opportunities to fuse data streams from both structural and optical data (Cook et al., 2013), which may enhance our ability to estimate and scale important foliar properties such as DP and DMD.

Strategies for estimating spatiotemporal variation in forage quality metrics are needed because northern ecosystems are rapidly changing. The range of northern herbivores is expanding as the quantity of forage resources increases (Tape et al., 2016; Zhou et al., 2017, 2020). However, the impact of climate warming on forage quality is less clear and will likely vary depending on region and species (Elmendorf et al., 2012; Hansen et al., 2006; Lenart et al., 2002; Turunen et al., 2009). Since forage quality strongly influences herbivore life-history traits like maternal body condition, pregnancy rates, and survival (Parker et al., 2009), monitoring 'nutritional landscapes' (*sensu* Merems et al., 2020) that include integrated metrics of forage quality – like DP and DMD – is urgently needed. In addition to the importance of forage quality on fitness, secondary effects related to changes in herbivore populations can have cascading effects on ecosystem structure and function.

We did not see any improvement in model fit or predictive power when we included the light environment (H3), which contrasted with previous work indicating that light conditions influenced fiber and nitrogen concentrations as well as DMD (Lenart et al., 2002; Molvar et al., 1993). This may in part be because the light modelling employed in this study did not account for variation throughout the canopy (i.e., we only modeled the surface foliage of the shrub canopy). Indeed, one study compared various techniques for quantifying the light environment of *Salix pulchra* and found that only lidar-based techniques captured photosynthetic partitioning of nitrogen and chlorophyll in canopies (Magney et al., 2016). Moreover, our findings may be related to the relatively coarse spatial scale of the atmospheric variables (with a spatial resolution of 32 km) included within the models of solar irradiance employed in this study. Future work may benefit from applying the approaches used in Magney et al, (2016) or ground-based sensors that estimate the instantaneous irradiance at the location of shrubs to determine how solar energy influences DP and DMD,

as we did see a modest increase in predictive power and a slight decrease in error when irradiance was added to DMD models (Table 4.2). Similarly, including topographic attributes produced no model improvements (H4). This is surprising considering that elevation, slope and aspect have been shown to influence forage quality (Knox et al., 2012; Pullanagari et al., 2018).

One limitation of our study was that we did not quantify shrub biomass, because we did not have the resources locally to do so. Yet, the total energy acquired through browsing is a function of both forage quantity and quality, and thus both of these metrics are needed to truly map nutritional landscapes. Additionally, forage quality is normally the highest after budburst and then declines throughout the remainder of the growing season as fiber content increases and digestibility and nitrogen decrease (Klein, 1990; McArt et al., 2009; Shively et al., 2019). Our study demonstrated that remote sensing of DP and DMD is possible during peak biomass. However, future work should consider the seasonal dynamics of these integrated metrics.

Finally, future work should investigate the possibility of scaling these plot-level assessments to airborne and satellite platforms. Although we advocate for future work to include both optical and structural data streams, we also observed strong relationships between hyperspectral SVIs and DP and DMD without additional shrub structural inputs (Table 4.2; A3.1). Therefore, we anticipate that as new hyperspectral satellite platforms – such as the Environmental Mapping and Analysis Program (EnMAP; Guanter et al., 2015) – become more widely available, our ability to monitor integrated forage quality metrics seasonally and interannually at the landscape scale will be enhanced. We also suggest that future work that employs satellite data should couple with finer scale structural remotely sensed data that would help characterize the uncertainty in canopy structure attributes as the spatial resolution will be much coarser than our shrub level assessments. Structural data may be sourced from aerial lidar transects, which can provide estimates of both plant height variability and LAI but would not provide wall-to-wall coverage. LAI may also be estimated from fine-spatial resolution satellites such as WorldView-2 (Pu & Cheng, 2015) or a combination of satellite platforms (Houborg & McCabe, 2018). One alternative to aerial lidar in high latitude regions would be canopy height models estimated from the ArcticDEM (Meddens et al., 2018), which could provide information on canopy height variability, which

we found to be an important predictor of both DP and DMD. Assessments would be needed for aerial lidar (~1m grid cells), satellite imagery, and canopy height models (~5m grid cells) to determine if these data sources are fine-scaled enough to provide useful information for LAI and canopy height variability, as our UAV SfM point clouds were 1cm spatial resolution.

Conclusion

Results from our study demonstrate that integrated forage quality metrics like DP and DMD can be successfully quantified using hyperspectral remote sensing data, and that models based on those data can be improved by incorporating additional shrub structural metrics. Mapping DP and DMD to create a spatially explicit representation of the nutritional landscape available to herbivores may assist in management decisions in the face of ongoing environmental change.

Literature Cited

Akaike, H. (1974). A new look at the statistical model identification. *IEEE Trans Automatic Control*, *AC-19*(6), 716–723.

Asner, G. P. (1998). Biophysical and biochemical sources of variability in canopy reflectance. *Remote Sensing of Environment*, *64*(3), 234–253.

Asner, G. P., Knapp, D. E., Boardman, J., Green, R. O., Kennedy-Bowdoin, T., Eastwood, M., Martin, R. E., Anderson, C., & Field, C. B. (2012). Carnegie Airborne Observatory-2: Increasing science data dimensionality via high-fidelity multi-sensor fusion. *Remote Sensing of Environment*, *124*, 454–465.

Ball, J. P., Danell, K., & Sunesson, P. (2000). Response of a herbivore community to increased food quality and quantity: An experiment with nitrogen fertilizer in a boreal forest. *Journal of Applied Ecology*, *37*(2), 247–255.

Ben-Dor, E., Inbar, Y., & Chen, Y. (1997). The reflectance spectra of organic matter in the visible near-infrared and short wave infrared region (400-2500 nm) during a controlled decomposition process. *Remote Sensing of Environment*, *61*(1), 1–15.

Bischof, R., Loe, L. E., Meisingset, E. L., Zimmerman, B., Van Moorter, B., & Mysterud, A. (2012). A migratory northern ungulate in the pursuit of spring: Jumping or surfing the green wave? *The American Naturalist*, *180*(4), 407–424.

Bryant, J. P. (1981). Phytochemical deterrence of Snowshoe Hare browsing by adventitious shoots of four Alaskan trees. *Science*, *213*(4510), 889–890.

Bryant, J. P., & Chapin, F. S. I. (1986). Browsing-woody plant interactions during boreal forest plant succession. In K. Van Cleve & F. S. I. Chapin (Eds.), *Forest Ecosystems in the Alaskan Taiga* (pp. 213–225). Springer-Verlag.

Butler, L. G., & Kielland, K. (2008). Acceleration of vegetation turnover and element cycling by mammalian herbivory in riparian ecosystems. *Journal of Ecology*, *96*, 136–144.

Chapin, F. S., Shaver, G. R., Giblin, A. E., Nadelhoffer, K. J., & Laundre, J. A. (1995). Responses of Arctic tundra to experimental and observed changes in climate. *Ecology*, *76*(3), 694–711.

Chaves, N., & Escudero, J. (1999). Variation of flavonoid synthesis induced by ecological factors. In K. M. M. Dakshini and C. L. Foy (Eds.), *Principles and Practices in Plant Ecology: Allochemical Interactions* (pp. 267–285). CRC Press.

Chen, J. M., & Cihlar, J. (1996). Retrieving leaf area index of boreal conifer forests using landsat TM images. *Remote Sensing of Environment*, *55*(2), 153–162.

Christie, K. S., Bryant, J. P., Gough, L., Ravolainen, V. T., Ruess, R. W., & Tape, K. D. (2015). The role of vertebrate herbivores in regulating shrub expansion in the Arctic: A synthesis. *BioScience*, *65*(12), 1123–1133.

Christie, K. S., Ruess, R. W., Lindberg, M. S., & Mulder, C. P. (2014). Herbivores influence the growth, reproduction, and morphology of a widespread arctic willow. *PLoS ONE*, *9*(7), 1–9.

CloudCompare (version 2.2) [GPL software]. (2020). Retrieved from http://www.cloudcompare.org/

Cook, B. D., Corp, L. a., Nelson, R. F., Middleton, E. M., Morton, D. C., McCorkel, J. T., Masek, J. G., Ranson, K. J., Ly, V., & Montesano, P. M. (2013). NASA goddard's LiDAR, hyperspectral and thermal (G-LiHT) airborne imager. *Remote Sensing*, *5*(8), 4045–4066.

Corripio, M. J. G. (2015). *Package 'insol.'*

Curran, P. J. (1989). Remote sensing of foliar chemistry. *Remote Sensing of Environment*, *30*(3), 271–278.

DeGabriel, J. L., Moore, B. D., Felton, A. M., Ganzhorn, J. U., Stolter, C., Wallis, I. R., Johnson, C. N., & Foley, W. J. (2014). Translating nutritional ecology from the laboratory to the field: Milestones in linking plant chemistry to population regulation in mammalian browsers. *Oikos*, *123*(3), 298–308.

Dodge, S., Bohrer, G., Weinzierl, R., Davidson, S., Kays, R., Douglas, D., Cruz, S., Han, J., Brandes, D., & Wikelski, M. (2013). The environmental-data automated track annotation (Env-DATA) system: Linking animal tracks with environmental data. *Movement Ecology*, *1*(1), 3.

Doiron, M., Gauthier, G., & Lévesque, E. (2014). Effects of experimental warming on nitrogen concentration and biomass of forage plants for an arctic herbivore. *Journal of Ecology*, *102*(2), 508–517.

Dormann, C. F., Elith, J., Bacher, S., Buchmann, C., Carl, G., Carr, G., Garc, J. R., Gruber, Lafourcade, B., Leit, P. J., Tamara, M., Mcclean, C., Osborne, P. E., Der, B. S., Skidmore, A. K., Zurell, D., & Lautenbach, S. (2013). Collinearity: A review of methods to deal with it and a simulation study evaluating their performance. *Ecography*, *36*, 27–46.

Eitel, J. U. H., Long, D. S., Gessler, P. E., & Hunt, E. R. (2008). Combined spectral index to improve ground-based estimates of nitrogen status in dryland wheat. *Agronomy Journal*, *100*(6), 1694–1702.

Eitel, J. U. H., Long, D. S., Gessler, P. E., & Smith, A. M. S. (2007). Using in-situ measurements to evaluate the new RapidEye TM satellite series for prediction of wheat nitrogen status. *International Journal of Remote Sensing*, *28*(18), 4183–4190.

Elmendorf, S. C., Henry, G. H. R., Hollister, R. D., Björk, R. G., Bjorkman, A. D., Callaghan, T. V., Collier, L. S., Cooper, E. J., Cornelissen, J. H. C., Day, T. A., Fosaa, A. M., Gould, W. A., Grétarsdóttir, J., Harte, J., Hermanutz, L., Hik, D. S., Hofgaard, A., Jarrad, F., Jónsdóttir, I. S., … Wookey, P. A. (2012). Global assessment of experimental climate warming on tundra vegetation: Heterogeneity over space and time. *Ecology Letters*, *15*(2), 164–175.

Elvidge, C. D. (1990). Visible and near-infrared reflectance characteristics of dry plant materials. *International Journal of Remote Sensing*, *11*(10), 1775–1795.

Ferwerda, J. G., Skidmore, A. K., & Stein, A. (2006). A bootstrap procedure to select hyperspectral wavebands related to tannin content. *International Journal of Remote Sensing*, *27*(7), 1413–1424.

Field, A., Miles, J., & Field, Z. (2012). *Discovering statistics using R*. Sage publications.

Foley, W. J., & Moore, B. D. (2005). Plant secondary metabolites and vertebrate herbivores - From physiological regulation to ecosystem function. *Current Opinion in Plant Biology*, *8*(4), 430–435. https://doi.org/10.1016/j.pbi.2005.05.009

Goetz, A. F. H. (2009). Three decades of hyperspectral remote sensing of the Earth: A personal view. *Remote Sensing of Environment*, *113*, 5–16.

Guanter, L., Kaufmann, H., Segl, K., Foerster, S., Rogass, C., Chabrillat, S., Kuester, T., Hollstein, A., Rossner, G., Chlebek, C., Straif, C., Fischer, S., Schrader, S., Storch, T., Heiden, U., Mueller, A., Bachmann, M., Mühle, H., Müller, R., … Sang, B. (2015). The EnMAP spaceborne imaging spectroscopy mission for earth observation. *Remote Sensing*, *7*(7), 8830–8857.

Hanley, T. A., Robbins, C. T., Hagerman, A. E., & Mcarthur, C. (1992). Predicting digestible protein and digestible dry matter in tannin-containing forages consumed by ruminants. *Ecology*, *73*(2), 537–541.

Hansen, A. H., Jonasson, S., Michelsen, A., & Julkunen-Tiitto, R. (2006). Long-term experimental warming, shading and nutrient addition affect the concentration of phenolic compounds in arctic-alpine deciduous and evergreen dwarf shrubs. *Oecologia*, *147*(1), 1–11.

Hensher, D. A., & Stopher, P. R. (1979). *Behavioural travel modelling*. Taylor & Francis.

Houborg, R., & McCabe, M. F. (2018). Daily Retrieval of NDVI and LAI at 3 m Resolution via the Fusion of CubeSat, Landsat, and MODIS Data. *Remote Sensing*, *10*(6), 890.

Jennewein, J. S., Eitel, J. U., Pinto, J. R., & Vierling, L. A. (2020). Toward Mapping Dietary Fibers in Northern Ecosystems Using Hyperspectral and Multispectral Data. *Remote Sensing*, *12*(16), 2579.

Kielland, K., & Bryant, J. P. (1998). Moose herbivory in Taiga: Effects on biogeochemistry and vegetation dynamics in primary succession. *OIKOS*, *82*(2), 377–383.

Klein, D. R. (1990). Variation in quality of caribou and reindeer forage plants associated with season, plant part, and phenology. *Rangifer*, *10*(3), 123–130.

Knox, N. M., Skidmore, A. K., Prins, H. H. T., Heitkönig, I. M. A., Slotow, R., Waal, C. Van Der, & Boer, W. F. De. (2012). Remote sensing of forage nutrients: Combining ecological and spectral absorption feature data. *ISPRS Journal of Photogrammetry and Remote Sensing*, *72*, 27–35.

Knyazikhin, Y., Schull, M. A., Stenberg, P., Mõttus, M., Rautiainen, M., Yang, Y., Marshak, A., Carmona, P. L., Kaufmann, R. K., Lewis, P., Disney, M. I., Vanderbilt, V., Davis, A. B., Baret, F., Jacquemoud, S., Lyapustin, A., & Myneni, R. B. (2013). Hyperspectral remote sensing of foliar nitrogen content. *Proceedings of the National Academy of Sciences of the United States of America*, *110*(3). https://doi.org/10.1073/pnas.1210196109

Kokaly, R. F., Asner, G. P., Ollinger, S. V, Martin, M. E., & Wessman, C. A. (2009). Characterizing canopy biochemistry from imaging spectroscopy and its application to ecosystem studies. *Remote Sensing of Environment*, *113*, 78–91.

Lenart, E. A., Bowyer, R. T., Hoef, J. Ver, & Ruess, R. W. (2002). Climate change and caribou: effects of summer weather on forage. *Canadian Journal of Zoology*, *80*(4), 664–678.

Lone, K., van Beest, F. M., Mysterud, A., Gobakken, T., Milner, J. M., Rudd, H. P., & Loe, L. E. (2014). Improving broad scale forage mapping and habitat selection analyses with airborne laser scanning: The case of moose. *Ecosphere*, *5*(11), 1–22.

Luo, S., Wang, C., Xi, X., Pan, F., Peng, D., Zou, J., Nie, S., & Qin, H. (2017). Fusion of airborne LiDAR data and hyperspectral imagery for aboveground and belowground forest biomass estimation. *Ecological Indicators*, *73*, 378–387.

Magney, T. S., Eitel, J. U. H., Griffin, K. L., Boelman, N. T., Greaves, H. E., Prager, C. M., Logan, B. A., Zheng, G., Ma, L., Fortin, E. A., Oliver, R. Y., & Vierling, L. A. (2016). LiDAR canopy radiation model reveals patterns of photosynthetic partitioning in an Arctic shrub. *Agricultural and Forest Meteorology*, *221*, 78–93.

McArt, S. H., Spalinger, D. E., Collins, W. B., Schoen, E. R., Stevenson, T., & Bucho, M. (2009). Summer dietary nitrogen availability as a potential bottom-up constraint on moose in south-central Alaska. *Ecology*, *90*(5), 1400–1411.

McFadden, D., & Zarembka, P. (1974). Conditional logit analysis of qualitative choice behavior. In P. Zarembka, (Ed.), *Frontiers in econometrics* (pp.105–142). Academic Press.

Meddens, A. J., Vierling, L. A., Eitel, J. U., Jennewein, J. S., White, J. C., & Wulder, M. A. (2018). Developing 5 m resolution canopy height and digital terrain models from WorldView and ArcticDEM data. *Remote Sensing of Environment, 218*, 174-188.

Melin, M., Matala, J., Mehtätalo, L., Suvanto, A., & Packalen, P. (2016). Detecting moose (*Alces alces*) browsing damage in young boreal forests from airborne laser scanning data. *NRC Research Press*, *46*(1), 10–19.

Merems, J. L., Shipley, L. A., Levi, T., Ruprecht, J., Clark, D. A., Wisdom, M. J., Jackson, N. J., Stewart, K. M., & Long, R. A. (2020). Nutritional-landscape models link habitat use to condition of mule deer (*Odocoileus hemionus*). *Frontiers in Ecology and Evolution*, *8*, 1–13.

Mirik, M., Norland, J. E., Crabtree, R. L., & Biondini, M. E. (2005). Hyperspectral One-Meter-Resolution Remote Sensing in Yellowstone National Park, Wyoming: I. Forage Nutritional Values. *Society for Range Management*, *58*(5), 452–458.

Molvar, E. M., Bowyer, R. T., & Van Ballenberghe, V. (1993). Moose herbivory, browse quality, and nutrient cycling in an Alaskan treeline community. *Oecologia*, *94*(4), 472–479.

Mysterud, A., Vike, B. K., Meisingset, E. L., & Rivrud, I. M. (2017). The role of landscape characteristics for forage maturation and nutritional benefits of migration in red deer. *Ecology and Evolution*, *7*(12), 4448–4455.

Ogawa, A., Shibata, H., Suzuki, K., Mitchell, M. J., & Ikegami, Y. (2006). Relationship of topography to surface water chemistry with particular focus on nitrogen and organic carbon solutes within a forested watershed in Hokkaido, Japan. *Hydrological Processes*, *20*(2), 251–265.

Parker, K. L., Barboza, P. S., & Michael, P. (2009). Nutrition integrates environmental responses of ungulates. *Functional Ecology*, *23*, 57–69. 2435.2008.01528.x

Pastor, J, Dewey, B., Naiman, R. J., McInnes, P. F., & Cohen, Y. (1993). Moose browsing and soil fertility in the boreal forests of Isle Royale National Park. *Ecology*, *74*(2), 467–480.

Pastor, John, Naiman, R. J., Dewey, B., Mcinnes, P., Forest, B., Pastor, J., Naiman, R. J., Dewey, B., & Mcinnes, P. (1988). Moose, microbes, and the boreal forest. *BioScience*, *38*(11), 770–777.

Peñuelas, J., & Estiarte, M. (1997). Trends in plant carbon concentration and plant demand for N throughout this century. *Oecologia*, *109*(1), 69–73.

Pinheiro, J., Bates, D., DebRoy, S., Sarkar, D., Heisterkamp, S., Van Willigen, B., & Maintainer, R. (2017). Package 'nlme.' *Linear and Nonlinear Mixed Effects Models, Version*, *3*(1).

Pix4D 2016. Pix4D—Drone Mapping Software. https://pix4d.com/.

Porter, Claire, Morin, Paul; Howat, Ian; Noh, Myoung-Jon; Bates, Brian; Peterman, Kenneth; Keesey, Scott; Schlenk, Matthew; Gardiner, Judith; Tomko, Karen; Willis, Michael; Kelleher, Cole; Cloutier, Michael; Husby, Eric; Foga, Steven; Nakamura, Hitomi; Platson, Melisa; Wethington, Michael, Jr.; Williamson, Cathleen; Bauer, Gregory; Enos, Jeremy; Arnold, Galen; Kramer, William; Becker, Peter; Doshi, Abhijit; D'Souza, Cristelle; Cummens, Pat; Laurier, Fabien; Bojesen, Mikkel, 2018, "ArcticDEM", https://doi.org/10.7910/DVN/OHHUKH, Harvard Dataverse, V1, 2018, Accessed 10/1/2018.

Pu, R., & Cheng, J. (2015). Mapping forest leaf area index using reflectance and textural information derived from WorldView-2 imagery in a mixed natural forest area in Florida, US. *International Journal of Applied Earth Observation and Geoinformation, 42*, 11-23.

Pullanagari, R. R., Kereszturi, G., & Yule, I. (2018). Integrating airborne hyperspectral, topographic, and soil data for estimating pasture quality using recursive feature elimination with random forest regression. *Remote Sensing*, *10*(1117), 1–14.

R Core Team. (2019). *R: A language and environment for statistical computing*. Vienna, Austria.

Ramoelo, A., Skidmore, A. K., Cho, M. A., Schlerf, M., Mathieu, R., & Heitkönig, I. M. A. (2012). Regional estimation of savanna grass nitrogen using the red-edge band of the spaceborne RapidEye sensor. *International Journal of Applied Earth Observations and Geoinformation*, *19*, 151–162.

Robbins, C. T., Hanley, T. A., Hagerman, A. E., Hjeljord, O., Baker, D. L., Schwartz, C. C., & Mautz, W. W. (1987a). Role of tannins in defending plants against ruminants: Reduction in protein availability. *Ecology*, *68*(1), 98–107.

Robbins, C. T., Mole, S., Hagerman, A. E., & Hanley, T. A. (1987b). Role of tannins in defending plants against ruminants: Reduction in dry matter digestion? *Ecology*, *68*(6), 1606–1615.

Rohrs-Richey, J., & Mulder, C. (2007). Effects of local changes in active layer and soil climate on seasonal foliar nitrogen concentrations of three boreal forest shrubs. *Canadian Journal of Forest Research*, *394*, 383–394.

Schmitz, O. J., Wilmers, C. C., Leroux, S. J., Doughty, C. E., Atwood, T. B., Galetti, M., Davies, A. B., & Goetz, S. J. (2018). Animals and the zoogeochemistry of the carbon cycle. *Science*, *362*(1127), 1–10. https://doi.org/10.1126/science.aar3213

Serreze, M. C., Walsh, J. E., Chapin, F. S. I., Osterkamp, T., Dyurgerov, M., Romanovsky, V., Oechel, W. C., Morison, J., Zhang, T., & Barry, R. G. (2000). Observational evidence of recent change in the northern high- latitude environment. *Climatic Change*, *46*(1-2), 159–207.

Shively, R. D., Crouse, J. A., Thompson, D. P., & Barboza, P. S. (2019). Is summer food intake a limiting factor for boreal browsers? Diet, temperature, and reproduction as drivers of consumption in female moose. *PLoS ONE*, *14*(10), 1–18.

Silva, C. A., Crookston, N. L., Hudak, A. T., Vierling, L. A., Klauberg, C., & Silva, M. C. A. (2017). Package 'rLiDAR.' *The CRAN Project*.

Skidmore, A. K., Ferwerda, J. G., Mutanga, O., Van Wieren, S. E., Peel, M., Grant, R. C., Prins, H. H. T., Balcik, F. B., & Venus, V. (2010). Forage quality of savannas - Simultaneously mapping foliar protein and polyphenols for trees and grass using hyperspectral imagery. *Remote Sensing of Environment*, *114*(1), 64–72.

Solberg, S., Næsset, E., Holt, K., & Christiansen, E. (2006). Mapping defoliation during a severe insect attack on Scots pine using airborne laser scanning. *Remote Sensing of Environment*, *102*, 364–376.

Spalinger, D. E., Collins, W. B., Hanley, T. A., Cassara, N. E., & Carnahan, A. M. (2010). The impact of tannins on protein, dry matter, and energy digestion in moose (*Alces alces*). *Canadian Journal of Zoology*, *88*(10), 977–987.

Sponseller, R. A., Gundale, M. J., Futter, M., & Ring, E. (2016). Nitrogen dynamics in managed boreal forests: Recent advances and future research directions. *Ambio*, *45*, 175–187.

Stouter, C. (2008). Intra-individual plant response to moose browsing: Feedback loops and impacts on multiple consumers. *Ecological Monographs*, *78*(2), 167–183.

Symonds, M. R. E., & Moussalli, A. (2011). A brief guide to model selection, multimodel inference and model averaging in behavioural ecology using Akaike's information criterion. *Behavioral Ecology and Sociobiology*, *65*(1), 13–21.

Tape, K. D., Gustine, D. D., Ruess, R. W., Adams, L. G., & Clark, J. A. (2016). Range expansion of moose in Arctic Alaska linked to warming and increased shrub habitat. *PLoS ONE*, *11*(7), 1–12.

ter Steege, H. (2018). *Hemiphot. R: free R scripts to analyse hemispherical photographs for canopy openness, leaf area index and photosynthetic active radiation under forest canopies [online]. Naturalis Biodiversity Center, Leiden, Netherlands*.

Thompson, D. P., & Barboza, P. S. (2014). Nutritional implications of increased shrub cover for caribou (Rangifer tarandus) in the Arctic. *Canadian Journal of Zoology*, *92*(4), 339–351.

Thulin, S., Hill, M. J., Held, A., Jones, S., & Woodgate, P. (2012). Hyperspectral determination of feed quality constituents in temperate pastures: Effect of processing methods on predictive relationships from partial least squares regression. *International Journal of Applied Earth Observation and Geoinformation*, *19*(1), 322–334.

Torabzadeh, H., Morsdorf, F., & Schaepman, M. E. (2014). Fusion of imaging spectroscopy and airborne laser scanning data for characterization of forest ecosystems - A review. *ISPRS Journal of Photogrammetry and Remote Sensing*, *97*, 25–35.

Turner, D. P., Cohen, W. B., Kennedy, R. E., Fassnacht, K. S., & Briggs, J. M. (1999). Relationships between leaf area index and Landsat TM spectral vegetation indices across three temperate zone sites. *Remote Sensing of Environment*, *70*(1), 52–68.

Turunen, M., Soppela, P., Kinnunen, H., Sutinen, M. L., & Martz, F. (2009). Does climate change influence the availability and quality of reindeer forage plants? *Polar Biology*, *32*(6), 813–832.

Vance, C. K., Tolleson, D. R., Kinoshita, K., Rodriguez, J., & Foley, W. J. (2016). Near infrared spectroscopy in wildlife and biodiversity. *Journal of Near Infrared Spectroscopy*, *24*(1), 1–25.

Vastaranta, M., Kantola, T., Lyytikäinen-Saarenmaa, P., Holopainen, M., Kankare, V., Wulder, M. A., Hyyppä, J., & Hyyppä, H. (2013). Area-Based Mapping of Defoliation of Scots Pine Stands Using Airborne Scanning LiDAR. *Remote Sensing*, *5*, 1220–1234.

Verbyla, D. (2008). The greening and browning of Alaska based on 1982-2003 satellite data. *Global Ecology and Biogeography*, *17*(4), 547–555.

Vierling, K. T., Vierling, L. a, Gould, W. a, Martinuzzi, S., & Clawges, R. M. (2008). Lidar: shedding new light on habitat characterization and modeling. *Frontiers in Ecology and the Environment*, *6*(2), 90–98.

Wallace, L., Lucieer, A., Malenovskỳ, Z., Turner, D., & Vopěnka, P. (2016). Assessment of forest structure using two UAV techniques: A comparison of airborne laser scanning and structure from motion (SfM) point clouds. *Forests*, *7*(3), 1–16.

Walton, K. M., Spalinger, D. E., Harris, N. R., Collins, W. B., & Willacker, J. J. (2013). High spatial resolution vegetation mapping for assessment of wildlife habitat. *Wildlife Society Bulletin*, *37*(4), 906–915.

Wang, W., Yao, X., Yao, X. F., Tian, Y. C., Liu, X. J., Ni, J., Cao, W. X., & Zhu, Y. (2012). Estimating leaf nitrogen concentration with three-band vegetation indices in rice and wheat. *Field Crops Research*, *129*, 90–98.

White, T. C. (1993). *The inadequate environment*: *Nitrogen and the abundance of animals.* Springer.

Wolken, J. M., Hollingsworth, T. N., Rupp, T. S., Chapin, F. S., Trainor, S. F., Barrett, T. M., Sullivan, P. F., McGuire, A. D., Euskirchen, E. S., Hennon, P. E., Beever, E. A., Conn, J. S., Crone, L. K., D'Amore, D. V., Fresco, N., Hanley, T. A., Kielland, K., Kruse, J. J., Patterson, T., … Yarie, J. (2011). Evidence and implications of recent and projected climate change in Alaska's forest ecosystems. *Ecosphere*, *2*(11), art124.

Wu, H., Levin, N., Seabrook, L., Moore, B., & Mcalpine, C. (2019). Mapping Foliar Nutrition Using WorldView-3 and WorldView-2 to Assess Koala Habitat Suitability. *Remote Sensing*, *11*(215), 1–17.

Youngentob, K. N., Renzullo, L. J., Held, A. A., Jia, X., Lindenmayer, D. B., & Foley, W. J. (2012). Using imaging spectroscopy to estimate integrated measures of foliage nutritional quality. *Methods in Ecology and Evolution*, *3*(2), 416–426.

Zamin, T. J., Côté, S. D., Tremblay, J. P., & Grogan, P. (2017). Experimental warming alters migratory caribou forage quality: *Ecological Applications*, *27*(7), 2061–2073.

Zhou, J., Prugh, L., D. Tape, K., Kofinas, G., & Kielland, K. (2017). The Role of Vegetation Structure in Controlling Distributions of Vertebrate Herbivores in Arctic Alaska. *Arctic, Antarctic, and Alpine Research*, *49*(2), 291–304.

Zhou, J., Tape, K. D., Prugh, L., Kofinas, G., Carroll, G., & Kielland, K. (2020). Enhanced shrub growth in the Arctic increases habitat connectivity for browsing herbivores. *Global Change Biology*, *00*, 1–12.

Tables

Table 4.1. Results comparing spatial autocorrelation structures for generalized least squares regression predicting dry matter digestibility (DMD) and digestible protein (DP). Model fit was assessed using Akaike's information criterion (AIC), where lower values are considered better.

Model	AIC	
	DP	DMD
Simple Linear	165.27	280.49
Spherical	158.79	276.14
Linear	Did not converge	276.11
Rational Quadratic	157.70	275.94
Gaussian	159.11	275.99
Exponential	157.33	275.81

Table 4.2. Digestible Protein (DP) and Digestible Dry Matter (DMD) Models. DP GLS models included a spherical correlation structure, while DMD GLS models included a rational quadratic correlation structure. The spectral vegetation index (SVI) was regressed against percent DP and DMD. Structural (leaf area index (LAI), coefficient of variation of height (HCV), variance of heights (HVAR), standard deviation of heights (HSD), topographic attributes, (topographic wetness index (TWI), aspect, slope, elevation), and total irradiance the week before sample harvest were sequentially added to models and evaluated based on two pseudo R^2s: McFadden and Nagelkerke. Root mean square error (RMSE) quantified error. We used Akaike information criterion (AIC) to assess model fit and AIC weights to assess the probability of a given model being the best model. We used slopes and Spearman Rank correlation coefficients (ρ) from leave-one-out cross validation (LOOCV) to assess bias and predictive ability of models. The best models for DP and DMD have been italicized for easy visualization.

Models	McFadden R^2	Nagelkerke R^2	RMSE	AIC	AIC weights	LOOCV Slope	LOOCV ρ
Digestible Protein							
SVI	0.33	0.82	1.42%	157.70	0.07	0.76	0.88
SVI + LAI	0.33	0.82	1.44%	158.81	0.05	0.74	0.86
SVI + HCV	0.31	0.80	1.37%	173.24	0	0.78	0.87
SVI + HVAR	*0.34*	*0.82*	*1.46%*	*154.08*	*0.56*	*0.72*	*0.85*
SVI + HSD	0.34	0.82	1.54%	155.29	0.31	0.72	0.85
SVI + TWI	0.30	0.78	1.41%	168.95	0	0.76	0.88
SVI + Aspect	0.32	0.80	1.43%	173.50	0	0.76	0.87
SVI + Slope	0.33	0.82	1.42%	164.00	0	0.74	0.88
SVI + Elevation	0.35	0.83	1.36%	167.59	0	0.80	0.89
SVI + Irradiance (1 week)	0.33	0.81	1.42%	190.93	0	0.75	0.88
Digestible Dry Matter							
SVI	0.14	0.62	5.11%	275.94	0	0.58	0.75
SVI + LAI	0.14	0.62	5.11%	273.98	0	0.58	0.75
SVI + HCV	0.15	0.66	4.87%	278.96	0.05	0.62	0.77
SVI + HVAR	0.17	0.69	4.99%	263.85	0.27	0.62	0.76
SVI + HSD	0.16	0.67	5.13%	267.01	0.05	0.59	0.76

SVI + TWI	0.14	0.63	5.11%	276.32	0	0.57	0.75
SVI + Aspect	0.14	0.63	5.11%	285.96	0	0.58	0.76
SVI + Slope	0.14	0.64	5.07%	277.27	0	0.59	0.76
SVI + Elevation	0.14	0.63	5.08%	284.72	0	0.58	0.76
SVI + Irradiance (1 week)	0.15	0.65	4.93%	302.71	0	0.60	0.78
SVI + HVAR +LAI	*0.17*	*0.70*	*4.96%*	*261.09*	*0.63*	*0.63*	*0.79*

Figures

Figure 4.1. Photographs depicting examples of broomed (A and D), browsed (B), and unbrowsed (C) willow shrubs in northcentral Alaska. Plants that show signs of browsing on ≥ 50% of current annual growth (CAG) are considered 'broomed,' while plants with < 50% of CAG are classified as 'browsed,' and plants with no sign of browsing are considered 'unbrowsed.' (photo credit: Jyoti Jennewein)

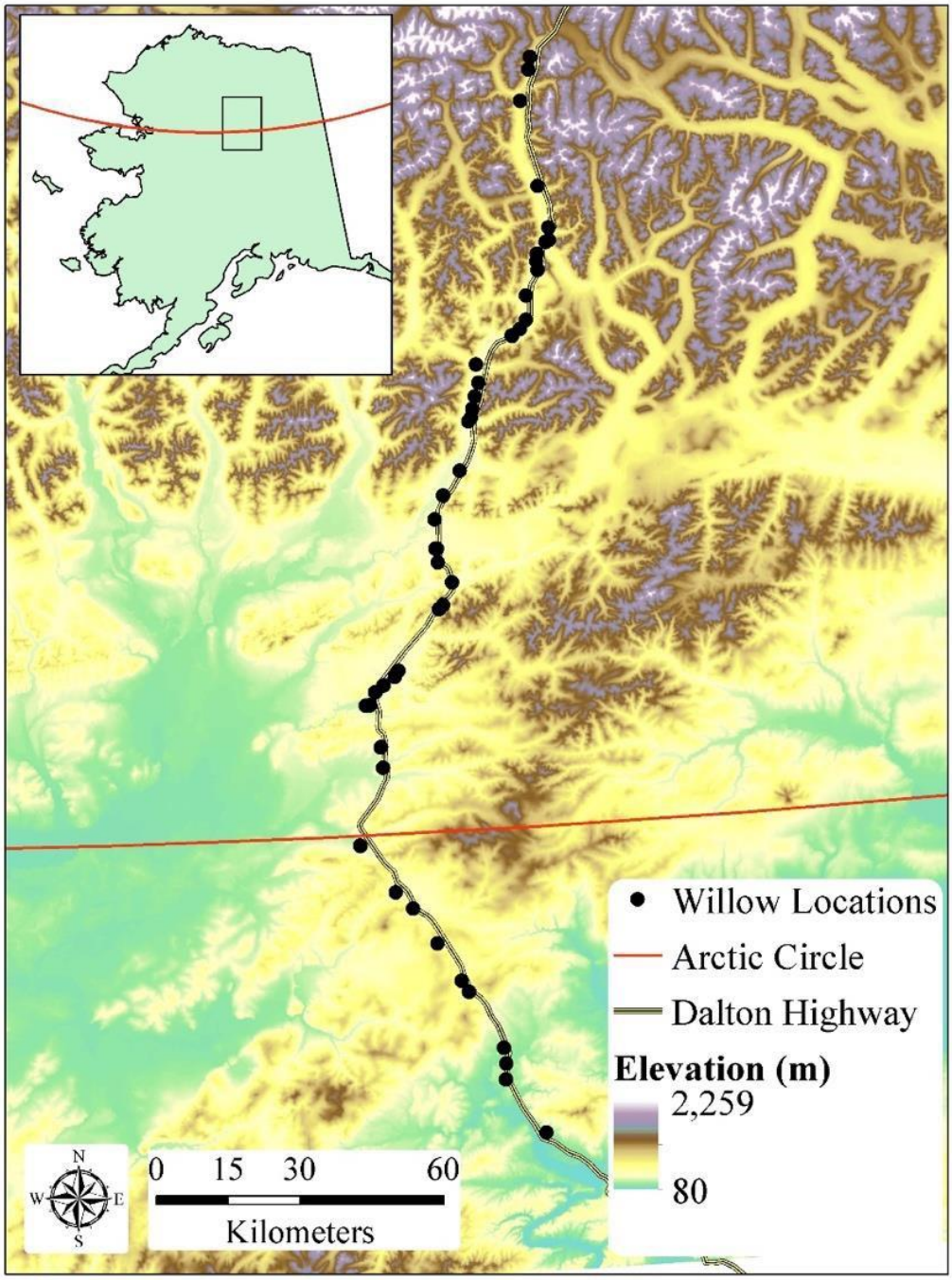

Figure 4.2. Study area in the upper Koyukuk River drainage. Willow **s**tudy sites (n=45) span a latitudinal gradient from the Yukon River to just below Atigun Pass along the Dalton Highway.

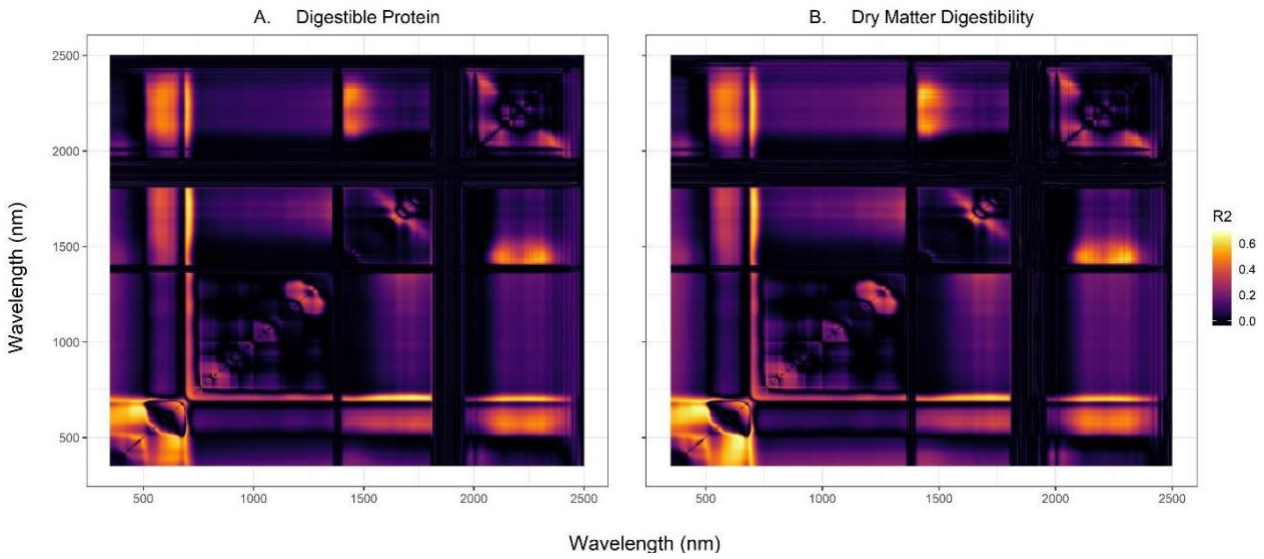

Figure 4.3. Coefficients of determination (R^2) between willow samples and simple ratio vegetation indices for digestible protein (A) and dry matter digestibility (B). The x- and y-axes are the wavelengths (nm) from the spectrometer used for simple ratio spectral vegetation indices for digestible protein and normalized differenced spectral vegetation indices for dry matter digestibility.

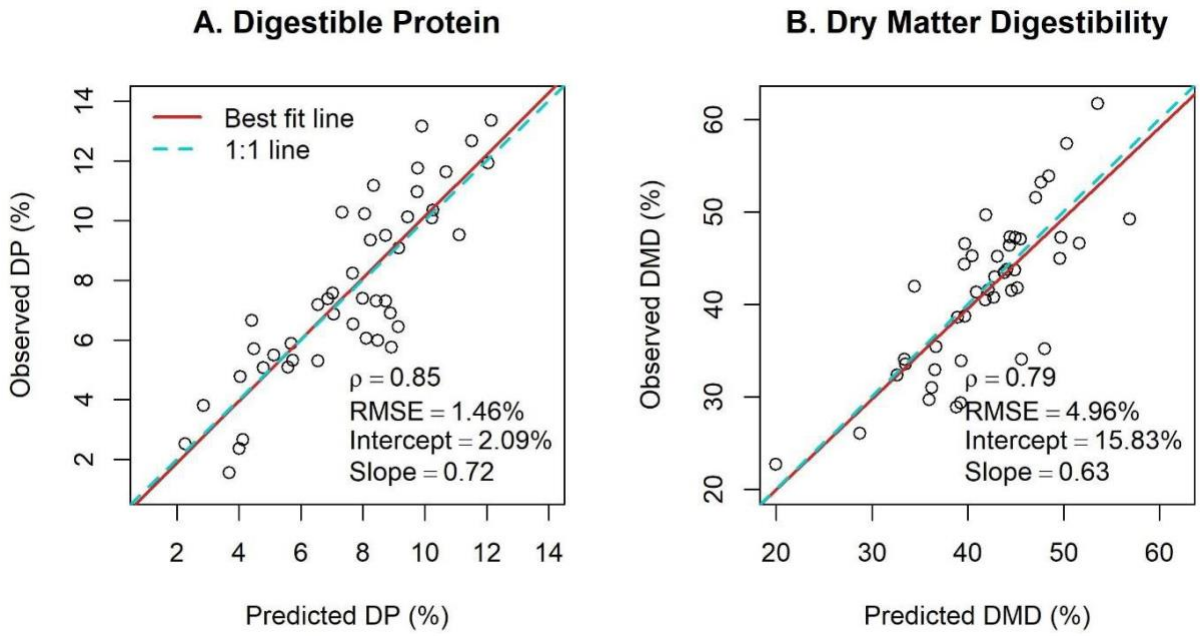

Figure 4.4. Observed vs. predicted concentrations of digestible protein (A) and dry matter digestibility (B) of the best performing models. DP's best model included a spectral vegetation index (SVI) and variance of shrub heights (HVAR). DMD's best model included a SVI, HVAR, and leaf area index (LAI).

Chapter 5: Conclusion

This dissertation includes three disciplinary chapters that explored geospatial tools for modeling habitat selection and habitat forage quality. Chapter two modeled habitat selection of a heat sensitive herbivore in response to temperature. To date, this research was the first to explore how moose behavior changed as a function of temperature in high northern latitude regions of North America. Results from this chapter indicated that denser canopied forests are an important habitat feature that enable behavioral thermoregulation of moose. Based on these findings, future land management decisions in Alaska should prioritize the conservation of denser canopied habitats (~50% coverage) to support an important component of maintaining moose biophysical needs. This is especially important in interior Alaskan communities that are expected to experience decreases in other subsistence species needed to main provisional and cultural services (Brinkman et al., 2016).

However, future work is still needed to further explore the relationship between behavioral thermoregulation strategies and moose. For instance, explicitly investigating how habitat selection in females who have a calf at heal would be an important next step as the demands of calving on female moose are substantial (Speakman & Król, 2010). Females are also known to alter their behavior when calves are present, and often opt for habitats that provide cover for predator avoidance (Dussault et al., 2005; Joly et al., 2016). Another avenue for future work on this topic should include delineation of plant communities. A major challenge to land management agencies in Alaska is a lack of landcover classes fine enough to inform habitat selection models. For instance, “shrub" in most vegetative classifications does not distinguish between shade forages and shade only species, which is critical for parsing selection behavior. It is also important to recognize that categorical land cover maps are not always the ideal product for studying other behaviors such as foraging (Coops & Wulder, 2019). Continuous metrics of forage quality such as the normalized differenced vegetation index (NDVI) are often used to predict habitat quality. However, NDVI often has mixed results when used to track forage quantity and quality (Doiron et al., 2013; Johnson et al., 2018). This limitation may be linked to the spectral resolution of broad band imagery that is not able to detect small absorption features associated with foliar biochemical traits.

Chapters 3-4 of this dissertation investigated new remote sensing approaches to monitor and map forage resources in high northern latitude regions, which is of great interest to wildlife managers (Vance et al., 2016; Walton et al., 2013). Numerous studies demonstrated that hyperspectral remote sensing can be used to successfully estimate a variety of important foliar properties known to influence forage quality such as crude protein, fiber, or defense chemicals like condensed tannins (Ferwerda et al., 2006; Mirik et al., 2005; Skidmore et al., 2010; Thulin et al., 2012). Chapters 3-4 add further evidence that hyperspectral remote sensing approaches can be used to estimate forage quality, but in a region previously unexplored for this purpose. The work presented in Chapter 4 was also one of the first to evaluate how well integrated metrics of forage quality – digestible protein (DP) and digestible dry matter (DMD) – could be estimated using hyperspectral remote sensing, and the first to do so in Arctic and boreal regions.

Additionally, this dissertation explored a novel remote sensing approach to fuse passive spectral remote sensing and structural data acquired from digital photographs as well as height variability from unmanned aerial vehicle (UAV) flights to estimate forage quality. Canopy structural variation strongly influences spectral reflectance characteristics by creating a more complex three-dimensional environment for photons to interact (Asner, 1998; Knyazikhin et al., 2013; Vierling et al., 1997). Additionally, herbivores influence plant canopy architecture of palatable forage species by decreasing shrub height, canopy openness, and branching structure (Christie et al., 2014, 2015; Kielland & Bryant, 1998), which in turn can affect the palatability of forage species (Bryant, 1981; Bryant & Chapin, 1986). To my knowledge, this was the first study to incorporate remotely sensed structural metrics as a proxy for browsing history in models to predict forage quality. These results indicated that incorporating shrub structure is an important, and often unconsidered, aspect of remotely sensed forage quality metrics that should be considered in future studies.

Future work on monitoring and mapping forage quality in high northern latitudes should also scale measurements to hyperspectral airborne platforms such as the Airborne Visible Infrared Imaging Spectrometer (AVIRIS-NG; Chapman et al., 2019) and Goddard's light detection and ranging (LiDAR), hyperspectral and thermal (G-LiHT) airborne imager (Cook et al., 2013), and ideally satellite platforms such as the environmental mapping and analysis program (EnMAP; Guanter et al., 2015). Scaling these measurements to the satellite

level will be important to effectively monitor and evaluate changes in forage quality over space and time in a region that is rapidly changing. After proper assessment and validation, these measures could then also serve as inputs into herbivore habitat selection models.

Each of these chapters adds important information to a growing body of research on habitat changes or animal behavior in high northern latitudes. These chapters all serve as an important benchmark that may be useful to state and federal land management agencies charged with the difficult task of monitoring the quickly changing landscapes of Arctic-boreal North America. In the pursuit of this knowledge, I have grown tremendously as a researcher and collaborator. However, I recognize that each chapter presented in this dissertation offers a small scientific contribution to the broader scope of work being conducted in these high northern latitude regions most vulnerable to climate change.

Literature Cited

Asner, G. P. (1998). Biophysical and biochemical sources of variability in canopy reflectance. *Remote Sensing of Environment*, *64*(3), 234–253.

Brinkman, T. J., Hansen, W. D., Chapin, F. S., Kofinas, G., BurnSilver, S., & Rupp, T. S. (2016). Arctic communities perceive climate impacts on access as a critical challenge to availability of subsistence resources. *Climatic Change*, *139*(3–4), 413–427.

Bryant, J. P. (1981). Phytochemical deterrence of Snowshoe Hare browsing by adventitious shoots of four Alaskan trees. *Science*, *213*(4510), 889–890.

Bryant, J. P., & Chapin, F. S. I. (1986). Browsing-woody plant interactions during boreal forest plant succession. In K. Van Cleve & F. S. I. Chapin (Eds.), *Forest Ecosystems in the Alaskan Taiga* (pp. 213–225). Springer, New York, NY.

Chapman, J. W., Thompson, D. R., Helmlinger, M. C., Bue, B. D., Green, R. O., Eastwood, M. L., Geier, S., Olson-Duvall, W., & Lundeen, S. R. (2019). Spectral and radiometric calibration of the Next Generation Airborne Visible Infrared Spectrometer (AVIRIS-NG). *Remote Sensing*, *11*(18), 2129.

Christie, K. S., Bryant, J. P., Gough, L., Ravolainen, V. T., Ruess, R. W., & Tape, K. D. (2015). The role of vertebrate herbivores in regulating shrub expansion in the Arctic: A synthesis. *BioScience*, *65*(12), 1123–1133.

Christie, K. S., Ruess, R. W., Lindberg, M. S., & Mulder, C. P. (2014). Herbivores influence the growth, reproduction, and morphology of a widespread Arctic willow. *PLoS ONE*, *9*(7), 1–9.

Cook, B. D., Corp, L. A., Nelson, R. F., Middleton, E. M., Morton, D. C., McCorkel, J. T., Masek, J. G., Ranson, K. J., Ly, V., & Montesano, P. M. (2013). NASA goddard's LiDAR, hyperspectral and thermal (G-LiHT) airborne imager. *Remote Sensing*, *5*(8), 4045–4066.

Coops, N. C., & Wulder, M. A. (2019). Breaking the Habit (at). *Trends in Ecology & Evolution*, *34*(7), 585–587.

Doiron, M., Legagneux, P., Gauthier, G., & Lévesque, E. (2013). Broad-scale satellite Normalized Difference Vegetation Index data predict plant biomass and peak date of nitrogen concentration in Arctic tundra vegetation. *Applied Vegetation Science*, *16*(2), 343–351.

Dussault, C., Ouellet, J., Courtois, R., Huot, J., Breton, L., & Jolicoeur, H. (2005). Linking moose habitat selection to limiting factors. *Ecography*, *28*(5), 619–628.

Ferwerda, J. G., Skidmore, A. K., & Stein, A. (2006). A bootstrap procedure to select hyperspectral wavebands related to tannin content. *International Journal of Remote Sensing*, *27*(7), 1413–1424.

Guanter, L., Kaufmann, H., Segl, K., Foerster, S., Rogass, C., Chabrillat, S., Kuester, T., Hollstein, A., Rossner, G., Chlebek, C., Straif, C., Fischer, S., Schrader, S., Storch, T., Heiden, U., Mueller, A., Bachmann, M., Mühle, H., Müller, R., … Sang, B. (2015). The EnMAP spaceborne imaging spectroscopy mission for earth observation. *Remote Sensing*, *7*(7), 8830–8857.

Johnson, H. E., Gustine, D. D., Golden, T. S., Adams, L. G., Parrett, L. S., Lenart, E. A., & Barboza, P. S. (2018). NDVI exhibits mixed success in predicting spatiotemporal variation in caribou summer forage quality and quantity. *Ecosphere*, *9*(10), e02461.

Joly, K., Sorum, M. S., Craig, T., & Julianus, E. L. (2016). The effects of sex, terrain, wildfire, winter severity, and maternal status on habitat selection by moose in north-central Alaska. *Alces*, *52*, 101–115.

Kielland, K., & Bryant, J. P. (1998). Moose herbivory in Taiga: Effects on biogeochemistry and vegetation dynamics in primary succession. *OIKOS*, *82*(2), 377–383.

Knyazikhin, Y., Schull, M. A., Stenberg, P., Mõttus, M., Rautiainen, M., Yang, Y., Marshak, A., Carmona, P. L., Kaufmann, R. K., Lewis, P., Disney, M. I., Vanderbilt, V., Davis, A. B., Baret, F., Jacquemoud, S., Lyapustin, A., & Myneni, R. B. (2013). Hyperspectral remote sensing of foliar nitrogen content. *Proceedings of the National Academy of Sciences of the United States of America*, *110*(3), E185-E192.

Mirik, M., Norland, J. E., Crabtree, R. L., & Biondini, M. E. (2005). Hyperspectral One-Meter-Resolution Remote Sensing in Yellowstone National Park, Wyoming: I. Forage Nutritional Values. *Society for Range Management*, *58*(5), 452–458.

Skidmore, A. K., Ferwerda, J. G., Mutanga, O., Van Wieren, S. E., Peel, M., Grant, R. C., Prins, H. H. T., Balcik, F. B., & Venus, V. (2010). Forage quality of savannas - Simultaneously mapping foliar protein and polyphenols for trees and grass using hyperspectral imagery. *Remote Sensing of Environment*, *114*(1), 64–72.

Speakman, J. R., & Król, E. (2010). Maximal heat dissipation capacity and hyperthermia risk: Neglected key factors in the ecology of endotherms. *Journal of Animal Ecology*, *79*(4), 726–746.

Thulin, S., Hill, M. J., Held, A., Jones, S., & Woodgate, P. (2012). Hyperspectral determination of feed quality constituents in temperate pastures: Effect of processing methods on predictive relationships from partial least squares regression. *International Journal of Applied Earth Observation and Geoinformation*, *19*(1), 322–334.

Vance, C. K., Tolleson, D. R., Kinoshita, K., Rodriguez, J., & Foley, W. J. (2016). Near infrared spectroscopy in wildlife and biodiversity. *Journal of Near Infrared Spectroscopy*, *24*(1), 1–25.

Vierling, L. A., Deering, D. W., & Eck, T. F. (1997). Differences in arctic tundra vegetation type and phenology as seen using bidirectional radiometry in the early growing season. *Remote Sensing of Environment*, *60*(1), 71–82.

Walton, K. M., Spalinger, D. E., Harris, N. R., Collins, W. B., & Willacker, J. J. (2013). High spatial resolution vegetation mapping for assessment of wildlife habitat. *Wildlife Society Bulletin*, *37*(4), 906–915.

Appendices

Appendix 1.1. Temperature Validation

Two moose populations (Koyukuk and Innoko) had temperature loggers on their GPS collars, enabling a comparison between these estimates and the temperature product (NARR) used in this study. GPS locations from the Koyukuk and Innoko populations were rarified to one randomly selected fix per individual per data to avoid issues with pseudoreplication. Using these rarified datasets, we regressed temperature estimates from NARR against recorded collar temperatures for both populations. To identify and remove outliers from temperature estimates, we used the Tukey method, which removed observations 1.5 times beyond the inner quartile range (Tukey, 1977). We used the Metrics package (Hamner & Frasco, 2018) to calculate the root mean square error (RMSE), which we used to assess bias of our regression estimates. Agreement between collar-based and NARR temperature estimates is moderate (Figure 1). These relationships are not as strong as we might have expected based on other studies comparing weather station data to collared estimated (R^2=0.90 and 0.97, respectively Street et al., 2015; van Beest et al., 2012). However, the primary interest in incorporating temperature in these analyses is to determine how selection changes as a function of temperature through interaction terms with other covariates. To that end, our relatively large temperature pixels (32 km) represent an ambient, neighborhood temperature, allowing us to investigate how moose respond to ambient variation in temperature via fine-scale selection for environmental characteristics that are likely to create cooler micro-climates. Therefore, we are confident the NARR temperature estimates used in this study are adequately representing ambient temperature for our purposes, while recognizing that no temperature data product will be completely accurate to on-the-ground conditions.

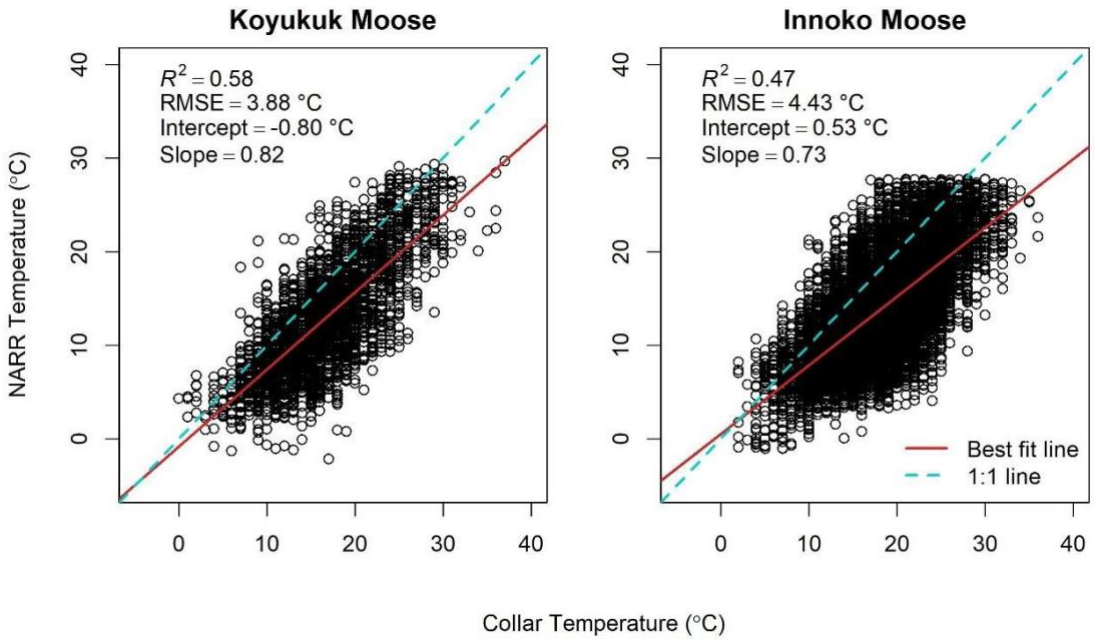

Figure A1.1. Temperature validation check between collared temperature estimates in the Koyukuk and Innoko populations and remote sensing derived temperature estimates from the North American Regional Reanalysis (NARR).

Appendix 1.2. Used-Available Tables of Covariates

Table A1.2.2 Used and available summaries by population for each covariate for female moose.

	Females							
	Koyukuk		**Susitna**		**Innoko**		**Tanana**	
Predictors	Used Mean (SD)	Available Mean (SD)	Used Mean (SD)	Available Mean (SD)	Used Mean (SD)	Available Mean (SD)	Used Mean (SD)	Available Mean (SD)
Elevation (meters)	472.7 (204.4)	476.8 (213.6)	773.3 (204.7)	784.9 (219.5)	44.4 (39.8)	44.5 (39.6)	193.6 (118.2)	193.5 (116.4)
Percent Canopy (%)	39.6 (32.2)	31.9 (31.9)	57.9 (29.6)	51.8 (32.9)	50.7 (33.9)	46.1 (35.7)	38.4 (28.3)	37.4 (28.9)
Solar Radiation Index (unitless)	0.04 (0.6)	0.03 (0.5)	-0.05 (0.69)	-0.05 (0.69)	-0.03 (0.66)	0.006 (0.66)	-0.01 (0.5)	0.02 (0.5)
Distance to Water (meters)	3969.8 (5885.7)	3991.4 (5887.4)	1373.3 (1017.3)	1372.5 (1028.1)	600.3 (1282.6)	591.6 (1278.9)	1427.7 (1113.4)	1433.1 (1115.8)

Table A1.2.2 Used and available summaries by population for each covariate for male moose.

	Males					
	Koyukuk		**Susitna**		**Innoko**	
Predictors	Used Mean (SD)	Available Mean (SD)	Used Mean (SD)	Available Mean (SD)	Used Mean (SD)	Available Mean (SD)
Elevation (meters)	520.0 (225.5)	524.3 (238.1)	805.4 (213.8)	816.7 (224.6)	54.9 (45.5)	55.8 (47.9)
Percent Canopy (%)	35.6 (31.9)	31.3 (31.5)	54.27 (31.3)	47.3 (34.4)	44.8 (35.2)	42.0 (36.2)
Solar Radiation Index (unitless)	0.02 (0.5)	0.01 (0.5)	-0.06 (0.6)	-0.06 (0.6)	-0.01 (0.7)	0.02 (0.7)
Distance to Water (meters)	2853.5 (2802.7)	2854.3 (2799.7)	1569.9 (1029.8)	1553.6 (1051.3)	1220.9 (2408.6)	1225.7 (2397.4)

Appendix 1.3. Regional Habitat Features

We explored regional differences in habitat features that may explain our habitat such as elevation (Figure 1E), temperature (Figure 2E), cloud cover (Figure 3D), and precipitation (Table 1E). Elevation (m) data was sourced from the ArcticDEM (Porter, et al., 2018), while temperature (originally in Kelvin, but transformed into °C), cloud cover (%), and precipitation (binary: yes-no raining at time of fix) were sourced from NARR data (Mesinger et al., 2006) and annotated in Env-DATA (Dodge et al., 2013).

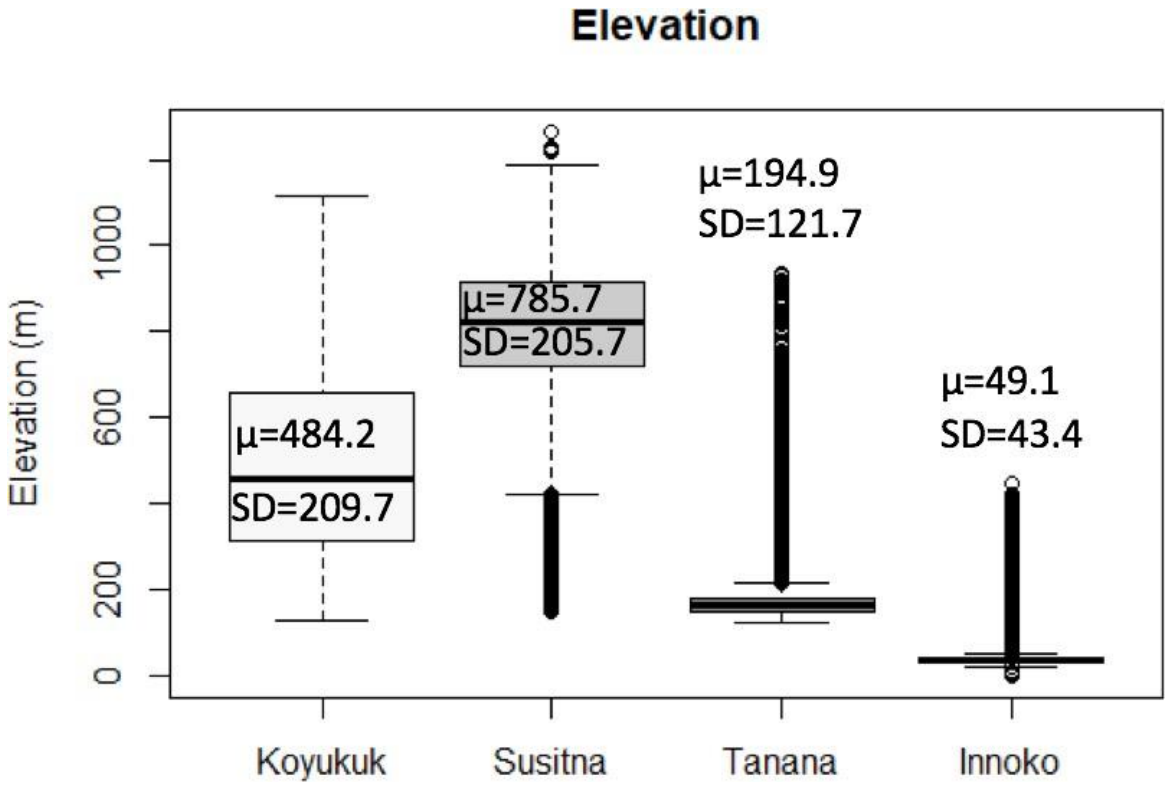

Figure A1.3.1. Regional variation in elevation. ANOVA results comparing regional variation in elevation show that all regions vary from each other statistically ($F=2705$, $p<0.001$).

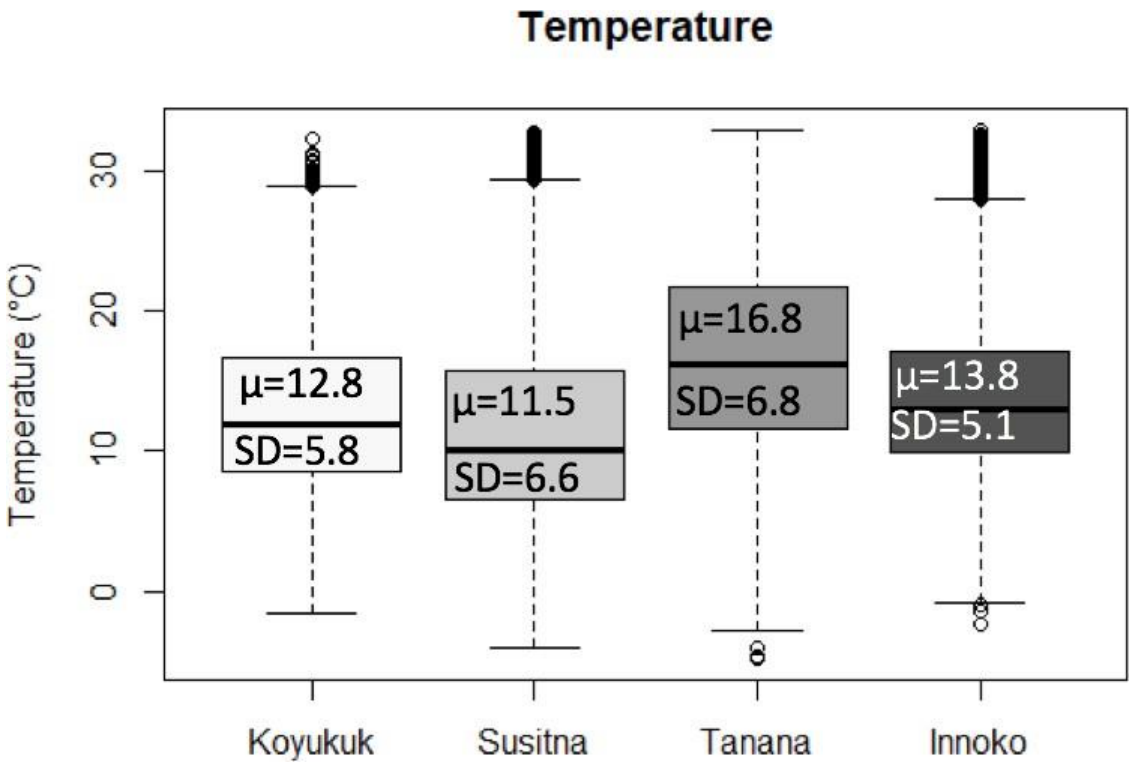

Figure A1.3.2. Regional variation in ambient temperature. ANOVA results comparing regional variation in ambient temperature show that all regions vary from each other statistically ($F=2705$, $p<0.001$). With Tanana showing the highest temperatures, Innoko second, Koyukuk third, and Susitna fourth.

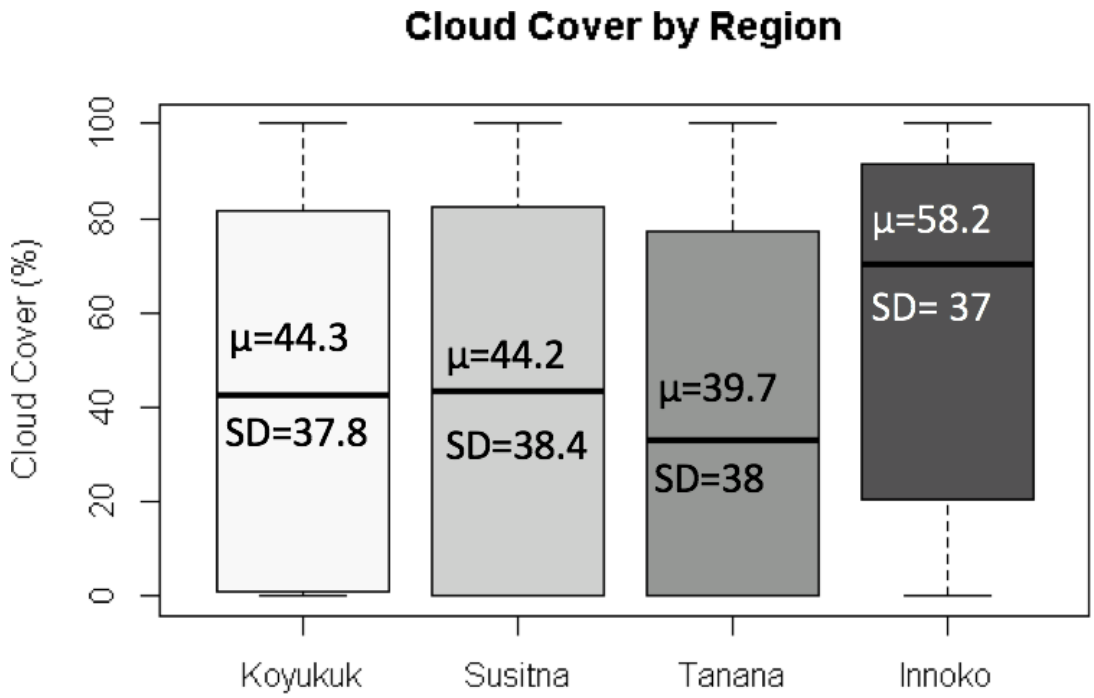

Figure A1.3.3. Regional variation in cloud cover. ANOVA results show all regions vary from each other statistically ($F=1472$, $p<0.001$), except Koyukuk and Susitna.

Table A1.3: Regional variation in fixes occurring in the rain. Percent estimated proportionally comparing number of fixes in the rain to total number of fixes regionally.

	Koyukuk	Susitna	Tanana	Innoko
% fixes in the rain	9.6%	12.1%	7.7%	15.2%

Appendix 2.1. Details on Nitrogen (N) Fertilizer Treatment Estimation

We estimated the native treatment N amount from soil samples collected adjacent to shrubs in the field (n = 3; 0–10 cm depth) and analyzed for total N and bulk density (g cm^{-3}) in the lab. Since not all soil N is available for plant uptake, we assumed 39% of these values were estimated to be plant available N (i.e., ammonium ($NH4^{+}$) or nitrate ($NO3^{-}$)). This uptake percentage is in accordance with a previous study that estimated available N uptake from a deciduous shrub (*Vaccinium uliginosum*) in interior Alaska to be 39% of the soil N pool throughout the growing season (i.e., Chapin, 1983). Plant available, soil-organic N concentrations were calculated using the following equation:

$$\text{SON (kg ha}^{-1}) = \text{SON (\%)} \times \text{BD} \times \text{SD} \times 1000$$

where SON is soil organic N, BD is bulk density (g cm^{-3}), and SD is soil depth (cm). The resultant values of soil organic N for available datasets were 36.40, 48.47, and 52.06 (kg ha^{-1}). These estimated values were averaged and served as our estimate for native soil conditions (45.64 kg ha^{-1}). All other fertilizer treatments were additions to this value.

Appendix 2.2. Summary Statistics for Dietary Fibers

Table A2.2. Table depicting summary statistics for dietary fibers: hemicellulose (HMC), cellulose (CLL), neutral detergent fiber (NDF), acid detergent fiber (ADF), acid detergent lignin (ADL), and acid insoluble ash (AIA).

Fiber	Range	Mean	Standard Deviation
HMC	5.13–7.77%	6.01%	0.79%
CLL	5.70–8.10%	6.87%	0.71%
NDF	12.24–18.51%	14.89%	1.48%
ADF	7.11–10.74%	8.89%	0.95%
ADL	1.26–2.64%	2.02%	0.37%
AIA	0.03–0.24%	0.12%	0.06%

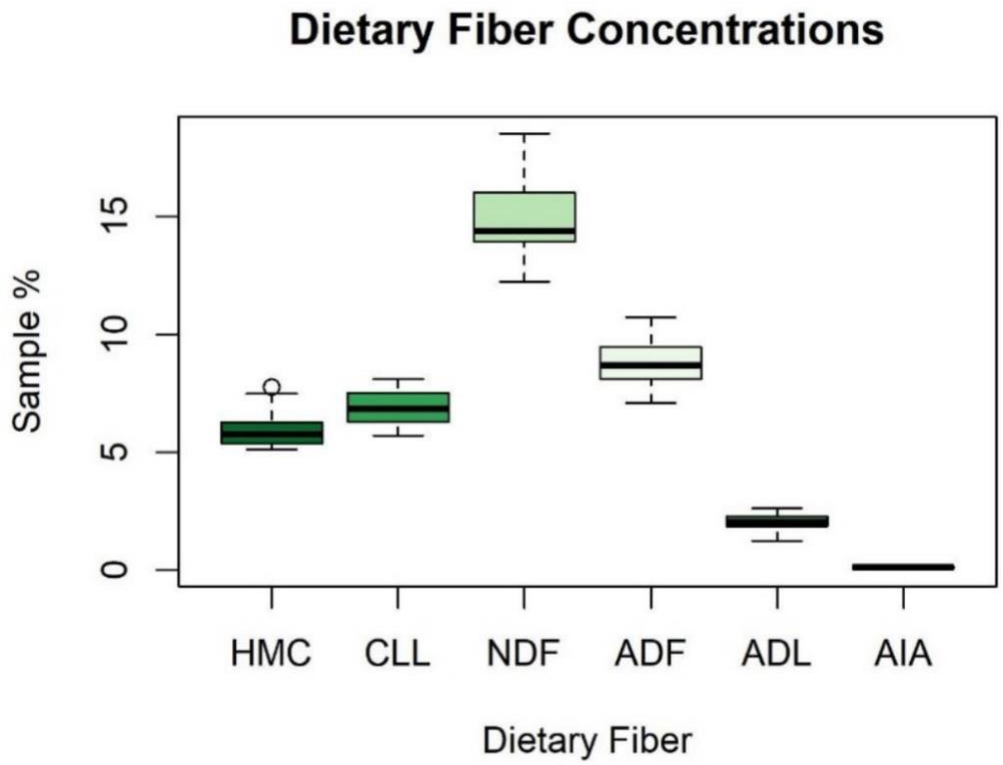

Figure A2.2. Boxplot depicting summary statistics for dietary fibers: hemicellulose (HMC), cellulose (CLL), neutral detergent fiber (NDF), acid detergent fiber (ADF), acid detergent lignin (ADL), and acid insoluble ash (AIA).

Appendix 2.3. Nitrogen Treatments and Cellulose, Neutral Detergent Fiber, and Acid Detergent Fiber

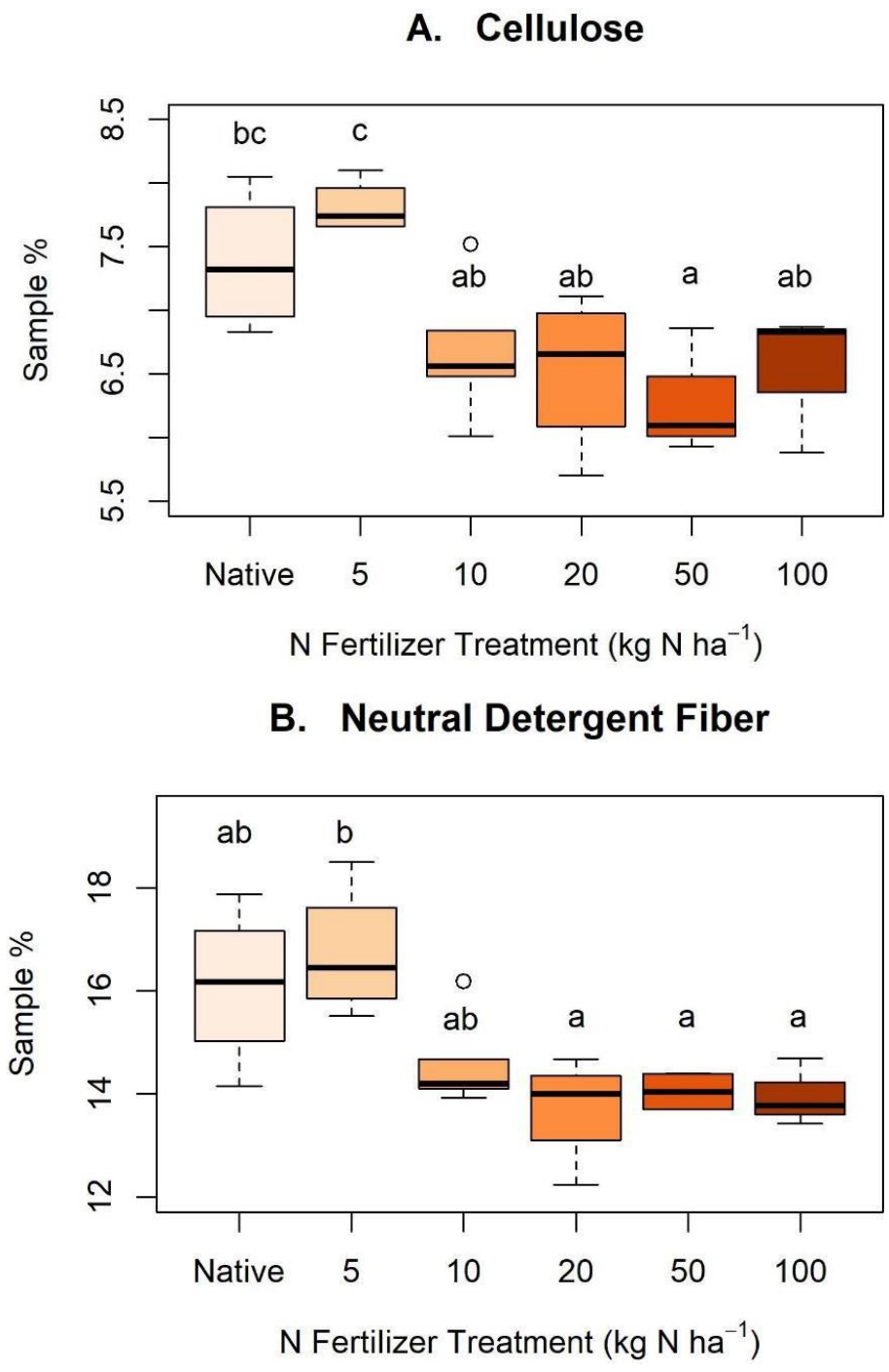

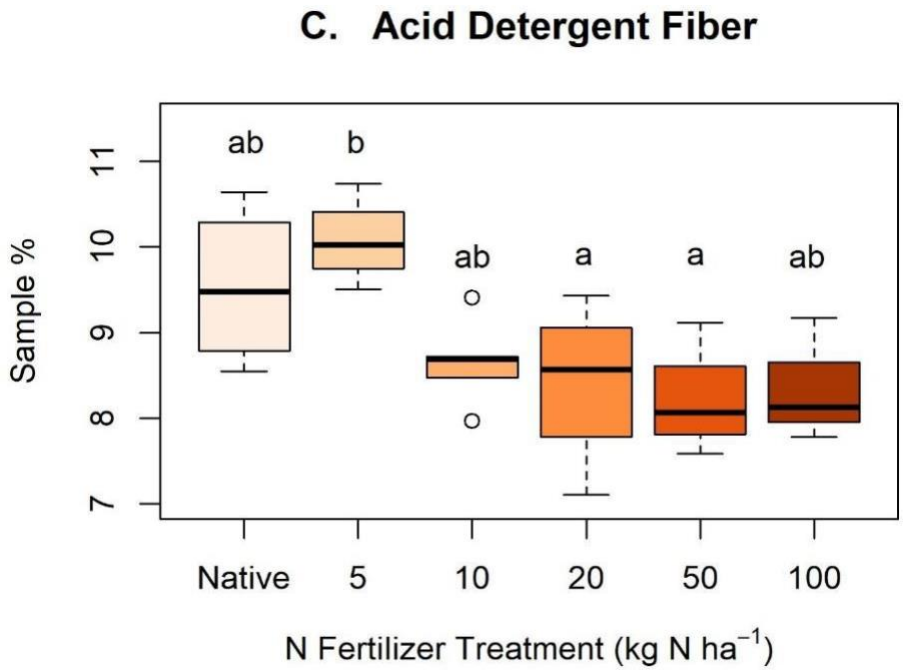

Figure A2. Boxplots depicting statistically significant differences ($p < 0.05$) between nitrogen (N) treatments and dietary fibers: (A) cellulose, (B) neutral detergent fiber, and (C) acid detergent fiber. Letters indicate statistically significant differences between groups within each figure but are not comparable across figures. No statistically significant differences were found between N treatments in hemicellulose, acid detergent lignin, or acid detergent ash.

Appendix 2.4. Results of Swapping Leaf Area for the Normalized Difference Vegetation Index

Table A2.4. Incorporating the normalized difference vegetation index (NDVI) as a proxy for leaf area into the best the band equivalent reflectance (BER) of WorldView3 (WV3) spectral vegetation index (SVI) results for hemicellulose, cellulose, neutral detergent fiber (NDF), acid detergent fiber (ADF), acid detergent lignin (ADL), and acid insoluble ash (AIA) and associated variance explained (R^2), root mean square error (RMSE), Akaike's information criterion for small sample sizes (ΔAICc), and leave-one-out cross validation (ΔLOOCV).

Models	R^2	RMSE	AICc	ΔAICc	LOOCV Slope	LOOCV ρ	ΔLOOCV
Hemicellulose (HMC)							
SVI	0.32	0.62%	52.65	-	0.27	0.52	-
SVI+ NDVI	0.37	4.28%	52.41	−0.24	0.67	0.53	+1%
Cellulose (CLL)							
SVI	0.25	0.59%	50.10	-	0.22	0.45	-
SVI+ NDVI	0.21	0.59%	53.00	+2.90	0.14	0.47	+5%
Neutral detergent fiber (NDF)							
SVI	0.31	1.18%	83.33	-	0.26	0.67	-
SVI+ NDVI	0.28	1.18%	86.09	+2.76	0.22	0.62	−5%
Acid detergent fiber (ADF)							
SVI	0.30	0.76%	62.10	-	0.28	0.57	-
SVI+ NDVI	0.27	0.76%	64.92	+2.82	0.21	0.58	+9%
Acid detergent lignin (ADL)							
SVI	0.34	0.28%	15.05	-	0.33	0.70	-
SVI+ NDVI	0.34	0.28%	16.99	+1.94	0.33	0.71	+1%
Acid detergent ash (AIA)							
SVI	0.13	0.05%	−66.35	-	0.11	0.31	-
SVI+ NDVI	0.13	0.05%	−64.44	+1.91	0.07	0.33	+2%

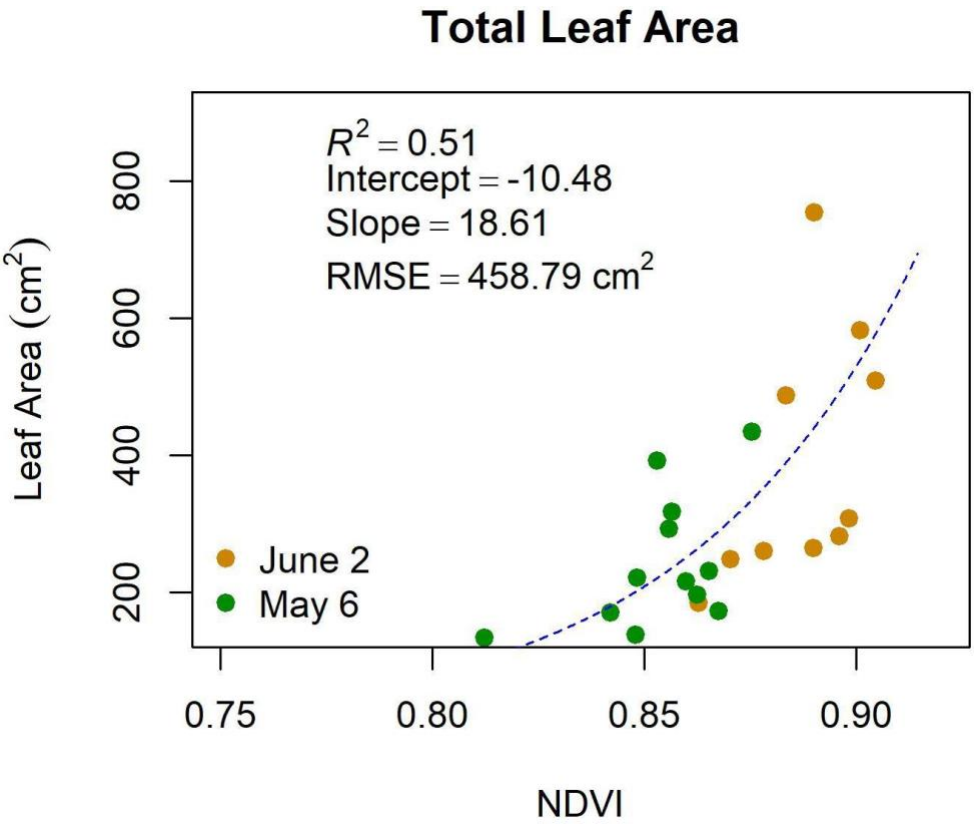

Figure A2.4. The relationship between total leaf area (cm^2) and the normalized differenced vegetation index (NDVI) of the band equivalent reflectance of the WorldView3 satellite.

Appendix 3.1. Best Spectral Vegetation Indices Cross Validation Results

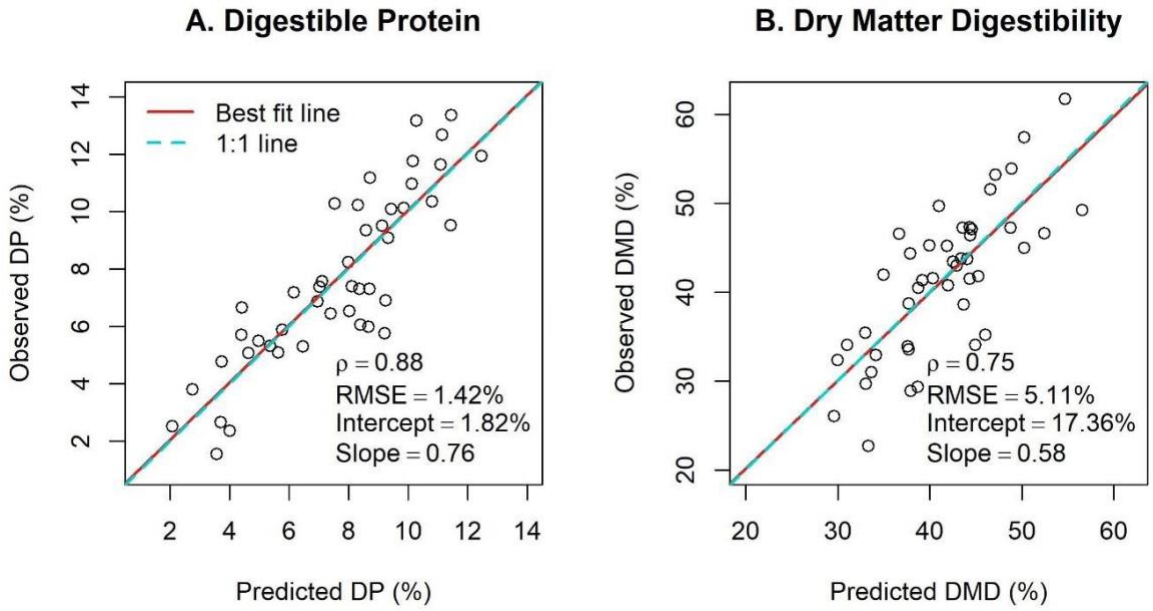

Figure A3.1. Observed vs. predicted concentrations of digestible protein (A) and dry matter digestibility (B) of the best performing spectral vegetation indices (SVI). The best performing SVI for DP included a red-edge and a SWIR band in the normalized difference format ($(R_{703nm} - R_{1719nm})/(R_{703nm} + R_{1719nm})$). The best performing SVI for DMD included a blue and a red band in the simple ratio format (R_{483nm}/R_{657nm}).